CHARACTERIZATION OF THE ADAPTIVE IMMUNE RESPONSES IN ENTEROVIRUS A71 INFECTION

AW YONG KAM LENG

DISSERTATION SUBMITTED IN FULFILMENT OF THE REQUIREMENT FOR THE DEGREE OF MASTER OF MEDICAL SCIENCE

FACULTY OF MEDICINE
UNIVERSITY OF MALAYA
KUALA LUMPUR

2016

UNIVERSITI MALAYA

ORIGINAL LITERARY WORK DECLARATION

Name of Candidate: **Aw Yong Kam Leng**

Registration/Matric No: **MGN120036**

Name of Degree: **Master of Medical Science**

Title of Project Paper/Research Report/Dissertation/Thesis ("this Work"):
Characterization of the adaptive immune responses in enterovirus A71 infection

Field of Study: **Molecular Virology**

I so solemnly and sincerely declare that:

(1) I am the sole author/writer of this Work;
(2) This Work is original;
(3) Any use of any work in which copyright exists was done by way of fair dealing and for permitted purposes and any excerpt or extract form, or reference to or reproduction of any copyright work has been disclosed expressly and sufficiently and the title of the Work and its authorship have been acknowledged in this Work;
(4) I do not have any actual knowledge nor do I ought reasonably to know that the making of this work constitutes an infringement of any copy work;
(5) I hereby assign all and every rights in the copyright to this Work to the University of Malaya ("UM"), who henceforth shall be owner of the copyright in this Work and that any reproduction or use in any form or by any means whatsoever is prohibited without the written consent of UM having been first had and obtained;
(6) I am fully aware that if in the course of making this Work I have infringed any copyright whether intentionally or otherwise, I may be subject to legal action or any other action as may be determined by UM.

Candidate's Signature Date

Subscribed and solemn declared before,

Witness's Signature

Name: Date

Designation:

ABSTRACT

Hand, foot and mouth disease (HFMD) is a common childhood disease caused by many enteroviruses, including enterovirus A71 (EV-A71). Understanding the adaptive immune responses in EV-A71 infection is critical for the development of diagnostic tools, and potential therapeutics and vaccines. The first objective of the study was to determine the antibody responses in HFMD patients. EV-A71-specific IgM antibodies in serum samples from 89 patients with HFMD were detected by commercial IgM-capture enzyme-linked immunosorbent assay (ELISA) and IgM-colloidal gold immunochromatographic assay (GICA). The sensitivity, specificity, positive predictive value, and negative predictive value rates were 78.4, 80.8, 74.4, and 84.0%, respectively, for the IgM-capture ELISA, and 75.7, 76.9, 70.0, and 81.6% for the IgM GICA. Concordance between the two assays was 91.1%. The overall performance suggests that both commercial diagnostic kits are suitable for early diagnosis of HFMD caused by EV-A71 in Malaysia. For the second objective, these sera were subsequently used to characterize antibody responses against the structural and non-structural proteins of EV-A71. Each viral protein was cloned and expressed in either bacterial or mammalian systems, and tested with antisera by Western bloting. The results revealed that all structural proteins (VP1-4), and non-structural proteins 2A, 3C and 3D were targets of EV-A71 IgM, whereas EV-A71 IgG recognized all the structural and non-structural proteins. Subsequent characterization of linear B-cell epitopes on EV-A71 was performed with 63 biotinylated peptides predicted to be immunogenic *in silico*. In total, 22 IgM and 4 IgG dominant linear epitopes were identified. The amino acid sequences of these epitopes were then aligned with 12 enterovirus species, and peptides were further tested with individual serum and mapped to their structural localization. PEP27 (VP1 142-156) and PEP23 (VP1 41-55) were identified as EV-A71 IgM-specific and IgG cross-reactive immunodominant epitopes, respectively. In addition to the antibody

responses, T cells have important functions in immune protection against viral diseases. Hence the final objective was to examine the T cell responses in enterovirus infection. Peripheral blood mononuclear cells collected from HFMD patients were stimulated with EV-A71, and T-cell markers and cytokines were analysed by flow cytometry. EV-A71-infected and coxsackievirus A6 (CV-A6)-infected patients showed similar T cell responses suggesting that the induced T-cell responses were cross-reactive. A higher frequency of IFN-γ expressing $CD4^+$ T cells was observed in children, but a higher frequency of IFN-γ expressing $CD8^+$ T cells was observed in adults. This may be because $CD4^+$ cells are involved in responses to primary infections, which mostly occur in children, while the $CD8^+$ responses in adults represent immune memory. Cytolytic enzymes such as granzyme B and perforin, which are critical mediators for anti-viral immunity, were expressed in both children and adults. Higher granzyme B compared to perforin was expressed in $CD8^+$ T cells in both children and adults, suggesting that a proportion of EV-A71-specific $CD8^+$ T cells may not be directly cytotoxic. Similar expression of $CD57^+$ $CD8^+$ T cells was observed in children and adults. The expression of CD57 cells suggests that immunosenescence common in chronic infection may also play a role in EV-A71 T-cell immunity. Overall, this study provides new knowledge in the immunoprotection mechanisms against EV-A71.

ABSTRAK

Penyakit kaki, tangan dan mulut (HFMD) merupakan penyakit kanak-kanak biasa yang disebabkan oleh banyak jenis enterovirus, termasuk enterovirus A71 (EV-A71). Oleh itu, memahami respon imun adaptif dalam jangkitan EV-A71 adalah penting untuk perkembangan alat diagnostik, terapeutik dan vaksin yang berpotensi. Objektif pertama untuk kajian ini adalah untuk menentukan respon antibodi pesakit HFMD. Antibodi IgM-spesifik EV-A71 dalam sampel serum daripada 89 pesakit HFMD telah dikesan oleh komersial asai imunojerapan berpaut enzim penangkapan IgM (ELISA) dan asai imunokromatografi koloid emas IgM (GICA). Kadar kepekaan, kekhususan, nilai ramalan positif dan nilai ramalan negatif adalah 78.4, 80.8, 74.4, and 84.0% bagi ELISA penangkapan IgM, manakala kadar untuk IgM GICA adalah 75.7, 76.9, 70.0, dan 81.6% . Keselarasan antara dua asai tersebut adalah 91.1%. Prestasi keseluruhan menunjukkan bahawa kedua-dua alat diagnostik komersial sesuai untuk digunakan di Malaysia bagi diagnosis awal HFMD yang disebabkan oleh EV-A71. Bagi objektif kedua, sera ini digunakan untuk mencirikan respon antibodi terhadap protein struktur dan bukan struktur EV-A71. Setiap protein virus telah diklon dan diekspreskan sama ada dalam sistem bakteria atau mamalia, dan diuji dengan antisera oleh pemedapan western. Hasil kajian menunjukkan bahawa semua protein struktur VP1-4 dan protein bukan struktur 2A, 3C dan 3D merupakan sasaran IgM EV-A71, manakala IgG EV-A71 mengecam semua protein struktur dan bukan struktur. Seterusnya, pencirian epitop linear B-sel pada EV-A71 dilakukan dengan 63 peptida biotinylated yang diramalkan imunogenik *in silico*. Keseluruhannya, 22 epitop linear IgM and 4 epitop linear IgG dominan telah dikenal pasti. Jujukan asid amino epitop dijajarkan dengan 12 spesies enterovirus, dan diuji dengan serum individu, dan dipetakan kepada penyetempatan struktur mereka. PEP27 (VP1 142-156) dan PEP23 (VP1 41-55) telah dikenal pasti sebagai epitop dominan imun spesifik IgM dan reaksi silang IgG bagi EV-A71. Sebagai

tambahan kepada respon antibodi, sel-sel T mempunyai fungsi penting dalam perlindungan imun terhadap penyakit-penyakit virus. Oleh demikian, objektif akhir kajian adalah untuk mengkaji respon sel-sel T dalam jangkitan enterovirus. Sel-sel mononuklear darah periferi daripada pesakit HFMD dirangsangkan dengan EV-A71, dan penanda sel T dan sitokin dianalisis dengan sitometri aliran. Pesakit yang dijangkiti oleh EV-A71 dan coxsackievirus A6 (CV-A6) menunjukkan respon sel T yang sama, menunjukkan respon sel T teraruh mempunyai tindak balas bersilang. Frekuensi IFN-γ sel $CD4^+$ T adalah lebih tinggi pada kanak-kanak, tetapi frekuensi IFN-γ $CD8^+$ T adalah lebih tinggi pada orang dewasa. Hal ini mungkin disebabkan oleh sel-sel $CD4^+$ terlibat dalam respon kepada jangkitan primer yang kebanyakannya berlaku pada kanak-kanak, manakala respon $CD8^+$ dalam orang dewasa merupakan memori imun. Enzim sitolisis seperti granzyme B dan perforin yang merupakan pengantara kritikal untuk imuniti anti-virus turut diekspreskan dalam kanak-kanak dan orang dewasa. Frekuensi granzyme B yang lebih tinggi berbanding dengan perforin diekspreskan dalam sel-sel $CD8^+$ T dalam kanak-kanak dan orang dewasa, menunjukkan bahawa sebahagian daripada sel-sel $CD8^+$ T spesifik EV-A71 mungkin tidak sitotoksik secara langsung. Pengekspresan yang serupa diperhatikan pada kanak-kanak dan orang dewasa. Pengekspresan sel CD57 menunjukkan bahawa imun senesens yang biasa dalam jangkitan kronik juga memainkan peranan dalam imuniti sel T EV-A71. Secara keseluruhan, kajian ini memberikan pengetahuan baru dalam mekanisme perlindungan imun terhadap EV-A71.

ACKNOWLEDGEMENTS

This dissertation would not have been achievable without the guidance and the help of several individuals, who contributed and extended their invaluable assistance along the way of preparation and completion of this study.

I would like to express the deepest appreciation to my supervisors, **Associate Professor Dr. Chan Yoke Fun, Professor Dr. Jamal I-Ching Sam and Associate Professor Dr. Shankar Esakimuthu** for supporting me throughout the course of this study with their continuous encouragement, patience, guidance and knowledge. It was a great pleasure to conduct my postgraduate studies under their close supervision.

I would like to offer my special thanks to **Professor Dr. Koh Mia Tuang, Dr. Hannah Wardiah Rosland, doctors and nurses** from Paediatric Trauma and Emergency Department of the University Malaya Medical Centre for helping me in the collection of patients' blood samples and throat swab specimens.

Special thanks to my fellow labmates in Lab A2-24 laboratory: **Dr. Tan Chee Wah, Dr. Chiam Chun Wei, Chua Chong Long, Loong Shih Keng, Chan Shie Yien, Khor Chee Sieng, Jeffrey Lai Kam Fatt, Nik Nadia, Wong Hui Vern, Tee Han Kang and interns** for their friendship, guidance and laboratory assistance in my study.

I am deeply grateful to **Department of Medical Microbiology, Immunotherapeutics Laboratory and Medical Biotechnology Laboratory** for the facilities provided.

I owe my deepest gratitude to **my parents, elder brother and friends**, whose were always supporting me and encouraging me with their best wishes.

Last but not least, I would like to thank everybody who supported me in any respect during the completion of this dissertation.

TABLE OF CONTENTS

LIST OF FIGURES

LIST OF TABLES

LIST OF SYMBOLS AND ABBREVIATIONS

%	Percentage
℃	Degree Celsius
κ	Cohen's kappa
µg	Microgram
µg/ml	Microgram per milliliter
µl	Microliter
µM	Micromolar
ANOVA	Analysis of variance
APC	Allophycocyanin
APCs	Antigen presenting cells
ASC	Antibody-secreting B cells
ATCC	American Type Culture Collection
BLAST	Basic Local Alignment Search Tool
bp	Base pair
BSA	Bovine serum albumin
CD	Cluster of differentiation
cm^2	Square centimeter
CNS	Central nervous system
CO_2	Carbon dioxide
CPE	Cytopathic effect
CTLA-4	Cytokine T lymphocyte antigen-4
CV	Coxsackievirus
DAB	3, 3'-Diaminobenzidine
DMEM	Dulbecco's modified Eagle's medium
DMSO	Dimethyl sulfoxide
DNA	Deoxyribonucleic acid
dNTP	Deoxynucleotide
DTT	Dithiothreitol
EDTA	Ethylenediaminetetraacetic acid
EGFP	Enhanced green fluorescence protein
ELISA	Enzyme-linked immunosorbent assay
ELISPOT	Enzyme-linked immunospot
EV	Enterovirus
FACS	Fluorescence-activated cell sorting
FBS	Fetal bovine serum
FITC	Flurescein Isothiocyanate Conjugate
FSC	Forward scatter
GICA	Gold immunochromatographic assay
HEK-293	Human Embryonic Kidney 293 cells
HEPES	4-(2-hydroxyethyl)-1-piperazineethanesulfonic acid
HFMD	Hand, foot, and mouth disease
HIV	Human immunodeficiency virus
HLA-DR	Human leukocyte antigen-antigen D related

HPD	Highest posterior density
HRP	Horseradish peroxidase
IFN	Interferon
Ig	Immunoglobulin
IL	Interleukin
IP-10	Interferon-gamma inducible protein 10
IRES	Internal ribosome entry site
IVIg	Intravenous immunoglobulin
KCl	Potassium chloride
LB	Luria-Bertani
M	Molar
mAb	Monoclonal antibody
MCMC	Markov chain Monte Carlo
mg	Milligram
mg/ml	Milligram per milliliter
$MgSO_4$	Magnesium sulfate
MHC	Major histocompatibility complex
ml	Milliliter
mM	Millimolar
mm	Millimeter
MOI	Multiplicity of infection
NaCl	Sodium chloride
NaH_2PO_4	Sodium dihydrogen phosphate
NEAA	Non-essential amino acids
ng	Nanogram
NK	Natural killer
nm	Nanometer
NPV	Negative predictive value
OD	Optical density
ORF	Open reading frame
PBMCs	Peripheral blood mononuclear cells
PBS	Phosphate-buffered saline
PBST	Tween-20 phosphate-buffered saline
PCR	Polymerase chain reaction
PDB	Protein Data Bank
PE	Pulmonary edema
PE	R-Phycoerythrin (fluorochrome)
PerCP-Cy5.5	Peridinin-chlorophyll-protein complex: Cy5.5 conjugate
PFU/ml	Plaque forming units per milliliter
PHA	Phytohemagglutinin
PPV	Positive predictive value
RD	Rhabdomyosarcoma
RdRp	RNA dependent RNA polymerase
RNA	Ribonucleic acid
RPMI-1640	Roswell Park Memorial Institute 1640 medium

RT-PCR	Reverse transcription polymerase chain reaction
S/CO	Signal/cut-off
SD	Standard deviation
SDS	Sodium dodecyl sulfate
SDS-PAGE	Sodium dodecyl sulfate-polyacrylamide gel electrophoresis
SSC	Side scatter
TAE	Tris-acetate-EDTA buffer
$TCID_{50}$	50% tissue culture infective dose
TE	Tris-EDTA buffer
TFH	T follicular helper cells
TMB	Tetramethylbenzidine
TNE	Tris-sodium chloride-EDTA buffer
Tris-HCl	Tris(hydroxymethyl)aminomethane hydrogen chloride
U/ml	Units per milliliter
UMMC	University Malaya Medical Centre
UTR	Untranslated regions
V	Voltage
VP	Viral protein
x g	Gravitational acceleration

LIST OF APPENDICES

CHAPTER 1

INTRODUCTION

1.1 Introduction

Hand, foot and mouth disease (HFMD) is a common viral infection frequently occurring in infants and children. HFMD usually results in mild and self-limiting illness, characterized by fever and the development of vesicular lesions on the palms and soles, and oral ulcers. The causative agents of HFMD are viruses from the genus of Enterovirus within the family of *Picornaviridae*, with enterovirus A71 (EV-A71) and coxsackievirus A16 (CV-A16) being the most commonly detected viruses. Over the last decade, EV-A71 was responsible for several large HFMD epidemics in the Asia Pacific region, raising serious public health concerns (Solomon *et al.*, 2010). Unlike other enteroviruses that cause HFMD, EV-A71 infection may result in fatality and severe neurological complications such as encephalitis, myocarditis, acute flaccid paralysis and aseptic meningitis, especially in children below 5 years old (Ooi *et al.*, 2010). To date, no effective licensed antivirals and vaccines are available to combat EV-A71 infection (Tan *et al.*, 2014).

Co-circulation of various enteroviruses was observed in several large HFMD outbreaks, such as Singapore (Ang *et al.*, 2009), Thailand (Linsuwanon *et al.*, 2014), China (Lu *et al.*, 2012, He *et al.*, 2013), Taiwan (Wei *et al.*, 2011) and Malaysia (Chua and Kasri, 2011, Ling *et al.*, 2014). However, the HFMD clinical manifestations caused by these enteroviruses are generally indistinguishable. Therefore, proper laboratory diagnosis is essential for prompt public health measures to provide appropriate treatment, control the spread of virus and minimize the risk of fatality. Traditionally, the standard laboratory diagnosis of EV-A71 was achieved by virus isolation, immunofluorescence assay and neutralization test (reviewed in Muir *et al.*, 1998). However, these approaches are time-

consuming and labour-intensive. Therefore there is a need for a more accessible, reliable and rapid diagnostic assay for EV-A71 during the HFMD outbreaks. In this study, the performance of the commercial EV-A71 IgM-capture enzyme-linked immunosorbent assay (ELISA) and EV-A71 IgM-colloidal gold immunochromatographic assay (GICA) was evaluated. This study further hypothesized that both diagnostic assays are suitable for the screening for EV-A71 during HFMD outbreaks in Malaysia.

Epitopes, which also known as antigenic determinants, are the parts of an antigen that are recognized by antibodies, B cells or T cells to stimulate immune responses against an infective microorganism. In EV-A71, a majority of the reported epitopes have been mainly identified with immunized animal antisera (Foo *et al*., 2007b, Li *et al.*, 2009, Liu *et al.*, 2011, Gao *et al.*, 2012, Lim *et al.*, 2012, Kiener *et al.*, 2014) and only one study of EV-A71 immunogenic epitopes has been conducted using human sera (Gao *et al.*, 2012). To date, all the reported EV-A71 epitopes focused only on EV-A71 structural proteins. Two main EV-A71 immunogenic sites were identified: the epitopes spanning amino acid positions 208-222 in VP1 (Foo *et al.*, 2007b, Li *et al.*, 2009, Chang *et al.*, 2011, Lim *et al.*, 2012, Deng *et al.*, 2015) and positions 136-159 in the VP2 capsid protein (Liu *et al.*, 2011, Gao *et al.*, 2012, Xu *et al.*, 2014). However, the immunogenicity of EV-A71 non-structural proteins remains unknown. This study is the first to characterize human antibody responses against the structural and non-structural proteins of EV-A71 with well-characterized EV-A71-infected patient sera. This study further hypothesized that the screening of 63 synthetic peptides (predicted as potential EV-A71 immunogenic epitopes) covering the structural and non-structural proteins of EV-A71 will enable identification of EV-A71-specific IgM and IgG immunogenic epitopes.

T cells play an important role in protecting the host from viral infections. Others have demonstrated that cellular rather than humoral immunity is correlated with clinical outcome of EV-A71 infection (Chang *et al.*, 2006). Interferon-gamma (IFN-γ) levels were reported to be high in the serum and cerebrospinal fluid samples of HFMD patients with pulmonary edema (PE) (Wang *et al.*, 2003, Wang *et al.*, 2007), but lower in peripheral blood mononuclear cells (PBMCs) stimulated with EV-A71 (Chang *et al.*, 2006). Nevertheless, the production and accumulation of IFN-γ in T cells after stimulation remain unknown. Granzyme B plays an important role in antiviral immunity by activation of programmed cell death in the presence of perforin (Tarpani *et al.*, 1998), and is generally produced by cytotoxic T cells and natural killer (NK) cells (Cullen *et al.*, 2010). Moreover, granzyme B and perforin have also been linked to CD57, a critical molecule associated with replicative senescence (Chattopadhyay *et al.*, 2009). The association of granzyme B, perforin and CD57 has been well studied in human immunodeficiency virus (HIV) infection, but largely remain unclear in EV-A71 infection. This knowledge gap of T cell immune responses in EV-A71 infection led to this first preliminary analysis of IFN-γ expression in $CD4^+$ and $CD8^+$ T cells and the association of granzyme B, perforin and CD57 with EV-A71 infection.

In summary, this study provides new knowledge in the immunoprotection mechanisms against EV-A71 infection, which may be beneficial in the development of diagnostic tools, potential therapeutics and vaccine candidates.

1.2 Objective of the study

Adaptive immunity plays an important role in protection against EV-A71 infection. The underlying B cell and T cell immune responses in EV-A71 infection are still not fully understood. Hence, the main objective was to study different aspect of humoral and cellular responses in EV-A71 infection.

The specific aims of the present study are as follows:

1. To identify causative agents of HFMD in University Malaya Medical Centre, Kuala Lumpur, in 2012-2013
2. To characterize EV-A71 IgM responses in patients with HFMD using commercial EV-A71 IgM assays for diagnosis
3. To characterize human antibody responses against EV-A71 structural and non-structural proteins with well-characterized EV-A71-infected patient sera
4. To identify EV-A71-specific IgM and IgG antigenic epitopes within EV-A71 structural and non-structural proteins
5. To examine the T cell responses in enterovirus infection

CHAPTER 2

LITERATURE REVIEW

2.1 The virology of enterovirus A71

2.1.1 Classification of enteroviruses

At present, the family of *Picornaviridae* consists of 50 species grouped into 29 genera, which includes *Aphthovirus*, *Aquamavirus*, *Avihepatovirus*, *Avisivirus*, *Cardiovirus*, *Cosavirus*, *Dicipivirus*, *Enterovirus*, *Erbovirus*, *Gallivirus*, *Hepatovirus*, *Hunnivirus*, *Kobuvirus*, *Megrivirus*, *Mischivirus*, *Mosavirus*, *Oscivirus*, *Parechovirus*, *Pasivirus*, *Passerivirus*, *Rosavirus*, *Salivirus*, *Sapelovirus*, *Senecavirus*, *Teschovirus*, *Tremovirus*, and three newly designated genera of *Kunsagivirus*, *Sakobuvirus* and *Sicinivirus* (Adams *et al.*, 2015).

Originally, the human enteroviruses were classified based on antigenic differences and their natural and experimental pathogenesis, and subdivided into poliovirus, coxsackievirus A (CV-A) and CV-B, and echovirus (reviewed in Muir *et al.*, 1998). However, based on molecular and biological properties of the viruses, human enteroviruses have been reclassified into four species, human enterovirus A-D. Classification based on phylogenetic and molecular analysis has led to a recent proposal to remove references to host species name from the enterovirus species nomenclature (Adams *et al.*, 2013). To date, the genus of enterovirus consists of 12 species: Enterovirus A-H, Enterovirus J and Rhinovirus A-C.

Enterovirus A consists of 25 serotypes, which includes coxsackievirus A2-A8, A10, A12, A14, A16, enterovirus A71, A76, A89-A92, A114, A119-A121, simian enteroviruses SV19, SV43, SV46 and baboon enterovirus BA13. EV-A71 is classified as a member of the species of enterovirus A.

2.1.2 Genomic and structural components of enterovirus A71

Similar to other picornaviruses, EV-A71 is a small (30 nm), non-enveloped, single-stranded, positive-sense RNA virus of approximately 7.4 kb in size. The EV-A71 genome comprises a 5' untranslated regions (UTR), single open reading frame (ORF) encoding a polyprotein of 2193 amino acids, a short 3' UTR and a poly-adenylated tail (Figure 2.1A). The polyprotein is subdivided into three regions, P1, P2 and P3. The P1 region encodes four structural proteins (VP1, VP2, VP3 and VP4), while the P2 and P3 regions encode seven non-structural proteins (2A, 2B, 2C and 3A, 3B, 3C, 3D, respectively) (Brown and Pallansch, 1995).

The 5' UTR of EV-A71 contains six putative stem-loop structures (Figure 2.1B). Stem-loop I (cloverleaf) is involved in viral RNA synthesis and stem-loop II-VI comprise the type I internal ribosome entry site (IRES) which plays an important role in cap-independent viral RNA translation (Thompson and Sarnow, 2003). The 3' UTR of EV-A71 contains three putative stem-loop structures (X, Y, Z), followed by a poly-adenylated tail which is important for genome replication (Rohll *et al.*, 1995). A small viral protein, VPg is covalently linked to the end of 5' UTR.

The EV-A71 virus particle consists of an icosahedral capsid with 60 identical units (promoters) each consisting of the four structural proteins VP1, VP2, VP3 and VP4 (Figure 2.2). VP1, VP2 and VP3 capsid proteins are the main structural components of the virion, whereas VP4 is located internally. VP1, VP2 and VP3 capsid proteins are exposed to the surface, hence they are most likely to be responsible for host receptor binding and antigenicity (Brown and Pallansch, 1995). The non-structural proteins mediate genomic RNA replication. $2A^{pro}$ and $3CD^{pro}$ are involved in polyprotein processing. 2B viroporin is involved in the integration of viral protein into the endoplasmic reticulum membrane. This alters the permeability of host cell membranes

to promote virus release (Martinez-Gil *et al.*, 2011). $2C^{ATPase}$ has several important functions in viral RNA replication, such as host membrane rearrangements associated with the formation of replication complexes, RNA binding domains, ATPase activity for the initiation of negative-stranded RNA synthesis and VPg uridylylation (reviewed in Steil and Barton, 2009). Protein 3A contains hydrophobic domains that facilitate anchoring of the replication complex to the virus-induced vesicles (Lin *et al.*, 2009a). The uridylylated VPg (viral protein 3B) primes RNA replication initiation whereas $3D^{pol}$ functions as the RNA dependent RNA polymerase (RdRp) which is involved in RNA elongation. However $3D^{pol}$ is error-prone with no proofreading, resulting in rapid virus mutation and evolution (reviewed in Solomon *et al.*, 2010).

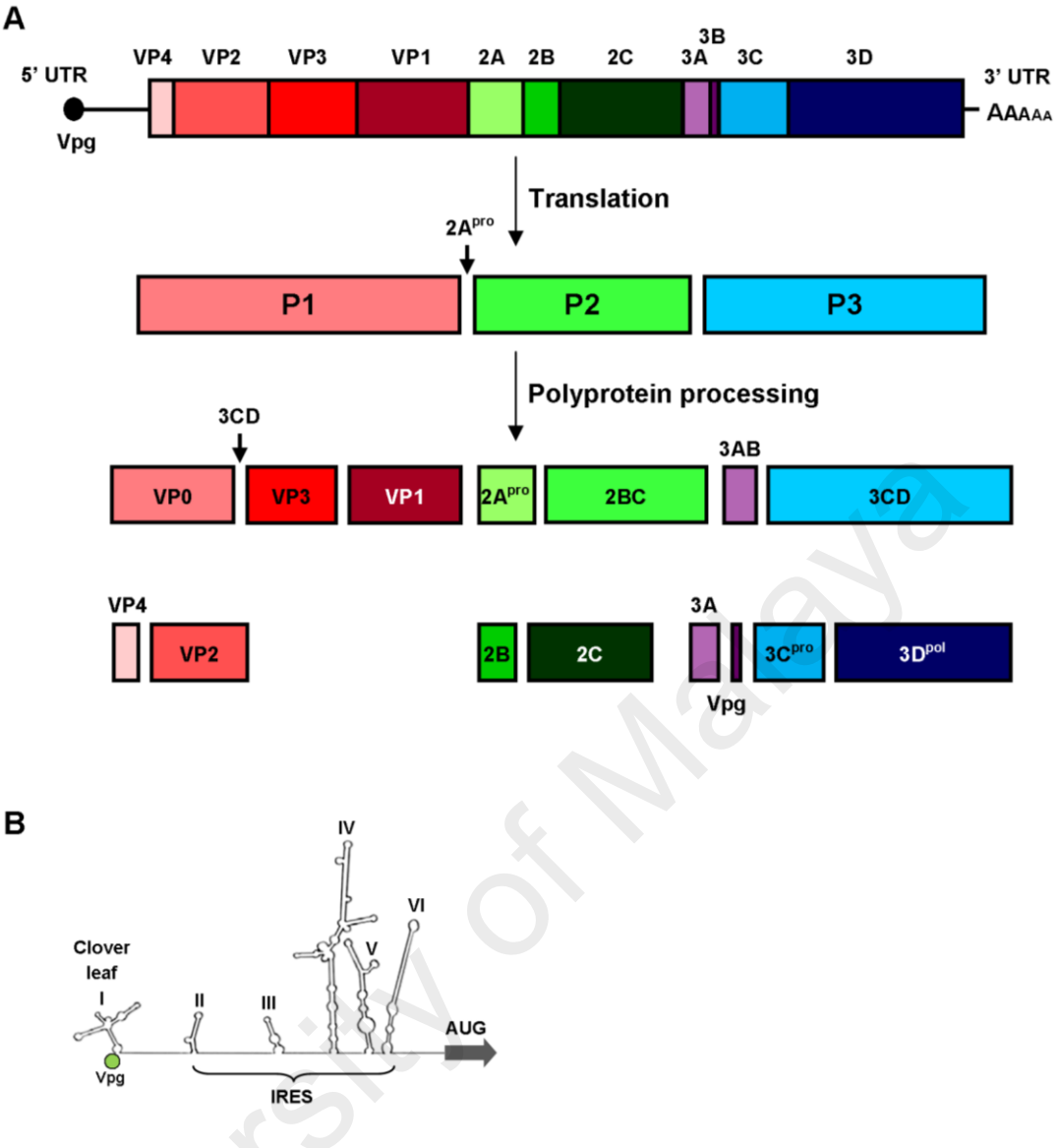

Figure 2.1: Schematic illustration of the EV-A71 genome. (A) Structure of the EV-A71 genome. The EV-A71 genome consists of a single ORF flanked by 5' UTR and 3' UTR. VP1-VP4 are structural proteins, while 2A-2C and 3A-3D are non-structural proteins. Image was adapted with modifications from Hober *et al.* (2013). (B) Schematic representation of EV-A71 5' UTR. The roman numerals (I-VI) represent the six putative stem-loop structures. Cloverleaf (stem-loop I) is involved in viral RNA synthesis while IRES (stem-loop II-VI) involved in cap-independent viral RNA translation. Image modified from Shih *et al*. (2011).

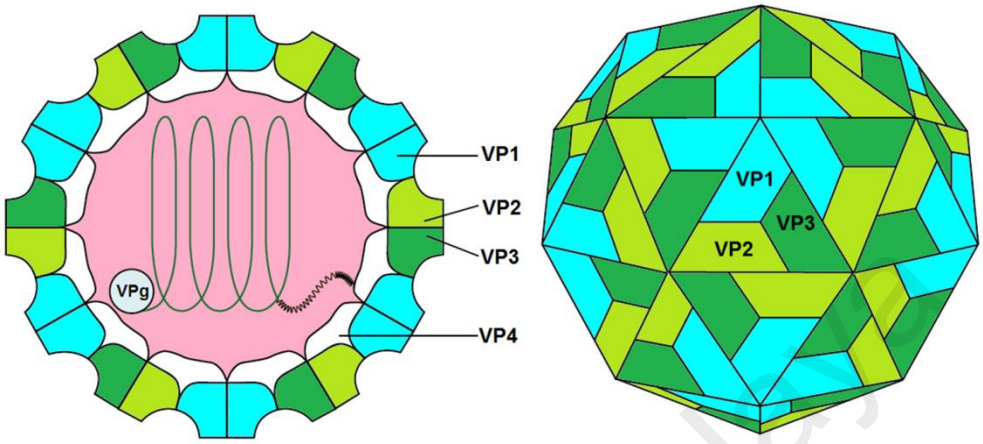

Figure 2.2: Enterovirus A71 virion structure. VP1, VP2 and VP3 capsid proteins are the main structural components of the virion, whereas VP4 is located internally. Image modified from Solomon *et al.* (2010) and ViralZone of Swiss Institute of Bioinformatics.

2.2 Clinical manifestations of enteroviruses infections

2.2.1 Hand, foot and mouth disease and herpangina

HFMD is a common viral infection in children and usually results in mild and self-limiting illness, characterized by fever and the development of papulo-vesicular lesions on the palms and soles, and oral ulcers. Other clinical symptoms frequently experienced include poor appetite, sleep disturbance, vomiting, and lethargy (Liu *et al.*, 2000). HFMD is commonly caused by EV-A71 and CV-A16, and other enterovirus serotypes such as CV-A4, A5, A10, B2 and B5 (reviewd in Chan *et al.*, 2011). The HFMD clinical manifestations caused by these enteroviruses are generally indistinguishable. However based on clinical observations in Japan, Malaysia and Western Australia, CV-A16 infection form larger papular and/or petechial vesicles, and are often located on the trunk and limbs (reviewed in McMinn, 2002). The HFMD clinical manifestations of CV-A6 are generally similar to those caused by EV-A71 and CV-A16, but more severe skin manifestations have been observed in CV-A6 infection (Kobayashi *et al.*, 2013, Puenpa *et al.*, 2013). The atypical CV-A6-associated HFMD outbreaks in Finland, Taiwan and Japan were associated with onychomadesis 1-2 months after illness (Fujimoto *et al.*, 2012, Kobayashi *et al.*, 2013, Osterback *et al.*, 2009, Wei *et al.*, 2011). Occurrence of onychomadesis suggested that CV-A6 virus replication damaged nail matrix and resulted in temporary nail dystrophy (Osterback *et al.*, 2009).

In addition to HFMD, enteroviruses also can cause herpangina, which is characterized by an abrupt onset of fever and the development of multiple oral ulcers on anterior pharyngeal folds, uvula, tonsils and soft palate (reviewed in Ooi *et al.*, 2010). Herpangina was the second most common diagnosis after HFMD during the Taiwan epidemic in 1998 (Ho *et al.*, 1999). Herpangina has been associated most with acute

coxsackievirus A infections, with CV-A8, CV-A10 and CV-A16 being most frequently implicated (reviewed in McMinn, 2002).

2.2.2 Neurological complications

More frequently, EV-71 has been associated with severe clinical presentations and potentially fatal neurological complications such as encephalitis, myocarditis, acute flaccid paralysis and aseptic meningitis, especially in children less than 5 years old (reviewed in Ooi *et al.*, 2010, Solomon *et al.*, 2010).

EV-A71 encephalitis generally involves the brainstem, cerebellum and spinal cord, and presents with myoclonic jerks, reduced consciousness, ataxia and cranial nerve palsies (reviewed in Chan *et al.*, 2011). Similar to poliomyelitis, EV-A71 encephalitis is frequently associated with severe cardiorespiratory symptoms such as pulmonary edema (PE) (reviewed in Ooi *et al.*, 2010). In Sarawak, where several epidemics occurred from 2000 to 2006, up to 10-30% of children hospitalized with EV-A71-associated HFMD also developed central nervous system (CNS) complications (Ooi *et al.*, 2007, Ooi *et al.*, 2009). Acute flaccid paralysis associated with EV-A71 infection was generally milder and had higher complete recovery rates than poliovirus infection (reviewed in McMinn, 2002).

Deaths caused by EV-A71 typically present with febrile illness, neurological syndromes, acute refractory cardiac dysfunction and fulminant pulmonary edema (Ooi *et al.*, 2009). Most of them died within a few hours after hospital admission (Lum *et al.*, 1998).

2.3 Epidemiology of enteroviruses

2.3.1 Outbreaks of hand, foot and mouth disease

Over the last decade, numerous large HFMD epidemics have occurred in the Asia-Pacific region. The common causative agents include EV-A71, CV-A16 and CV-A6.

2.3.1.1 Enterovirus A71 outbreaks

EV-A71 was first isolated in California in 1969 from the stool of a 9-month-old infant with encephalitis (Schmidt *et al.*, 1974). Since then, EV-A71 spread to Europe and caused outbreaks in Sweden (1973), Bulgaria (1975) and Hungary (1978) (Blomberg *et al.*, 1974, Chumakov *et al.*, 1979, Nagy *et al.*, 1982). Outbreaks of EV-A71 infection were also reported in Asia, such as Japan in 1973 (Hagiwara *et al.*, 1978) and Australia in 1986 (Gilbert *et al.*, 1988).

Over the last decade, EV-A71 has become endemic in the Asia-Pacific region, and large HFMD epidemics have been reported in Malaysia (AbuBakar *et al.*, 1999), Singapore (Wu *et al.*, 2010), Taiwan (Wu *et al.*, 1999, Huang *et al.*, 1999), Korea (Ryu *et al.*, 2010), Japan (Hagiwara *et al.*, 1978, Hosoya *et al.*, 2006), Hong Kong (Ng *et al.*, 2001), Brunei (AbuBakar *et al.*, 2009) and China (Zheng *et al.*, 1995).

In mid-1997 in Sarawak, Malaysia, there was a large outbreak of HFMD caused primarily by EV-A71, with 34 children aged <6 years old dying of rapidly progressive cardiorespiratory failure (Cardosa *et al.*, 1999). In the same year, HFMD outbreaks were reported in Peninsular Malaysia and four children with sudden cardiopulmonary collapse also died within a few hours of admission (Lum *et al.*, 1998). In 1998, 129,106 EV-A71 cases were reported in Taiwan. A total of 405 children with serious

neurological complications were admitted to hospital and 78 of them died (Ho *et al.*, 1999).

In 2000, Singapore experienced large HFMD outbreaks with 3,790 cases and 5 deaths reported (Chan *et al.*, 2003). Another fatal HFMD outbreak was reported in Malaysia in 2000. Three children with CNS infection and rapid cardiorespiratory decompensation were admitted to hospital, two of whom died (Lum *et al.*, 2002). In addition to EV-A71, echovirus 7 was identified as another possible causative agent for these three cases. The fatal HFMD outbreaks caused by EV-A71 continued to be seen in Sarawak in 2000, 2003, 2006 and 2008/2009 (Ooi *et al.*, 2009, Ooi *et al.*, 2010, Solomon *et al.*, 2010).

The largest EV-A71 epidemics were reported in China in 2008, with 488,955 HFMD cases and 126 fatal cases reported (Yang *et al.*, 2009). The outbreak continued in 2009, with 1,161,131 HFMD cases and 353 fatalities reported (Tan *et al.*, 2011). In addition, 200 deaths and 567 fatality cases were reported in Vietnam in 2011/2012 (Khanh *et al.*, 2012) and in China in 2012 (Wang *et al.*, 2015b). The emergence of EV-A71 outbreaks shows that EV-A71 has become a serious public health threat with pandemic potential.

2.3.1.2 Coxsackievirus A16 outbreaks

HFMD caused by CV-A16 infection is generally milder and self-limiting, therefore reports of CV-A16 outbreaks are limited. In Singapore, CV-A16 has become the predominant etiological agent of HFMD for three epidemic years (2000, 2005 and 2007), whereas EV-A71 was responsible for the 2006 epidemic (Ang *et al.*, 2009). Similarly in Vietnam in 2005, 52% of the HFMD cases were caused by CV-A16 and 42% were caused by EV-A71 (Tu *et al.*, 2007). In China, EV-A71 and CV-A16 often circulated alternatively or together (Mao *et al.*, 2014). In Beijing, CV-A16 were

responsible for a HFMD outbreak in 2007, then EV-A71 became the predominant causative agent in 2008 and 2009 (Zhu *et al.*, 2013). In Guangzhou, EV-A71 was the predominant agent for HFMD in 2008 and 2010, while CV-A16 was the main agent in 2009 (Zou *et al.*, 2012).

The clinical symptoms of HFMD caused by EV-A71 and CV-A16 are very similar, but EV-A71 infection can potentially cause more severe and fatal infections in children less than 5 years old (reviewed in Ooi *et al.*, 2010, Solomon *et al.*, 2010). However, severe and fatal CV-A16 cases also have been reported in the United States (Wright *et al.*, 1963), France (Legay *et al.*, 2007), Japan (Goto *et al.*, 2009), China (Xu *et al.*, 2012) and Taiwan (Wang *et al.*, 2004b). Rhombencephalitis associated with HFMD, which is a combination of brainstem encephalitis and cerebellitis was diagnosed in a 23-month-old infant with CV-A16 infection (Goto *et al.*, 2009). Of the 92 HFMD patients with nervous system damage in Shenyang, China, 19 were infected with CV-A16; two patients had brainstem encephalitis and one had acute flaccid paralysis (Xu *et al.*, 2012). Recently, a case of sudden unexpected death in infancy attributable to CV-A16 infection was reported in Denmark (Astrup *et al.*, 2016). The 3 and ½ months old infant displayed no symptoms before the sudden death. The post mortem investigation concluded that pulmonary involvement of a systemic infection with CV-A16 was the most likely cause of death (Astrup *et al.*, 2016).

2.3.1.3 Coxsackievirus A6 and other enterovirus outbreaks

In recent years, other enteroviruses have emerged as causative agents for large HFMD outbreaks. Since 2008, unusual HFMD outbreaks caused by CV-A6 have been reported in Finland (Osterback *et al.*, 2009, Blomqvist *et al.*, 2010), Singapore (Wu *et al.*, 2010), Taiwan (Lo *et al.*, 2011, Wei *et al.*, 2011), China (Lu *et al.*, 2012, He *et al.*, 2013),

Japan (Fujimoto *et al.*, 2012), France (Mirand *et al.*, 2012), United States (Flett *et al.*, 2012), Spain (Montes *et al.*, 2013), Thailand (Puenpa *et al.*, 2013), Malaysia (Ling *et al.*, 2014), Cuba (Fonseca *et al.*, 2014) and most recently Israel (Renert-Yuval *et al.*, 2015). In countries such as Cuba, Thailand and China, CV-A6 has been replaced CV-A16 as the second most common agent after EV-A71 for HFMD epidemics (Fonseca *et al.*, 2014, Puenpa *et al.*, 2013). In many of these outbreaks, more severe skin manifestations were observed (Kobayashi *et al.*, 2013, Puenpa *et al.*, 2013). Immunocompetent adults with CV-A6-induced HFMD have also been reported (Lott *et al.*, 2013, Shea *et al.*, 2013, Stewart *et al.*, 2013, Downing *et al.*, 2014).

Co-circulation of CV-A6 and CV-A10 has been increasingly associated with HFMD outbreaks in China (2008-2012), Finland (2008) and France (2010) (He *et al.*, 2013, Blomqvist *et al.*, 2010, Mirand *et al.*, 2012, Lu *et al.*, 2012). In addition, co-circulation of CV-A10 and CV-A5 has also been reported in Thailand (Linsuwanon *et al.*, 2014). Other enterovirus serotypes such as CV-A2, CV-A4, CV-A5, CV-B5, echovirus 4 and echovirus 30 were identified in Taiwan (Wei *et al.*, 2011). Lu *et al.* (2012) identified 16 enterovirus serotypes that caused HFMD outbreaks in China in 2009-2011, in addition to the common causative agents of EV-A71, CV-A16, CV-A6 and CV-A10.

2.3.2 Molecular epidemiology of enteroviruses

2.3.2.1 Molecular epidemiology of enterovirus A71

EV-A71 is classified into three genotypes, A, B (B1-B5) and C (C1-C5), based on the first phylogenetic analysis of structural VP1 gene, with nucleotide sequence divergence of 16-20% between genotypes and of ≤12% between subgenotypes (Brown *et al.*, 1999). Genotype A is represented by the prototype EV-A71 strain BrCr (GenBank accession

number: U22521), which was first isolated from an infant with encephalitis in California in 1969 (Schmidt *et al.*, 1974). No circulation of genotype A has been detected thereafter but in 2008, five EV-A71 isolates with 97.4% sequence identity were isolated in Anhui province of China (Yu *et al.*, 2010). Genotype B is predominant in Malaysia and Singapore (reviewed in Solomon *et al.*, 2010). Subgenotype B1 was predominant in the United States and Australia in 1980s, whilst subgenotype B2 was circulating in the United States in 1981-1987 (Brown *et al.*, 1999). EV-A71 subgenotypes B3 and B4 have circulated in Singapore, Malaysia and Japan since 1997 (Cardosa *et al.*, 2003, Podin *et al.*, 2006), whereas subgenotypes B5 was circulating in Malaysia and Singapore in 2000 (Chan *et al.*, 2012), Japan and Taiwan in 2003 (Huang *et al.*, 2009), Brunei in 2006 (AbuBakar *et al.*, 2009, Zaini and McMinn, 2013) and Thailand in 2008 (Linsuwanon *et al.*, 2014). Genotype C has been predominant in east Asia, especially in Taiwan, China and Vietnam (reviewed in Solomon *et al.*, 2010). Subgenotype C1 replaced genotype B as the predominant genotype in the United States and Europe from 1987 (Brown *et al.*, 1999, McMinn, 2012). Subgenotype C2 emerged in the United States and Australia from 1995 to 1998 (Brown *et al.*, 1999) and subgenotype C3 was reported in Korea in 2003 (Cardosa *et al.*, 2003). Subgenotype C4 has emerged as the predominant circulating subgenotype in China since 2000, and has been reported in Taiwan, Japan, Thailand and Vietnam (Zhang *et al.*, 2010b, Lin *et al.*, 2006, Tu *et al.*, 2007, Yip *et al.*, 2013). Subgenotype C5 was reported in Vietnam in 2005 and Taiwan in 2006-2007 (Tu *et al.*, 2007, Huang *et al.*, 2008).

In Malaysia, only subgenotypes B3, B4, B5, C1 and C2 have been reported (Chan *et al.*, 2012). In mid-1997, a large HFMD outbreak with fatalities was reported. EV-A71 subgenotype B3 was the predominant genotype in that outbreak and was co-circulating with other subgenotypes B4, C1 and C2. In the 2000 HFMD outbreak, subgenotypes C1 and B4 were found. Since 2005, subgenotype B5 has been predominantly circulating in

both Peninsular Malaysia and Sarawak (Cardosa *et al.*, 2003, Chua *et al.*, 2007, Chan *et al.*, 2012, Solomon *et al.*, 2010).

2.3.2.2 Molecular epidemiology of coxsackievirus A16

CV-A16 is classified into two genotypes, A and B, with genotype B further divided into subgenotypes B1a, B1b, B1c, B2a, B2b and B2c. Based on VP1 nucleotide sequence analysis, the nucleotide sequence divergence of CV-A16 was 27.5-30.2% between genotypes and 11.8% between subgenotypes B1 and B2 (Zhang *et al.*, 2010a). Genotype A is represented by the prototype CV-A16 strain G10 (GenBank accession number: U05876). Subgenotypes B1a and B1b were predominant in Australia and China from 1999 to 2006 and 1999 to 2008, respectively (Zhou *et al.*, 2011, Zhang *et al.*, 2010a). These were renamed as subgenotype B2a and B2b based on the chronological year of isolation (Zong *et al.*, 2011). Subgenotype B2 was predominant in Malaysia from 1981 to 2000 (Chan *et al.*, 2012).

In Malaysia, only subgenotypes B1, B2a and B2c have been reported (Chan *et al.*, 2012). The CV-A16 isolates in Sarawak from 1998 and 2000 belonged to subgenotype B1, and were subsequently replaced by subgenotypes B2a and B2c. Subgenotype B2a was dominant in 1997-2003, 2005 and 2007, whereas subgenotype B2c only emerged after 2005. In 2012/2013, subgenotype B2b was reported in Seri Kembangan (Ling *et al.*, 2014).

2.3.2.3 Molecular epidemiology of coxsackievirus A6

Classification of CV-A6 into genotypes and subgenotypes has not yet been standardized. Lu and his colleagues identified distinct geographic clusters of CV-A6 (Lu *et al.*, 2012), while other studies distinguish CV-A6 genotypes with cut-off values of ≥15% in the VP1 gene (He *et al.*, 2013).

2.4 Laboratory diagnosis

During a HFMD outbreak, rapid laboratory diagnosis is critical to identify the causative agents and prompt public health to control the spread of virus and minimize the risk of fatality.

2.4.1 Virus isolation and immunofluorescence assay

The gold standard laboratory diagnosis of enteroviruses is by virus isolation with subsequent confirmation using specific monoclonal antibodies by indirect immunofluorescence assay. Clinical specimens such as throat swabs, ulcer swabs, vesicle swabs, cerebrospinal fluid, rectal swabs, stool and brain tissues are suitable for virus isolation (reviewed in Chan *et al*., 2011). Mammalian cell cultures such as Vero (African green monkey kidney) cells, human rhabdomyosarcoma (RD) cells, MRC-5 (human foetal lung fibroblast) cells, and Vero cells are used for culture and isolation of enteroviruses (Ho *et al.*, 1999, Wang *et al.*, 2000). Cytopathic effects (CPE) can be observed within a few days under optimal conditions. However, a presumptive diagnosis may require more than two weeks when samples contain mixture of viruses (reviewed in Muir *et al.*, 1998). Additionally, the yield of enteroviruses from clinical specimens may be low, as some enteroviruses, particularly the coxsackievirus A group,

do not readily grow in cell culture (Lipson *et al.*, 1988). Furthermore, type and quality of the specimens, the timing of specimen collection as well as the adequacy of specimen storage before laboratory processing greatly affect the sensitivity of the tests (reviewed in Muir *et al.*, 1998).

Indirect immunofluorescence assay is used for virus identification by the use of specific monoclonal antibodies. In the diagnostic virology laboratory of University Malaya Medical Centre (UMMC), enterovirus-infected cells are immunostained with Light Diagnostics Pan-Enterovirus Blend (Millipore, USA) and the antigen-antibody complex is detected with a capture FITC-labeled antibody conjugate. However, the Pan-Enterovirus Blend of anti-EV-A71 monoclonal antibodies was reported to cross-react with CV-A16 (Yan *et al.*, 2001). Overall, these approaches are time-consuming, labour intensive and insensitive.

2.4.2 Neutralization assay

Neutralization test is used to detect specific antibodies that inhibit viral-induced CPE (reviewed in Muir *et al.*, 1998). The result is considered positive when a fourfold increase in neutralizing antibody titers against EV-A71 is observed in paired sera collected from patients during acute and convalescent phases (Shindarov *et al.*, 1979). However, the neutralization test is not widely used for diagnosis purposes as it is difficult to perform, labor intensive, time-consuming (6-8 days), requires the use of infectious virus in a biosafety level II laboratory, and requires paired patient sera to confirm seroconversion.

2.4.3 Enzyme-linked immunosorbent assay

A serological test such as ELISA is an alternative diagnostic method as the results can be obtained in 2-3 hours and most diagnostic laboratories will have access to the equipment, and IgM can be detected early in EV-A71 infection (Zhao *et al.*, 2011). However, cross-reaction between enteroviruses is an important issue for specificity as human enteroviruses shared high protein homology (Mao *et al.*, 2014). For example, EV-A71 is genetically closely related with CV-A16, with both sharing relative high 77% nucleotide and 89% amino acid similarities (Brown *et al.*, 1999). Commercial IgM-capture ELISA assays are now available for EV-A71 and CV-A16 diagnosis (Yu *et al.*, 2012).

2.4.4 Molecular diagnosis

Molecular diagnosis methods such as reverse transcription polymerase chain reaction (RT-PCR) are far more sensitive and quicker, and are the new "gold standard" for enterovirus detection (Hamilton *et al.*, 1999, Robinson *et al.*, 2002). Highly conserved 5' UTR is frequently used for enterovirus typing, whereas VP1 is mainly used for genotyping (reviewed in Chan *et al.*, 2011). 5' UTR is not suitable for genotyping as this region is a hot spot of recombination in enteroviruses (van der Sanden *et al.*, 2011, Santti *et al.*, 1999). Most of the phylogenetic analyses are performed based on the VP1 gene as it shows a high degree of genetic diversity and no homologous recombination has been reported (Oberste *et al.*, 1999). However molecular diagnosis may not be widely available throughout developing countries where EV-A71 is more common, as it requires specialized equipment and well-trained personnel.

2.5 Potential treatment and vaccines

Currently there are no effective antivirals and vaccines against EV-A71 and other enteroviruses (Tan *et al.*, 2014). Treatment is generally not required for HFMD. Occasionally, symptomatic treatment is required. In more severe infection, intravenous immunoglobulin (IVIg) has been used as treatment. IVIg is the intravenous injection of polyvalent IgG antibodies purified from collectively pooled plasma from thousands of healthy donors, which functions as a treatment in providing protection against viral infection (Jolles *et al.*, 2005). In Taiwan and Malaysia, IVIg has been used on HFMD patients with CNS complications (particularly those with encephalitis and acute flaccid paralysis) to reduce mortality rate (Ooi *et al.*, 2009, Wang *et al.*, 2006). Among children with EV-A71 in Sarawak, 95% of the children with severe central nervous complications survived after IVIg treatment (Ooi *et al.*, 2009). Infection biomarkers such as IFN-γ, interleukin-6 (IL-6), IL-8, IL-10 and IL-13 levels were significantly decreased in plasma of patients with PE after IVIg administration, while decreasing of plasma levels of IL-6 and IL-8 were observed in patients with autonomic nervous system dysfunction after administration of IVIg (Wang *et al.*, 2006).

Presently, at least 58 natural products such as flavonoids, polyphenols, terpenoids, steroids and alkaloids have been tested for anti-EV-A71 effect. Most of these natural products are derived from territorial plants, while the remaining five are from marine sources (reviewed Wang *et al.*, 2015a). Further investigations will be required to explore the potential of these natural antiviral compounds as drug candidate for EV-A71 and other enteroviruses.

A number of potential antiviral drugs with significant antiviral activities against enterovirus infection have been discovered. Ribavirin is a conventional nucleoside analogue that exhibited remarkably broad spectrum antiviral activity against

picornaviruses (Kirsi *et al.*, 1983, Kishimoto *et al.*, 1988). Ribavirin demonstrated protective effect by reducing EV-A71 replication *in vitro* and *in vivo* (Li *et al.*, 2008). Pleconaril has broad spectrum antiviral activity against enteroviruses *in vitro* and *in vivo* (Pevear *et al.*, 1999), but failed to inhibit the CPE induced by EV-A71 (Chen *et al.*, 2008). Other antiviral compounds with anti-EV-A71 activity include lactoferrin, pyridyl imidazolidinone, BTA39/BTA188, amantadine, quinacrine, siRNA/ShRNA, rupintrivir, fisetin, rutin, DIDS, metrifudil, GW5074, 17-AAG and so forth (reviewed in Tan *et al.* 2014).

Several EV-A71 and CV-A16 vaccine candidates have been investigated in animal models, such as recombinant viral proteins (Ch'ng *et al.*, 2011, Wang *et al.*, 2013), virus-like particles and DNA vaccines (Lin *et al.*, 2012, Tung *et al.*, 2007), peptide vaccines (Foo *et al.*, 2007a, Liu *et al.*, 2010), live attenuated vaccines (Chiu *et al.*, 2006, Arita *et al.*, 2007) and formalin-inactivated whole virus vaccines (Dong *et al.*, 2011, Bek *et al.*, 2011, Ong *et al.*, 2010). However in human clinical trials, only inactivated EV-A71 vaccines have been evaluated (Zhao *et al.*, 2013). To date, five EV-A71 vaccine candidates have been evaluated in China, Singapore and Taiwan. Inactivated EV-A71 vaccines by National Health Research institutes (NHRI), Taiwan and Inviragen of Singapore have completed their Phase I clinical trials, whereas Vigoo, Sinovac and Chinese Academy of Medical Sciences from China have completed their Phase III clinical trials in more than 30,000 infants and children, and are currently waiting for approval from the appropriate authorities (reviewed in Liang *et al.*, 2013, Liang and Wang, 2014, Ng *et al.*, 2015). All three vaccine candidates were reported to have good safety and > 90% vaccine efficacy for EV-A71-associated HFMD in Phase III clinical trials (reviewed in Li *et al.*, 2015a).

Despite the fact that Phase III clinical trials reported good efficacy against EV-A71, the effectiveness of vaccines containing a single subgenotype when deployed worldwide against multiple different genotypes is unknown. To understand the cross-neutralizing immunity, 119 sera collected from infants and children aged 6 months to 11 years in two clinical trials of EV-A71 subgenotype C4 vaccines were used to detect neutralizing antibody against the worldwide prominent epidemic EV-A71 strains. The results revealed that the antibodies of vaccinated children have broad cross-neutralizing activity against EV-A71 subgenotypes B4, B5, C2, C4 and C5 (Mao *et al.*, 2013). Similar results were observed by Liu *et al.* (2015), where 160 sera collected from vaccinated children aged 6 to 71 months showed remarkable cross-neutralizing activity against nine EV-A71 strains (A, B3, B4, B5, C1, C2, C3, C4 and C5). Overall, these studies indicated that inactivated EV-A71 vaccines composed of a single genotype strain were capable of inducing adequate protective immunity against EV-A71 infection by different genotypes.

2.6 Immune responses to enterovirus A71 infection

2.6.1 Immune responses in animal models

Appropriate animal models are required for the understanding of EV-A71 pathogenesis and immune responses to develop effective antivirals and vaccines. Non-human primates such as cynomolgus and rhesus monkeys are susceptible to EV-A71 infection (Hashimoto *et al.*, 1978, Hashimoto and Hagiwara, 1982, Chumakov *et al.*, 1979). Although non-human primate models mimic human disease closely, they have not been used extensively due to financial and ethical constraints (reviewed in McMinn, 2012). Murine models such as BALB/c and ICR mice are frequently used for studying the pathogenesis and immune responses related to EV-A71 infection. Neonatal mice are

susceptible to EV-A71 clinical isolates (Yu *et al.*, 2000), while mice aged more than 2 weeks are generally resistant to EV-A71 regardless of the route of infection (reviewed in Wang and Yu, 2014), suggesting that mice show age-dependent susceptibility to EV-A71 infection (Chua *et al.*, 2008, Fujii *et al.*, 2013). Mouse-adapted EV-A71 strains are required for infection of mice, hence the murine model is not an appropriate model to evaluate and characterize the virulence of clinical isolates (Chen *et al.*, 2004). However it can be used to understand the protective immunity against EV-A71 infection in mice (Wu *et al.*, 2007). Type I IFNs are produced, which activate several antiviral effectors to provide protection against viral infection (Takaoka and Yanai, 2006). Pretreatment of mice with the potent IFN inducer polyriboinosinic: polyribocytidylic acid (poly (I:C)) was shown to improve the survival rates and decrease tissue viral titres after EV-A71 challenge (Liu *et al.*, 2005). Early administration of recombinant mouse IFN-αA protected mice against lethal EV-A71 infection, suggesting that type I IFNs play an important role in exerting direct protective effect on EV-A71 (Liu *et al.*, 2005).

IL-6 is a pleiotropic cytokine typically induced during pathogen stimulation as part of innate inflammatory responses, and it functions as the main inducer of the acute phase response, T cells and B cells stimulation (Kanda *et al.*, 1996). Khong *et al.* (2011) discovered sustained high levels of IL-6 led to severe tissue damage and death in a neonate mouse model. Administration of anti-IL-6 neutralizing antibodies increased the survival rates and clinical scores, and subsequently protected the mice by reduced tissue destruction, absence of splenic atrophy, increased immune cell activation and marked elevated systemic levels of IL-10 (Khong *et al.*, 2011). The protective effect of anti-IL-6 neutralizing antibodies was independent of viral load. This finding suggests that anti-IL-6 antibody treatment is a potential therapeutic approach to protect against severe EV-A71 complication.

Shen and colleagues found that EV-A71 infection significantly enhanced interferon-gamma-inducible protein 10 (IP-10) expressions in the serum and brains of infected mice. Moreover, IP-10 deficiency significantly reduced monokine induced by IFN-γ levels in serum, and IFN-γ levels and $CD8^+$ T cell counts in the mice brains. Absence of IP-10 also increased the mortality rates of infected mice and reduced virus clearance in several tissues (Shen *et al.*, 2013).

Neutralizing antibodies are produced in animals immunized with EV-A71 (see section 2.6.3.1). These antibodies can efficiently bind and neutralize the virus, hence neutralizing antibodies play a critical role in protection against EV-A71 infection. Passive administration of neutralizing antibodies protects animals against lethal challenge (Foo *et al.*, 2007a, Chang *et al.*, 2010, Lim *et al.*, 2012).

The virus load, B cells, $CD4^+$ T cells and $CD8^+$ T cells in brains and antibody titer in sera were increased when the mice succumbed to death, similar to those observed in fatal EV-A71-infected patients (Lin *et al.*, 2009b). The study showed that lymphocytes and antibody responses protect mice from EV-A71 infection and reduced the disease severity, mortality and tissue viral loads. Wang *et al.* (2012) further demonstrated that $CD4^+$ T cell-deficient mice were resistant to EV-A71 infection, although B cell-deficient mice were highly susceptible to viral infection. Infected $CD4^+$ T cell-deficient mice produced EV-A71-specific neutralizing antibodies, which also protected B cell-deficient mice from viral infection by decreasing tissue viral loads (Wang *et al.*, 2012). This study concluded that B cells rather than $CD4^+$ T cells play a critical role in mediating protective effects against EV-A71 infection. However the results are contradicted by studies in humans, where cellular but not humoral immunity has been correlated with clinical outcome and disease progression of EV-A71 (Yang *et al.*, 2001, Chang *et al.*, 2006).

2.6.2 Immune responses in humans

Cardiopulmonary failure or PE occurs during the initial stages of EV-A71 CNS involvement (Chang *et al.*, 1999). High levels of the proinflammatory cytokine IL-6 have been detected in the early stages of CNS infection (Lin *et al.*, 2002, Lin *et al.*, 2003, Wang *et al.*, 2007), suggesting that the combination of CNS and systemic inflammatory response may play an important role in the development of EV-A71-related cardiopulmonary collapse (Lin *et al.*, 2003). The secretion of IFN-γ was found to enhance IL-6 transcription and protein expression in monocytes (Biondillo *et al.*, 1994), suggesting that IFN-γ may play an important role in modulating the secretion of other cytokines during inflammatory processes. Significant elevation of IFN-γ in serum and cerebrospinal fluid samples from EV-A71 patients with PE and autonomic nervous system dysregulation has been reported (Wang *et al.*, 2003, Wang *et al.*, 2007). Other cytokines such as IL-1β, IL-6, IL-10, IL-13 and tumor necrosis factor-α were also reported to be high in PE patients (Lin *et al.*, 2002, Lin *et al.*, 2003, Wang *et al.*, 2007).

Maternal antibodies are important to protect neonates and young infants from infectious diseases during the time of maturation of their immune system. In humans, maternal antibodies are transferred before birth transplacentally. A study conducted in Taiwan demonstrated that EV-A71 antibody titers in seropositive neonates were strongly associated with the EV-A71 antibody titers in their mothers, however the maternal neutralizing antibodies declined to almost undetectable levels by 6 months of age (Luo *et al.*, 2009). Furthermore, younger children (<6 months of age) were more likely to develop asymptomatic EV-A71 infections (Lee *et al.*, 2012, Chang *et al.*, 2002).

Neutralizing antibodies bind and neutralize virus efficiently, thus preventing further progression of disease. Hence neutralizing antibodies play an important role in immunoprotection from viral infection. Humoral immune response was elicited when

clinical symptoms appeared and 80% of HFMD patients became positive for neutralizing antibodies against EV-A71 one day after the onset of illness (Yang *et al.*, 2011). High levels of neutralizing antibodies were reached within 3-6 days after disease onset (Wang *et al.*, 2015b). Notably, the antibody titers in the patients with mild HFMD were not significantly different from those of patients with CNS involvement or PE, suggesting that neutralizing antibody response was not correlated with disease severity (Yang *et al.*, 2011, Chang *et al.*, 2006). Conversely, Xie *et al.* (2010) revealed that B cells and IgG levels were significantly elevated in severe cases in the acute stages of EV-A71 infection, before both recovered to normal levels during the convalescent phase, with an increase in EV-A71-specific neutralizing antibody titres.

Virus-specific antibody-secreting B cells (ASCs) in adults are derived from pre-existing memory B cell subsets that have undergone activation, differentiation and proliferation upon repeated viral exposure; however the percentage of memory B cell subsets are lower in children (Li *et al.*, 2012, Morbach *et al.*, 2010). An EV-A71-specific ASC response was detected as early as the first day and became predominant on days 4-7 after illness onset. EV-A71-specific ASCs in children aged ≥3 years produced IgG predominantly, whereas EV-A71-specific ASCs produced IgM predominantly in younger children (Huang *et al.*, 2015). EV-A71 ASC responses also correlated with throat viral load, fever duration and serological genotype-specific neutralizing titer in EV-A71 infected children.

T cell immunity plays an important role in protection against EV-A71 infection. Some studies have demonstrated that cellular but not humoral immunity is correlated with disease progression and clinical outcome of EV-A71 (Chang *et al.*, 2006, Yang *et al.*, 2001). Significant increase of Th1 and proinflammatory cytokines was observed when PBMCs were stimulated with EV-A71. PBMCs collected from patients with PE had

significantly lower IFN-γ, IL-1β, IL-6, TNF-α and macrophage inflammatory protein-1α in response to inactivated EV-A71 stimulation (Chang *et al.*, 2006). Children who died of encephalitis and PE also demonstrated low expression of IFN-γ, IL-4 and CD40-L (Yang *et al.*, 2001). This suggests an inverse correlation between antigenic-specific T cell responses and disease severity (Chang *et al.*, 2006).

Host genetic factors may play an important role in EV-A71 disease severity. Cytokine T lymphocyte antigen-4 (CTLA-4) polymorphism is an important negative regulator for T cell cytotoxicity. Polymorphism of CTLA-4 exon 1 at position 49 with A or G genotype was reported to be associated with autoimmune diseases (Marron *et al.*, 1997). In one Taiwan study, children with EV-A71 meningoencephalitis had higher frequency of the G/G allele in the CTLA-4 polymorphism at position 49 of exon 1, suggesting that altered cellular immunity associated with CTLA-4 polymorphism may correlate with disease severity (Yang *et al.*, 2001). Another recent study showed that chemotactic chemokine ligand 5 polymorphism may contribute to severe EV-A71 infection (Li *et al.*, 2015b).

Patients with PE had lower circulating $CD4^+$ T cells, $CD8^+$ T cells and NK cells (Wang *et al.*, 2003). Similarly, circulation of total $CD3^+$ T cells, $CD4^+$ T cells, $CD8^+$ T cells and NK cells was decreased in patients with autonomic nervous system dysregulation and was lowest in PE patients (Fu *et al.*, 2009). A study performed by Li *et al.* (2013) revealed that HFMD patients have an imbalance in peripheral T lymphocyte subsets. Th1 cells, Tc1 cells, Th1/Th2 ratio and IFN-γ levels were significantly higher in mild and severe patients, while Th17 cells, IL-17A levels and Th17/Treg cell ratio were highest in severe HFMD patients. This suggests that the imbalance of Th1/Th2 and Th17/Treg is involved in the pathogenesis of EV-A71 infection, and could serve as a potential biomarker for severe HFMD (Li *et al.*, 2014).

T follicular helper cells (TFH) are a subset of specialized $CD4^+$ T cells, localized to B cell follicles of the germinal centers to regulate humoral immune responses (Ma *et al.*, 2009). In the acute stage of EV-A71 infection, TFH with inducible costimulator ($ICOS^{high}$) and programmed death-1 ($PD\text{-}1^{high}$) expression were significantly increased in patients and positively correlated with levels of IL-21, IL-6 and neutralizing antibodies against EV-A71, suggesting that TFH cells might play a critical role in modulating the humoral response during pathogenesis of EV-A71 infection (Wu *et al.*, 2014).

2.6.3 Epitopes and neutralizing antibodies

2.6.3.1 Enterovirus A71 neutralizing antibodies produced by animals

Passive transfer of specific antibodies reduces the severity of viral infections, as shown in Japanese encephalitis infection (Kimura-Kuroda and Yasui, 1988), varicella infection (Huang *et al.*, 2001) and coxsackievirus infection (Geller and Condie, 1995). In EV-A71, passive transfer of mouse anti-SP70 sera (Foo *et al.*, 2007a), mAb 4E8 (Chang *et al.*, 2010) and mAb 51 (Lim *et al.*, 2012) demonstrated up to 100% *in vivo* passive protection against lethal EV-A71 infection. Hence mAbs with high specificity, avidity and neutralizing activity are promising candidates for treatment of EV-A71 infection.

SP70 (amino acids 208-222) in VP1 region was identified as a neutralizing epitope (Foo *et al.*, 2007b). Neutralizing anti-SP70 antibodies were able to confer 80% *in vivo* protection against a lethal dose of 1000 50% tissue culture infective dose ($TCID_{50}$) of EV-A71 (Foo *et al.*, 2007a). Another study conducted in China also demonstrated that monoclonal antibody (mAb; clone 22A12) generated by SP70-immunized mice and mAb 2G8 generated from EV-71 strain AH/08/06-immunized mice elicited potent

neutralizing activity against EV-A71 in an *in vitro* neutralization assay (Li *et al.*, 2009, Deng *et al.*, 2015). Moreover, mAb 51 derived from mice immunized with inactivated EV-A71 strain NUH0083/SIN/08 further identified KQEKD (amino acids 215-219, Table 2.1) located within SP70, with neutralizing activity against homologous and heterologous EV-A71 (Lim *et al.*, 2012).

Kiener *et al.* (2012) demonstrated that mAb 7C7 derived from mice immunized with an inactivated EV-A71 B5 strain was mapped to EDSHP (amino acids 142-146, Table 2.1) in the EF loop of VP2, within the VP2-28 previously reported as a cross-neutralization epitope. Mutation analysis showed that the aspartic acid to asparagine mutation for EV-A71 genotype A (BrCr prototype strain) at position 143 of VP2 did not interfere with antibody recognition, however a serine to threonine mutation for the EV-A71 subgenotype C4 Fuyang-08 strain at position 144 of VP2 abolished the antigenicity of VP2 protein (Kiener *et al.*, 2012).

Although VP4 capsid proteins were located internally, Zhao *et al.* (2013) proven that the immunization of the N-terminus of VP4 was able to elicit cross-protective antibody responses. Immunization of chimeric virus-like particles (HBc-N149-VP4N20) in a mouse model was able to produce VP4N20 specific antibodies and neutralize EV-A71. Furthermore, passive transfer of mice anti-chimeric VLP sera was able to protect 90% of neonatal mice against EV-A71 infection (Zhao *et al.*, 2013).

2.6.3.2 B-cell epitopes recognized by immunized animal antisera

VP1 protein is known to be the most immunogenic viral protein. Sera from rabbits immunized with inactivated EV-A71 BJ08 strain (subgenotype C4) identified four rabbit anti-EV-A71 IgG epitopes which mapped to VP1 (Gao *et al.*, 2012). Anti-rabbit

serum raised following injection of the N-terminal region of VP1 protein (1-100) in a Newcastle disease virus backbone elicited strong immune responses against the EV-A71 VP1 protein (Sivasamugham *et al.*, 2006). Mice antisera raised against 95 overlapping synthetic peptides spanning the VP1 capsid protein of EV-A71 strain 41 (subgenotype B4) were used for characterization of neutralization epitopes. Two synthetic peptides, SP55 and SP70 (Table 2.2) were capable of inducing neutralizing antibodies against EV-A71 in an *in vitro* microneutralization assay (Foo *et al.*, 2007b). The antisera from SP70-immunized mice shown better neutralizing activity compared to the SP55-immunized mice antisera. Moreover, passive transfer of mouse anti-SP70 antisera was able to protect 80% of sucking Balb/c mice against lethal EV-A71 infectivity (Foo *et al.*, 2007a).

Sera generated from mice and rabbits immunized with formalin-inactivated EV-A71 E59 strains (subgenotype B4) vaccine identified two epitopes (located at VP1) and four epitopes (one mapped to VP1 and the remaining mapped to VP2), respectively (Liu *et al.*, 2011). VP2-28 and VP1-43 (Table 2.2) were recognized as a cross-neutralization epitope and a genotype-specific neutralization epitope, respectively. VP2-28 was only recognized by neutralizing antisera from immunized rabbit but not by antisera from immunized mice and rats.

2.6.3.3 B-cell epitopes recognized by human antibodies

A screening study based on ELISA revealed that human sera with high titres of neutralizing antibodies (1:640) against EV-A71 were found to react strongly with the N-terminal half of VP1 protein (Tan and Cardosa, 2007). Capsid proteins VP1, VP2 and VP3 are exposed on the virion surface, and are responsible for host-receptor binding and immune responses (Brown and Pallansch, 1995). Nine enterovirus IgG linear epitopes

were identified with sera from patients with aseptic meningitis, where most reactive E1, E2 and E4 peptides were derived from the conserved region of VP1 N-terminal (Table 2.3, Cello *et al.*, 1993). The study also demonstrated that peptides from structural capsid proteins VP2, VP3 and VP4, and non-structural protein 3D RNA polymerase show no or poor reactivity. However, this study was unable to identify IgM linear epitopes by indirect IgM assays due to the high background problems (Cello *et al.*, 1993).

Gao and his colleagues (2012) synthesized 256 partial overlapping peptides covering external capsid proteins VP1, VP2 and VP3 to identify IgM and IgG epitopes in EV-A71 infected children at acute or recovery phase. Ten human anti-EV-A71 IgM epitopes were identified in the acute phase sera, mainly mapped at VP2 and VP3 (Table 2.3, Gao *et al.*, 2012). However, only one human IgG epitope in VP1 was identified in the recovery phase sera.

2.6.3.4 $CD4^+$ T-cell epitopes

T cells recognize linear epitopes derived from peptides that are processed by antigen presenting cells (APCs). Proteolytic enzymes in APCs cleave the antigenic proteins into peptide fragments and only 2% with the right amino acid side chains are presented on the surface of APCs and bind to major histocompatibility complex (MHC). Therefore, the binding affinity of T-cell epitopes to MHC molecules is one of the important determinants of immunogenicity (Weber *et al.*, 2009).

Three synthetic peptides (SP1, SP2 and SP3) located at the VP1 protein were predicted to bind more than 25 HLA-DR alleles by the ProPred algorithm. These peptides induced $CD4^+$ T-cell proliferative responses from EV-A71-positive volunteers with different HLA-DR alleles (Foo *et al.*, 2008). Significant levels of IL-2 and IFN-γ were produced,

indicating that $CD4^+$ T cells undergo Th-1-subtype differentiation. Among the three peptides tested, SP2 (Table 2.4) was identified as the main immunodominant MHC class II-restricted $CD4^+$ T-cell epitope (Foo *et al.*, 2008).

Subsequently, 37 epitopes were predicted by EpiMatrix, 15 were identified as $CD4^+$ T-cell epitopes, and 3 of them (A3, A8 and A14) were dominant EV-A71 epitopes (Table 2.4, Wei *et al.*, 2012). Of the three dominant epitopes, A3 (mapped to VP2) and A8 (mapped to VP3) are conserved amongst EV-A71 isolates. These distributions of $CD4^+$ T-cell epitopes are consistent with the study by Cello *et al.* (1996). Moreover, A3 is identified to be highly conserved among human enteroviruses (Table 2.4).

A comprehensive screening study based on four EV-A71 structural proteins was performed to identify $CD4^+$ T-cell epitopes in a non-HLA-restricted manner. A total of 31 epitopes were identified, with VP2 antigens dominating the T cell responses with a broad distribution of immunogenic peptides (n=13), followed by VP1 (n=9), VP3 (n=7) and VP4 (n=2) (Table 2.4, Tan *et al.*, 2013). The study also demonstrated that T cells responsive to VP2 were mainly $CD4^+$ T cells. Furthermore, identification of the VP2-24 (amino acids 176-193) epitope is consistent with the highly conserved dominant A3 epitopes reported in the study by Wei *et al.* (2012).

Another comprehensive study based on the VP1 structural protein and RdRp non-structural protein (also known as 3D protein) was conducted with *ex vivo* IFN-γ ELISPOT analysis. CD4-dependent RdRp-specific responses were observed in most of the EV-A71-infected children, at rates of 82% for individuals in the acute phase, 84% for those in the convalescent phase, and 100% for those with past exposure (Table 2.4, Dang *et al.*, 2014). The VP1-33 and VP1-19 epitopes were also found to be consistent with previously reported T-cell epitopes (Foo *et al.*, 2008).

Table 2.1: Summary of reported EV-A71 neutralizing antibodies

Neutralizing antibody	EV-A71 genotype	Region	Epitope type	Amino acid position	Epitope sequence	Reference
mAb 1D9	Strain 3437-SIN-06 (GU222654), subgenotype C5	VP1	Linear	3-8	RVADVI	Man-Li *et al.*, 2012
mAb 4	Strain NUH0083/SIN/08 (FJ461781), subgenotype B5	VP1	Linear	12-19	IGDSVSRA	Lim *et al.*, 2013
mAb MA28-7	Strain 1095, subgenotype C2	VP1	Conformational	145	Glycine (VP1-145)	Lee *et al.*, 2013
anti-SP70 antibodies	Immunized with synthetic peptide SP70 derived from strain 5865/SIN/000009 (AF316321), subgenotype B4	VP1	Linear	208-222	YPTFGEHKQEKDLEYC	Foo *et al.*, 2007a
mAb clone 22A12	Immunized with synthetic peptide SP70 derived from strain 5865/SIN/000009 (AF316321), subgenotype B4	VP1	Linear	208-222	YPTFGEHKQEKDLEYC	Li *et al.*, 2009
mAb clone 22A12	Strain1096/Shiga, subgenotype C2	VP1	Linear	208-222	YPTFGEHKQEKDLEYC	Shingler *et al.*, 2015
mAb 2G8	Strain AH/08/06 (HQ611148), subgenotype C4	VP1	Linear	208-222	YPTFGEHKQEKDLEYC	Deng *et al.*, 2015
mAb N1 mAb N3 mAb N4 mAb N6	Strain EV71/59, subgenotype B4	VP1	Linear	211-224	FGEHKQEKDLEYGAC	Chang *et al.*, 2011
mAb 51	Strain NUH0083/SIN/08 (FJ461781), subgenotype B5	VP1	Linear	215-219	KQEKD	Lim *et al.*, 2012
mAb H3B10 mAb K8G2	Not known	VP1	Linear	215-218	KQEK	He *et al.*, 2012

Table 2.1, continued.

Neutralizing antibody	EV-A71 genotype	Region	Epitope type	Amino acid position	Epitope sequence	Reference
mAb 4E8	Strain Hn2 (GQ994992), subgenotype C4	VP1	Linear	240-250 250-260	SSKSEYSLVI RIYMRMKHVR	Chang *et al.*, 2010
mAb D5 mAb H7 mAb C4	Immunized with EV-A71 VLPs (coexpression of P1 and 3CD proteins) derived from EV71 strain G082	VP1	Linear	Not known	VP1 protein, but not VP0 protein	Ku *et al.*, 2012
mAb 7C7	EV-A71 subgenotype B5	VP2	Linear	142-146	EDSHP	Kiener *et al.*, 2012
BB1A5	Strain52-3 (FJ600325), subgenotype C4	VP2	Linear	141-155	TEDSHPPYKQTQPGA (T141A, E142A, S144A & H145A abolish neutralizing activity)	Xu *et al.*, 2014
10D3	Strain 5865/SIN/000009 (AF316321), subgenotype B4	VP3	Conformational	59, 62, 67	P, A, E (P59L, A62D & E67D abolish neutralizing activity)	Kiener *et al.*, 2014
anti-VP4N20 antibodies	Immunized with HBc-N149-VP4N20 VLPs derived from strain BJ08, subgenotype C4	VP4	Linear	1-20	GSQVSTQRSGSSHENSNSATE	Zhao *et al.*, 2013

Table 2.2: Summary of reported B-cell epitopes recognized by immunized animal antisera

Epitope	EV-A71 genotype	Region	Amino acid position	Peptide sequence	Reference
In rabbits					
N-terminal of VP1	Strain S2/86/1 (AF376085), subgenotype B4	VP1	1-100	Not known	Sivasamugham *et al.*, 2006
VP1-14	Strain BJ08, subgenotype C4	VP1	40-51	DTGKVPALQAAE	Gao *et al.*, 2012
VP1-31		VP1	91-102	GEIDLPLEGTTN	
VP1-54		VP1	160-171	APKPDSRESPAW	
VP1-71		VP1	211-222	FGEHKQEKDLEY	
VP1-01	Strain TW/2086/98 (AF119796), genotype C	VP1	1-15	GDRVADVIESSIGDS	Liu *et al.*, 2011
VP2-27		VP2	131-145	VIGTVAGGTGTEDSH	
VP2-28		VP2	136-150	AGGTGTEDSHPPYKQ	
VP2-29		VP2	141-155	TEDSHPPYKQTQPGA	
In mice					
SP55	Strain 5865/SIN/000009 (AF316321), subgenotype B4	VP1	163-177	PESRESLAWQTATNPC	Foo *et al.*, 2007b
SP70		VP1	208-222	YPTFGEHKQEKDLEYC	
VP1-42	Strain TW/2086/98 (AF119796), genotype C	VP1	206-220	DGYPTFGEHKQEKDL	Liu *et al.*, 2011
VP1-43		VP1	211-225	FGEHKQEKDLEYGAC	

Table 2.3: Summary of reported B-cell epitopes recognized by human sera

Epitope	EV-A71 genotype	Region	Amino acid position	Peptide sequence	Reference
anti-enteroviruses IgG epitopes					
E1	Synthesized from conserved region among enteroviruses	VP1	42-55	PALTAVETGATNPL	Cello *et al.*, 1993
E2		VP1	42-50	PALTAVETG	
E3		VP1	57-75	PSDTMQTRHVKNYHSRSES	
E4		VP1	71-80	SRSESSIENF	
E5		VP1	129-139	RFDLELTFVIT	
E9		VP2	8-21	GYSDRVRSITLGNS	
E12		VP2	198-209	INLRTNNSATIV	
E14		VP3	153-163	HVIWDVGLQSS	
E17		VP4	47-58	QDPSKFTEPVKD	
anti-EV-A71 IgM epitopes					
VP1-14	Strain BJ08, subgenotype C4	VP1	40-51	DTGKVPALQAAE	Gao *et al.*, 2012
VP2-6		VP2	16-27	LTIGNSTITTQE	
VP2-21		VP2	61-72	NRFYTLDTKLWE	
VP2-40		VP2	118-129	HQGALLVAVLPE	
VP2-50		VP2	148-159	YKQTQPGADGFE	
VP3-10		VP3	28-39	FHPTPCIHIPGE	
VP3-12		VP3	34-45	IHIPGEVRNLLE	
VP3-15		VP3	43-54	LLELCQVETILE	
VP3-24		VP3	70-81	RFPVSAQAGKGE	
VP3-75		VP3	223-234	NFTMKLCKDASD	
anti-EV-A71 IgG epitopes					
N-terminal half of VP1 protein	Strain MS/7423/87 (U22522)	VP1	Not known	Not known	Tan and Cardosa, 2007
VP1-15	Strain BJ08, subgenotype C4	VP1	43-54	KVPALQAAEIGA	Gao *et al.*, 2012

Table 2.4: Summary of reported CD4+ T-cell epitopes

Epitope	EV-A71 genotype	Region	Amino acid position	Peptide sequence	Reference
Enteroviruses					
E1	Synthesized from conserved region among enteroviruses	VP1	42-55	PALTAVETGATNPL	Cello *et al.*, 1996
E2		VP1	42-50	PALTAVETG	
E3		VP1	57-75	PSDTMQTRHVKNYHSRSES	
E4		VP1	71-80	SRSESSIENF	
E7		VP1	175-184	WQTSTNPSVF	
E10		VP2	16-27	ITLGNSTITTQE	
E12		VP2	198-209	INLRTNNSATIV	
E13		VP3	12-22	QFLTSDDFQSP	
E14		VP3	153-163	HVIWDVGLQSS	
EV-A71					
SP1	Strain 5865/SIN/000009 (AF316321), subgenotype B4	VP1	66-77	IETRCVLNSHSTAET	Foo *et al.*, 2008
SP2		VP1	145-159	EVVPQLLQYMFVPPG	
SP3		VP1	247-261	LVVRIYMRMKHVRAW	
A9	Strain FY573 (HM064456)	VP1	733-747[a]	SLAWQTATNPSVFVK	Wei *et al.*, 2012
A11		VP1	833-849[a]	NQNYLFKANPNYAGNSI	
A12		VP1	899-914[a]	SRDLLVSSTTAQGCDT	
A13		VP1	933-947[a]	HYPVSFSKPSLIYVE	
VP1-11	Strain EV71/HENAN/DC/2010 (ADX87405)	VP1	75-90	TAETTLDSFFSRAGLV	Tan *et al.*, 2013
VP1-16		VP1	112-129	DITGYAQMRRKVELFTYM	
VP1-17		VP1	120-137	RRKVELFTYMRFDAEFTF	
VP1-19		VP1	137-154	FVACTPTGGVVPQLLQYM	
VP1-20		VP1	145-162	EVVPQLLQYMFVPPGAPK	
VP1-23		VP1	169-187	AWQTATNPSVFVKLSDPPA	
VP1-33		VP1	244-261	KYPLVVRIYMRMKHVRAW	
VP1-34		VP1	252-267	YMRMKHVRAWIPRPMR	
VP1-37		VP1	271-285	YLFKANPNYAGNSIK	

Table 2.4, continued.

Epitope	EV-A71 genotype	Region	Amino acid position	Peptide sequence	Reference
VP1-23	Strain EV71/HubeiChina/2009 (GU434678)	VP1	742-759[b]	PSVFVKLSDPPAQVSVPF	Dang *et al.*, 2014
VP1-22		VP1	734-751[b]	LAWQTATNPSVFVKLSDP	
VP1-25		VP1	758-775[b]	PFMSPASAYQWFYDGYPT	
VP1-30		VP1	798-815[b]	FSVRTVGSSKSKYPLVIR	
VP1-33		VP1	822-839[b]	HVRAWIPRPMRNQNYLFK	
VP1-28		VP1	782-799[b]	EKDLEYGACPNNMMGTFS	
VP1-19		VP1	710-727[b]	EVVPQLLQYMFVPPGAPK	
VP1-34		VP1	830-847[b]	PMRNQNYLFKSNPNYAGD	
A1	Strain FY573 (HM064456)	VP2	164-180[a]	NAQFHYLYRSGFCIHVQ	Wei *et al.*, 2012
A2		VP2	224-244[a]	ADGFELQHPYVLDAGISISQL	
A3		VP2	248-263[a]	PHQWINLRTNNCATII	
A4		VP2	278-292[a]	HCNFGLLVVPISPLD	
VP2-3	Strain EV71/HENAN/DC/2010 (ADX87405)	VP2	14-31	AQLTIGNSTITTQEAANI	Tan *et al.*, 2013
VP2-5		VP2	29-47	ANIIVGYGEWPSYCSDDDA	
VP2-9		VP2	62-79	RFYTLDTKLWEKSSKGWY	
VP2-10		VP2	70-86	LWEKSSKGWYWKFPDVL	
VP2-11		VP2	77-92	GWYWKFPDVLTETGVF	
VP2-12		VP2	83-100	PDVLTETGVFGQNAQFHY	
VP2-15		VP2	107-224	CIHVQCNASKFHQGALLV	
VP2-16		VP2	115-132	SKFHQGALLVAVLPEYVI	
VP2-19		VP2	139-155	TGTEDTHPPYKQTQPGA	
VP2-21		VP2	152-169	PGADGFELQHPYVLDAGI	
VP2-24		VP2	176-193	TVCPHQWINLRTNNCATI	
VP2-25		VP2	184-201	NLRTNNCATIIVPYINAL	
VP2-26		VP2	192-209	TIIVPYINALPFDSALNH	
A6	Strain FY573 (HM064456)	VP3	445-466[a]	TGSFMATGKMLIAYTPPGGPLP	Wei *et al.*, 2012
A7		VP3	479-499[a]	IWDFGLQSSVTLVIPWISNTH	
A8		VP3	533-551[a]	NTAYIIALAAAQKNFTMKL	

Table 2.4, continued.

Epitope	EV-A71 genotype	Region	Amino acid position	Peptide sequence	Reference
VP3-6	Strain EV71/HENAN/DC/2010 (ADX87405)	VP3	41-58	RNLLELCQVETILEVNNV	Tan *et al.*, 2013
VP3-7		VP3	49-66	VETILEVNNVPTNATSLM	
VP3-14		VP3	99-115	TMLGQLCGYYTQWSGSL	
VP3-17		VP3	118-135	TFMFTGSFMATGKMLIAY	
VP3-18		VP3	126-143	MATGKMLIAYTPPGGPLP	
VP3-20		VP3	142-169	LPKDRATAMLGTHVIWDF	
VP3-23		VP3	173-190	SSVTLVIPWISNTHYRAH	
VP4(18-34)	Strain EV71/HENAN/DC/2010 (ADX87405)	VP4	18-34	SATEGSTINYTTINYYK	Tan *et al.*, 2013
VP4(29-41)		VP4	29-41	INYTTINYYKDSYAATA	
A14	Strain FY573 (HM064456)	2A	1034-1048[a]	SREVEALKNYFIGSE	Wei *et al.*, 2012
A19		2B	1128-1143[a]	GLEWVSNKISKFIDWL	
A30	Strain FY573 (HM064456)	3D	1914-1929[a]	DSVYLRMAFGHLYETF	Wei *et al.*, 2012
A31		3D	1923-1940[a]	GHLYETFHANPGTITGSA	
RdRp-55	Strain EV71/HubeiChina/2009 (GU434678)	3D	2164-2181[b]	FVSTIRSVPIGRALAIPN	Dang *et al.*, 2014
RdRp-41		3D	2052-2069[b]	ELKMVAYGDDVLASYPFP	
RdRp-21		3D	1892-1909[b]	ELRSLDKIRKGKSRLIEA	
RdRp-56		3D	2172-2189[b]	PIGRALAIPNFENLRRNW	
RdRp-57		3D	2180-2193[b]	PNFENLRRNWLELF	
RdRp-20		3D	1884-1901[b]	PYSTYVKDELRSLDKIRK	
RdRp-27		3D	1940-1957[b]	AVGCNPDVFWSKLPILLP	
RdRp-19		3D	1876-1893[b]	MDKYGLDLPYSTYVKDEL	
RdRp-32		3D	1980-1997[b]	LELVLREIGYSEEAVSLI	
RdRp-33		3D	1988-2005[b]	GYSEEAVSLIEGINHTHH	
RdRp-26		3D	1932-1949[b]	NPGTVTGSAVGCNPDVFW	
RdRp-10		3D	1804-1821[b]	YVTQAALHYANQLKQLDI	
RdRp-25		3D	1924-1941[b]	HLYEVFHANPGTVTGSAV	
RdRp-12		3D	1820-1837[b]	DINTSKMSMEEACYGTEY	

[a] amino acid position based on whole EV-A71 virus strain FY573 (HM064456)

[b] amino acid position based on whole EV-A71 virus strain EV71/HubeiChina/2009 (GU434678)

CHAPTER 3

MATERIALS AND METHODS

3.1 Mammalian cell lines and viruses

3.1.1 Mammalian cell lines

Established adherent mammalian cell lines purchased from American Type Culture Collection (ATCC, USA) were used in this study. Human RD cells (ATCC CCL-136) and human embryonic kidney cells (HEK293, ATCC CRL-1573) were cultured in Dulbecco's Modified Eagle Medium (DMEM) supplemented with growth medium containing 10% heat-inactivated fetal bovine serum (FBS; Hyclone, USA), 2 mM L-glutamine (Hyclone, USA), 1X non-essential amino acids (NEAA; Hyclone, USA), 100 U/ml penicillin and 100 µg/ml streptomycin (Hyclone, USA). Growth media for HEK293 cells requires additional 1 mM sodium pyruvate (Hyclone, USA). All cell lines were maintained at 37 ℃ in the presence of 5% CO_2.

3.1.2 Viruses

3.1.2.1 Virus strains and propagation

The virus strain used in this study was EV-A71 isolate UH1/PM/1997 (GenBank accession number: AM396587), of subgenotype B4. EV-A71 isolate UH1/PM/1997 was propagated in RD cells with DMEM supplemented with 2% FBS (Hyclone, USA), 2 mM L-glutamine (Hyclone, USA), 1X NEAA (Hyclone, USA), 100 U/ml penicillin and 100 µg/ml streptomycin (Hyclone, USA). The culture supernatants were harvested and freeze-thawed when more than 70% of CPE was observed. The culture supernatants

were centrifuged at 40,000 x g for 20 minutes at 4℃ to remove cell debris. The virus supernatants were kept at -80℃ until later use.

3.1.2.2 Virus sucrose cushion purification

A volume of 32 ml of virus supernatant was carefully layered over 4 ml of sucrose-TNE buffer (30% sucrose, 50 mM Tris-HCl, 100 mM NaCl, 0.5 mM EDTA, pH7.4) in a ultracentrifuge tube. The sample was centrifuged at 125,000 x g for 4 hours at 4℃. After 4 hours, the supernatant was removed and 400 µl of TE buffer (10 mM Tris-HCl, 1 mM EDTA) was added to the pellet, followed by 30 minutes incubation on ice. The pellet was resuspended with TE buffer and kept at -80℃. The virus titers were determined by plaque assay.

3.1.2.3 Virus RNA extraction

Viral RNA was extracted from throat swabs in viral transport medium using QIAamp Viral RNA Mini Kit (Qiagen, Germany) according to the manufacturer's instructions. Briefly, 140 µl of the viral transport medium was lysed with 560 µl of buffer AVL containing carrier RNA, followed by 560 µl of absolute ethanol. The viral RNA-containing mixture was then added to the column and washed with 500 µl of buffer AW1 and buffer AW2. The viral RNA was eluted with 50 µl Ambion RNA storage solutions (Life Technologies, USA) and kept at -80℃ until later use.

3.1.2.4 Plaque assay

RD cells were seeded in a 24-well plate with 1.5 x 10^5 cells/well and incubated overnight at 37℃ in 5% CO_2. Ten-fold serially diluted virus sample was prepared in serum-free medium. The growth medium was removed and an aliquot of 100 µl of each virus dilution was inoculated onto RD cells for 1 hour at room temperature with gentle rocking. The excess inocula were removed after 1 hour of incubation and replaced with 500 µl of plaque medium (DMEM supplemented with 2% FBS and 0.9% carboxylmethyl cellulose). After 3 days of incubation, the plaque medium was removed, and the cells were fixed with 3.7% formaldehyde and subsequently stained with 0.5% crystal violet. Plaque forming units per milliliter (PFU/ml) were calculated with the following formula:

$$\text{PFU/ml} = \frac{\text{Number of plaque} \times \text{dilution factor}}{\text{Volume of inoculum (ml)}}$$

3.2 Clinical specimen processing and virus identification

3.2.1 Clinical specimens

From May 2012 to September 2013, blood and throat swabs specimens were collected from children clinically diagnosed with HFMD at the Paediatric Trauma and Emergency Department of UMMC, Kuala Lumpur. BD vacutainer blood collection tubes with lithium heparin (Becton Dickinson, USA) were used to prevent blood clotting. The throat swabs were placed in viral transport medium to maintain virus viability during transport to the laboratory. Demographic and clinical data were reviewed retrospectively from the medical notes. This study was approved by the UMMC Medical Ethics Committee (reference number: 932.17).

3.2.2 Virus identification

3.2.2.1 Virus isolation

Throat swabs in viral transport media were used for virus isolation. Specimens were inoculated into RD cell cultures in a 24-well plate. Viral cultures showing CPE were harvested and kept in -80 ℃ for further analysis.

3.2.2.2 Reverse transcription polymerase chain reaction

To detect any enterovirus, the 5' UTR was amplified with primers CoxbanS and CoxbanR (Arola *et al.*, 1995) using Access RT-PCR system (Promega, USA). The reaction mix was prepared as stated in Table 3.1. Each reaction was subjected to reverse transcription at 42 ℃ for 60 minutes and reverse transcriptase inactivation at 94 ℃ for 2 minutes, followed by 40 cycles of 94 ℃ for 30 s, 50 ℃ for 1 minute, and 68 ℃ for 2 minutes, and final extension of 68 ℃ for 7 minutes. Detection and genotyping of EV-A71, CV-A16 and CV-A6 were performed with previously published primer sets (Table 3.2) and protocols. The electrophoresis was performed with agarose gel pre-stained with GelRed nucleic acid stain (Biotium Inc, USA) prepared in 0.5X TAE buffer (20mM Tris, 10mM acetic acid, 0.5mM EDTA). Electrophoresis was carried out at 80 V and the expected PCR products of 502 bp (enteroviruses), 835 bp (EV-A71), 989 bp (CV-A16) and 657 bp (CV-A6) were visualized under ultraviolet transillumination.

The amplicons were purified using the Expin Combo GP (GeneAll, Korea) according to the manufacturer's instructions. Briefly, the DNA bands of interest were excised from the agarose gel using a clean blade. Buffer GB was added to the agarose gel slide (300 µl per 100 mg of gel), followed by 10 minutes incubation at 50 ℃. The DNA-containing mixture was then added to the column and washed with 700 µl of buffer NW. The DNA

was eluted with 50 µl buffer EB and kept at -20 ℃. The concentration of purified DNA was quantified using an Epoch microplate spectrophotometer (BioTek Instruments, USA) with Gen5 3.0 software.

3.2.2.3 Virus genotyping

The purified amplicons were sequenced by First BASE Laboratories (Selangor, Malaysia) using BigDye Terminator v3.1 Cycle Sequencing Kit (Applied Biosystems, USA) with a 3730xl DNA Analyzer (Applied Biosystems, USA). Sequencing results were subjected to BLAST analysis to identify the enterovirus serotypes.

Sequences were trimmed and assembled using Geneious R6 (Biomatters Ltd., New Zealand), and aligned with relevant sequences available in the GenBank. The best substitution model was determined using the jModelTest v2 (Posada, 2008). Phylogenetic trees were constructed for enteroviruses and EV-A71 using the partial 5' UTR and complete VP4 sequences, while for CV-A16 and CV-A6, complete and partial VP1 sequences were used, respectively. The phylogenetic trees were constructed using the Bayesian Markov chain Monte Carlo (MCMC) method implemented in the BEAST, version 1.7.4 (Drummond and Rambaut, 2007), run for 30 million generations with a 10% burn-in. All runs reached convergence with estimated sample sizes of > 200. The tree prior was coalescent GMRF Bayesian Skyride and the clock model was uncorrelated lognormal relaxed. The maximum clade credibility tree was viewed using the FigTree v1.4.0 (Rambaut, 2012). Substitution rates with 95% highest posterior density (HPD) intervals were determined by using Bayesian uncorrelated lognormal relaxed molecular clock model.

Table 3.1: Reaction mix preparation for RT-PCR

Reagent	Volume	Final concentration
Nuclease-free water	10 µl	-
AMV/T*fl* 5X reaction buffer	5 µl	1X
dNTP mix (10 mM each dNTP)	1 µl	0.2 mM
30 µM forward primer	1 µl	1.2 µM
30 µM reverse primer	1 µl	1.2 µM
25mM MgSO4	1 µl	1 mM
AMV reverse trancriptase (5 u/µl)	0.5 µl	0.1 u/µl
T*fl* DNA polymerase (5 u/µl)	0.5 µl	0.1 u/µl
RNA sample	5 µl	-
Total	25 µl	

Table 3.2: Primers for enteroviruses, EV-A71, CV-A16 and CV-A6 detection

Virus	Gene region	Primers name	Nucleotide sequence (5' – 3')	Nucleotide position	Product size (bp)	Annealing temp (℃)	Polarity	References
Enterovirus	5' UTR	CoxbanS	GTAMCYTTGTRCGCCWGTTT	66-567	502	50	Sense	Arola *et al.*,
		CoxbanR	GAAACACGGACACCCAAAGTA				Antisense	1995
EV-A71	VP4	EntabF	TCCTCCGGCCCCTGAATGCGGCTAAT	448-1282	835	55	Sense	Yoke-Fun and
		EV1R	TGMACRTGRATGCARAACC				Antisense	AbuBakar, 2006
CV-A16	VP1	CVVP1F	CACAGAGGACATTGAGCAAAC	2412-3401	989	55	Sense	Chan *et al.*,
		CVVP1R	AGGTGCCGATTCACTACCC				Antisense	2012
CV-A6	VP1	CU-EVF2632	TGTGTGATGAATCGAAACGGGGT	2632-3288	657	55	Sense	Puenpa *et al.*,
		CU-EVR3288	TGCAGTGTTAGTTATTGTTTGGCT				Antisense	2013

3.2.2.4 Nucleotide accession numbers

The sequences reported in this study have been deposited into the GenBank with the accession numbers KJ815033-KJ815044 and KT908004-KT908038 (Appendix I).

3.3 Cloning and expression of enterovirus A71 proteins

3.3.1 Cloning

3.3.1.1 Bacterial strains and plasmid vectors

Bacterial strains used in this study were *Escherichia coli* TOP10F (Invitrogen, USA) and *E. coli* BL21 (DE3) (New England Biolabs, USA). The plasmid vectors used in this study were pUC57 (GenScript standard vector), pET-52b(+) (Novagen, Germany) and pEGFP-N1 (Clontech Laboratories Inc., USA). The restriction maps of plasmid vectors are shown in Appendix II, Appendix III and Appendix IV.

3.3.1.2 Design and synthesis of enterovirus A71 genes

Codon-optimized cDNA clones encoding the entire EV-A71 isolate UH1/PM/1997 proteome (both structural and non-structural) based on consensus sequence alignments of different EV-A71 sequences were synthesized (GenScript, USA). An additional cassette with domain linker, StrepTag II, FLAG Tag and 8X His-Tag functions was designed and synthesized (Figure 3.1). The synthesized plasmid DNAs were reconstituted with 20 µl of sterile water and subcloned into pEGFP-N1 vector to form pEGFP-N1-cassette-VP1, -VP2, -VP3, -VP4, -3C and -3D expression plasmids. The pEGFP-N1-2B, -2C and -3AB expression plasmids were obtained from the laboratory. The synthesized 2A plasmid DNA was then subcloned into pET-52b(+) to form a pET-

52b(+)-2A expression plasmid. The workflow of preparation of plasmid DNAs for the mammalian expression system and the bacterial expression system are shown in Figure 3.2.

3.3.1.3 Transformation of competent *Escherichia coli*

E. coli TOP10F was transformed with pEGFP-N1 expression plasmids and pUC57 expression plasmids whereas *E. coli* BL21 (DE3) was transformed with pET-52b(+) expression plasmids. In brief, *E. coli* strains were cultured in 5 ml Luria Bertani (LB) broth (supplemented with 12.5 µg/ml tetracycline for *E. coli* TOP10F) for 6 hours at 37 ℃. The *E. coli* culture was aliquoted into 1.5 ml centrifuge tubes and pelleted by centrifugation at 1,000 x g for 3 minutes. The *E. coli* pellet was resuspended with 1.5 ml of 100 mM calcium chloride and incubated overnight at 4 ℃. The cells were pelleted with centrifugation at 1,000 x g for 3 minutes and resuspended with 80 µl of fresh 100 mM calcium chloride. Then, 1 µl of reconstituted plasmid DNAs or 4 µl of ligation mixtures were added to the cells, followed by incubation on ice for 45 minutes. The mixture was heat shocked at 42 ℃ for 1 minute and immediately placed on ice for another 5 minutes. An aliquot of 1 ml of LB broth was added to the transformed *E. coli* strains and incubated at 37 ℃ for 1 hour. The transformed *E. coli* was pelleted and resuspended with 80 µl of fresh LB broth. Approximately 40 µl of transformed *E.coli* was spread on LB agar plate supplemented with antibiotics (50 µg/ml kanamycin for pEGFP-N1 expression plasmids; 100 µg/ml ampicillin for pET-52b(+) and pUC57 expression plasmids). The plate was incubated overnight at 37 ℃ and stored at 4 ℃. All positive clones were screened by restriction enzyme digestion analysis and confirmed by DNA sequencing.

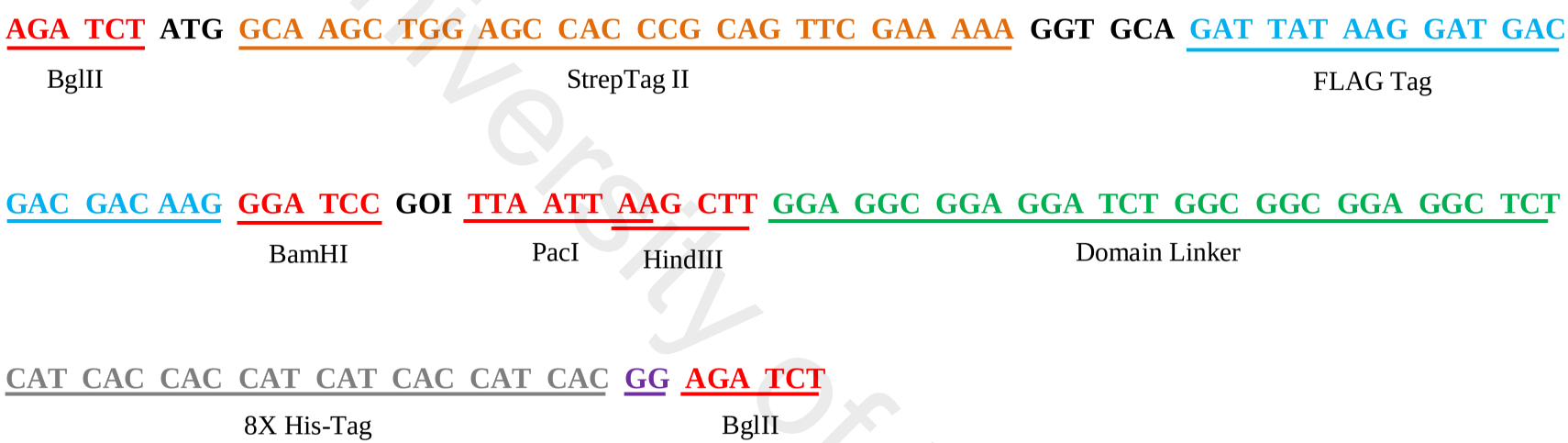

Figure 3.1: EV-A71 expression cassette in the pEGFP-N1 vector. The total length of the expression cassette was 149 bases. The available restriction enzyme cutting sites (shown in red), StrepTag II (orange), FLAG Tag (blue), domain linker (green) and 8X His-Tag (grey) are shown. Two bases (GG, in purple) were added to synchronize the reading frame with GFP expression. The EV-A71 genes used (indicated as GOI, gene of interest) in the expression cassette were VP1, VP2, VP3, VP4, 3C and 3D.

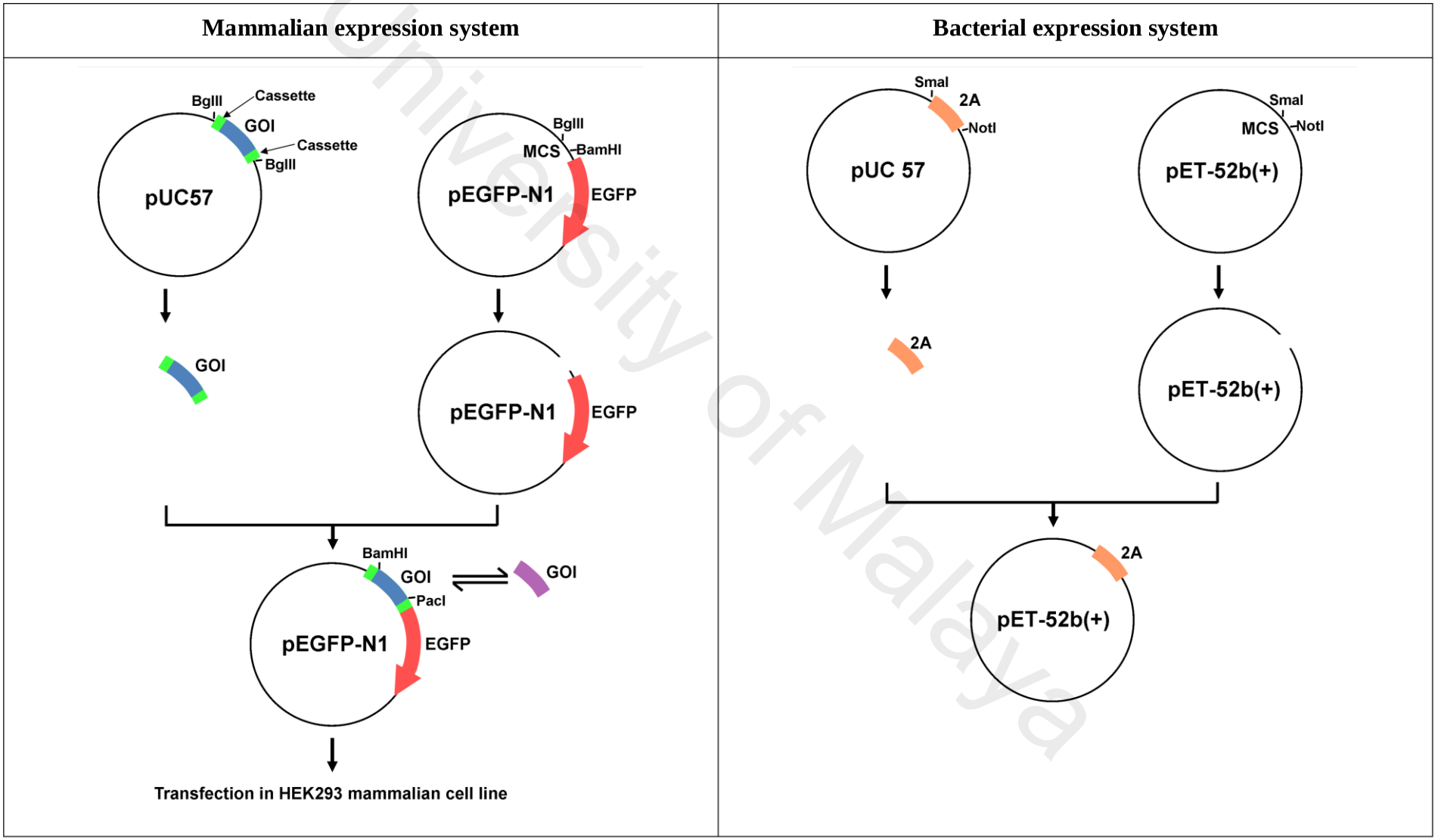

Figure 3.2: Workflow of plasmid DNA preparation for the mammalian and bacterial expression systems. The mammalian expression system included pEGFP-cassette-VP1, -VP2, -VP3, -VP4, -3C and 3D expression plasmids, whereas the bacterial expression system was the pET-52b(+)-2A expression plasmid. In the mammalian expression system, the synthesized EV-A71 cassettes with the gene of interest (GOI) in pUC57 vectors were digested by restriction enzyme BglII. The pEGFP-N1 vectors were digested by restriction enzymes BglII and BamHI at the multiple cloning site (MCS), which is a short DNA segment that contains various restriction sites and functions as an ideal place for foreign DNA fragment insertion for cloning. The digested cassette with GOI was subcloned into pEGFP-N1 vectors. The GOI in pEGFP-cassette expression plasmid is interchangeable with others by digestion of restriction enzymes BamHI and PacI. In bacterial expression system, the synthesized 2A plasmid DNA in pUC57 vectors and pET-52b(+) vectors were digested by restriction enzymes SmaI and NotI. Subsequently the digested 2A plasmid DNA was then subcloned into pET-52b(+) vector to form a pET-52b(+)-2A expression plasmid.

3.3.1.4 Restriction endonuclease digestion of DNA

Digestion of DNA was carried out with specific FastDigest restriction endonuclease (Thermo Scientific, USA) according to the manufacturer's instructions. Restriction enzymes BglII, BamHI and PacI were used in pEGFP-cassette expression plasmids, while restriction enzymes SmaI and NotI were used in pET-52b(+) expression plasmids (Figure 3.2). In brief, the reaction was carried out with 1-3 µg of DNA, FastDigest restriction enzymes and 1X FastDigest buffer in a thin-wall PCR tube. All reactions were incubated for 1 hour at optimal temperatures suggested by the manufacturer. The double digested DNA was purified using the Expin Combo GP as mentioned in section 3.2.2.2.

3.3.1.5 DNA ligation

DNA ligation was carried out with 150 ng of purified DNA and 120 ng of purified vector, 1X T4 DNA ligase buffer and 1 U T4 DNA ligase (Thermo Scientific, USA) in a thin-wall PCR tube and incubated at 4 ℃ for overnight. The ligated DNA was used for bacterial transformation as mentioned in section 3.3.1.3.

3.3.1.6 Plasmid extraction and confirmation

The endotoxin-free plasmid DNA maxi-preparation kit (BioTeke Corporation, China) was used for large scale plasmid DNA extraction. The plasmid DNA purification was carried out according to the manufacturer's instructions. A volume of 500 ml of bacterial culture was pelleted by centrifugation for 10 minutes at 8,000 x g. The bacterial cell pellet was resuspended with 9 ml of Buffer P1 supplemented with RNase A. The cell pellet was lysed with 9 ml of Buffer P2 for 5 minutes, and then neutralized

with 14.4 ml of Buffer P3. The resulting precipitate was removed through centrifugation for 15 minutes at 8,000 x g. The plasmid-containing supernatant was added to the column and then washed with 10 ml of Buffer PE, followed by 10 ml of Buffer WB twice. The plasmid DNA was eluted with 1.5 ml of Buffer EB. The eluted plasmid DNA was filtered using the purification-column ED and concentrated to around 500 µl by incubation at 50 ℃ for a few hours. Concentration of the purified plasmid DNA was quantified using an Epoch microplate spectrophotometer (BioTek Instruments, USA). The integrity of the plasmid DNA was then verified by agarose gel electrophoresis and its nucleotides were sequenced by First BASE Laboratories (Selangor, Malaysia) with primers pEGFP-CMV (5'-TAA CAA CTC CGC CCC ATT-3') and pEGFP-rev (5'-GTC CAG CTC GAC CAG GAT GGG-3').

3.3.2 Transfection of enhanced green fluorescent protein-expressing enterovirus A71 genes

The pEGFP-cassette-VP1, -VP2, -VP3, -VP4, -3C and -3D and pEGFP-N1-2B, -2C and -3AB plasmids were used for transfection. HEK293 cells were seeded in 75cm^2 tissue culture flasks at a density of 4 x 10^6 cells and incubated overnight at 37 ℃ in 5% CO_2. The transfection mixture was prepared with a ratio of plasmid DNA to lipofectamine LTX reagent (Invitrogen, USA) of 1:3. Cells were transfected (16 µg of plasmid DNA per 4 x 10^6 cells) in Opti-MEM (Invitrogen, USA) for 24 hours at 37 ℃ in 5% CO_2. The transfection medium was removed and replaced with fresh maintenance medium for another 24 hours incubation.

3.3.3 Protein expression

3.3.3.1 Protein extraction and purification from the mammalian expression system

Enhanced green fluorescent protein (EGFP)-expressing recombinant proteins were harvested at 48 hours post-infection. Cells were washed with PBS (137 mM NaCl, 2.7 mM KCl, 10mM Na_2HPO_4, 1.8 mM KH_2PO_4) twice and lysed with ice cold lysis buffer (20 mM HEPES (pH 7.5), 280 mM KCl, 1 mM EDTA, 1% Triton X-100) containing protease inhibitors (Sigma Aldrich, Germany). The recombinant protein was vortexed vigorously for 30 minutes at 4 ℃. The cell debris was removed through centrifugation at 20,000 x g for 10 minutes at 4 ℃. The protein lysate was kept at -20 ℃.

Recombinant EV-A71-EGFP proteins were purified using the µMACS GFP isolation kit (Miltenyi Biotec, Germany) according to the manufacturer's instructions. Briefly, 50 µl of anti-GFP microbeads were added to the protein lysate to magnetically label the epitope-tagged target protein and incubated on ice for 30 minutes. The column was placed in the magnetic field of the µMACS separator, followed by addition of 200 µl of lysis buffer into the column. The protein lysate-microbeads mixture was then added to the column and washed with 800 µl of Wash Buffer 1 and 100 µl of Wash Buffer 2. The denatured protein was eluted with 70 µl of pre-heated 95 ℃ hot elution buffer. The purified proteins were kept at -20 ℃.

3.3.3.2 Protein expression and purification from the bacterial expression system

Colony of the pET-52b(+)-2A expression bacteria was inoculated in 5 ml of LB broth supplemented with 100 µg/ml ampicillin at 37 ℃ overnight. About 2 ml of overnight bacteria culture was inoculated into 200 ml of fresh LB broth supplemented with 100 µg/ml ampicillin for 2 hours 15 minutes at 37 ℃. Protein expression was induced with

isopropyl-beta-D-thiogalactopyranoside (Vivantis Technologies, Malaysia) to a final concentration of 1 mM and incubated for 4 hours 30 minutes at 37℃. The bacteria culture was pelleted by centrifugation at 8,000 x g for 10 minutes. The cell pellet was lysed with denatured lysis buffer (8 M urea, 50 mM NaH_2PO_4, 300 mM NaCl, 10 mM imidazole, pH 8.0), followed by sonication, and centrifugation at 14,000 x g for 1 hour to remove the insoluble cell pellet. Profinity IMAC Ni-charged resins (Bio-Rad, USA) were added to a polypropylene column (Qiagen, Germany) and the column was activated with lysis buffer. Protein supernatant was added into the column and incubated for 30 minutes at 4℃ with gentle rocking. The flow-through was discarded and the column was washed twice with denatured washing buffer (8 M urea, 50 mM NaH_2PO_4, 300 mM NaCl, 20 mM imidazole, pH 8.0). The purified protein was eluted with 4 ml elution buffer (8 M urea, 50 mM NaH_2PO_4, 300 mM NaCl, 300 mM imidazole, pH 8.0).

3.4 Identification of immunogenic proteins and peptides

3.4.1 Human sera

Four panels of human sera were used in present study. Panel A consisted of 36 residual serum samples obtained during 2000 HFMD outbreaks, and panel B consisted of 53 sera prospectively collected during the 2012-2013 outbreak. All patients from panel A and B showed clinical signs of HFMD (including ulcers in the mouth/tongue, rash/vesicles on the palms and soles, with/without fever), and were positive for EV-A71 or non-EV-A71 enteroviruses by virus culture (or PCR, for panel B) from throat swabs, vesicle swabs and/or rectal swabs. Panel C, the non-HFMD (negative control) samples, consisted of 47 residual serum samples which previously tested positive for IgM for other viral infections, such as dengue, chikungunya, measles, herpes simplex virus or

varicella-zoster virus. Samples from panels A-C were obtained from the diagnostic virology laboratory, UMMC. Panel D consisted of 5 healthy adult volunteer donors.

3.4.2 Antibody detection

3.4.2.1 Enterovirus A71 IgM-capture enzyme-linked immunosorbent assay

EV-A71 specific-IgM antibody in serum specimens were detected using the EV-A71 IgM-capture ELISA (Beijing Wantai Biological Pharmacy Enterprise CO., Ltd., China) according to the manufacturer's instructions. In brief, 100 µl of diluent and 10 µl of sera were mixed in an anti-human IgM µ-chain microplate, followed by 30 minutes incubation at 37 ℃. The plate was washed with diluted washing buffer (PBS) five times. Then, 50 µl of purified EV-A71 antigens and 50 µl of horseradish peroxidase (HRP)-conjugate anti-EV-A71 monoclonal antibody were added into the microplate and incubated for 30 minutes at 37 ℃. The plate was washed, followed by addition of 50 µl of urea peroxidase and 50 µl of TMB substrate, and further incubated in the dark for 15 minutes at 37 ℃. The reaction was terminated with 50 µl of 2.0 M sulfuric acid. Optical density (OD) of each well was measured at 450 nm with a reference filter of 630 nm with a microplate reader (BioTek Instruments, USA). The cut-off value was calculated as 0.1 + mean OD of the negative controls. If the mean OD of negative controls was lower than 0.05, the value was considered to be 0.05. Serum specimens were considered positive if the signal/cut-off (S/CO) value is ≥ 1.0.

3.4.2.2 Enterovirus A71 IgM-colloidal gold immunochromatographic assay

EV-A71 specific-IgM antibody in serum specimens was detected with EV-A71 IgM GICA (Beijing Wantai Biological Pharmacy Enterprise CO., Ltd., China) according to the manufacturer's instructions. An aliquot of 15 µl of serum was added to the 1.5 ml specimen diluent and mixed well. Aliquots of 80 µl of diluted samples were pipetted into the sample wells of the EV-A71 IgM GICA cassette and the results were read within 30 min. EV-A71 specific-IgM antibodies were captured by immobilized EV-A71 antigen and formed an antibody-antigen complex on the test line. Serum specimens were considered positive if bands appeared at the test line and control line.

3.4.2.3 IgG detection by Western bloting

EV-A71 specific-IgG antibody in serum specimens was determined by immunoblotting analysis. The detailed methods were explained in sections 3.4.3.1 and 3.4.3.2. Briefly, the denatured proteins from the EV-A71 isolate UH1/PM/1997 were separated by sodium dodecyl sulfate-polyacrylamide gel electrophoresis (SDS-PAGE) at 80 V for 2 hours. The protein was then transferred onto a polyvinylidene fluoride membrane (Millipore, USA) using a semidry transfer method. The membrane was blocked with blocking buffer for 1 hour. The membrane was washed and clamped in a Mini-PROTEAN II multiscreen apparatus (Bio-Rad, USA), which can quickly and efficiently screen up to 18 different sera per membrane. The 1:100 diluted serum specimens were added into each lane and incubated for 1 hour. The membrane was washed, then incubated with HRP-conjugated polyclonal rabbit anti-human IgG (1:1000; Dakocytomation, Denmark) antibodies for 1 hour. The immunoblots were developed with DAB substrate in stable peroxide substrate solution (Pierce Biotechnology, USA).

The sizes of the desired protein bands were determined based on the PageRuler prestained protein marker (Thermo Scientific, USA).

3.4.2.4 Neutralization assay

The neutralization activity of antibodies from healthy donor and HFMD patients was tested in triplicate and analysed by microneutralization assay as previously described (Ang *et al.*, 2011), with some modifications. Briefly, the human serum samples were heat-inactivated at 56 ℃ for 30 minutes. Two-fold serial dilutions from 1:8 to 1:32 were performed for all serum samples. An aliquot of 90 µl of each dilution was mixed with 90 µl of 1000 $TCID_{50}$ of EV-A71 isolate UH1/PM/1997. The virus-antibody mixtures were incubated for 2 hours at 37 ℃ in the presence of 5% CO_2. The virus-antibody mixtures were inoculated into a 96-well plate in triplicate. RD cells were added at a density of 1 x 10^4 cells/well. Pooled positive sera of known titer were included as positive controls. Diluted serum, virus alone and uninfected RD cells were also included as controls. The plates were incubated for 5 days at 37 ℃ in the presence of 5% CO_2. The CPE were observed and the neutralizing antibody titer was defined as the highest dilution that prevents the development of CPE in 50% of the inoculated wells. A serum sample was considered as positive if the neutralizing titer was ≥1:8 (Ji *et al.*, 2012, Luo *et al.*, 2009).

3.4.3 Antigenic protein identification

3.4.3.1 Viral protein separation by sodium dodecyl sulfate-polyacrylamide gel electrophoresis

Protein was separated by SDS-PAGE using a vertical slab gel unit in a Mini-Protean tetra cell (Bio-Rad, USA). The SDS-PAGE was casted with a 10% polyacrylamide separating gel and a 5% polyacrylamide stacking gel. An aliquot of the desired amount of protein samples was boiled with Laemmli loading buffer (375 mM Tris, 12% SDS, 60% glycerol, 0.6 M DTT, 0.3% bromophenol blue) at 100 ℃ for 10 minutes and loaded into each well. The denatured proteins were separated in Laemmli electrophoresis running buffer (25 mM Tris, 192 mM glycine, 0.1% SDS) at 80 V for 2 hours. The SDS-PAGE gel was either stained for visualization of the separated proteins, or processed further for Western blot analysis (section 3.4.3.2). For visualization, the SDS-PAGE gel was stained in Coomassie brilliant blue R-250 staining solution (0.025% Coomassie brilliant blue R-250, 40% methanol and 7% acetic acid) for 1 hour with gentle rocking. Then, the stained gels were destained in destaining solution (40% methanol and 7% acetic acid) for 30 minutes. The gels were washed with deionized water overnight and gel images were captured by a GS-800 Calibrated Densitometer (Bio-Rad, USA) with Quantity One 1D Analysis software version 4.6.9 (Bio-Rad, USA).

3.4.3.2 Western blot analysis by chemiluminescence detection

The proteins in the SDS-PAGE gel were transferred onto an Amersham Hybond ECL nitrocellulose membrane (GE Healthcare, Germany) using a Trans-Blot SD semi-dry transfer cell (Bio-Rad, USA). The assembly of the protein transfer sandwich was in the following order, starting from the bottom: two layers of filter papers pre-wetted in

chilled anode buffer I (0.3 M Tris, 10% methanol, pH 10.4), followed by a layer of filter paper pre-wetted in chilled anode buffer II (25 mM Tris, 10% methanol, pH 10.4), nitrocellulose membrane pre-wetted in chilled anode buffer II, SDS-PAGE gel pre-soaked in chilled cathode buffer (25 mM Tris, 40 mM glycine, 10% methanol, pH 9.4) and three layers of filter papers pre-wetted in chilled cathode buffer. Proteins were transferred onto the membrane at 10 V for 30 minutes and 1 hour for the 0.75 mm and 1.5 mm gels, respectively.

The membrane was blocked with 5% skimmed milk in 0.05% Tween-20 phosphate buffered saline (0.05% PBST) for 1 hour. The membrane was washed thrice with 0.05% PBST, with 5 minutes per wash with rocking. For IgM specific antibody detection, the pooled human serum samples were pre-treated additionally with RIDA RF-Absorbens (R-Biopharm AG, Germany). For IgG specific antibody detection, the pooled human serum samples were pre-treated with DTT (Invitrogen, USA) to a final concentration of 5 mM prior to primary antibody incubation. The membrane was then incubated with 1:5000 diluted anti-GFP-HRP (Miltenyi Biotec, Germany), 1:300 diluted pooled human serum, 1:100 diluted Light Diagnostics EV-A71 monoclonal antibody 3323 (Millipore, USA), 1:1000 diluted EV-A71 specific monoclonal antibody 979 (mAb 979; Millipore, USA) or 1:100 diluted mouse sera immunized with inactivated EV-A71 (a gift from Dr. Ong Kien Chai, University Malaya) for 1 hour at room temperature with rocking. The membrane was washed thrice with wash buffer, followed by incubation with the 1:5000 diluted HRP-conjugated polyclonal rabbit anti-human IgM (KPL, USA), 1:3000 diluted Amersham ECL human IgG, HRP-linked whole Ab from sheep (GE Healthcare, USA) or 1:5000 diluted HRP-conjugated goat anti-mouse (Gene Tex, USA) antibody for 1 hour at room temperature. The immunoblot was developed with Clarity Western ECL Substrate (Bio-Rad, USA) and detected by chemiluminescence. The protein size was determined using the Precise Plus Protein Western C Standard (Bio-Rad, USA).

3.4.4 Identification of B-cell epitopes

3.4.4.1 Design and synthesis of synthetic peptides

A total of 63 biotinylated peptides consisting of 15-mer peptides (Pepscan, Netherlands) were generated from consensus alignment of different EV-A71 amino acid sequences. The synthetic biotinylated peptides were either potential EV-A71 antibody epitopes predicted by the Emini surface accessibility scale (Emini *et al.,* 1985) or published EV-A71 epitope sequences. The calculation of Emini surface accessibility scale was based on surface exposure of a product instead of an addition within the window. The accessibility profile was obtained using the formula $Sn = (\prod_{i-1}^{6} \delta n + 4 + i) \times (0.37)^{-6}$ where Sn is the surface probability, δn is the fractional surface probability value, and *i* varies from 1 to 6. A hexapeptide sequence with Sn greater than 1.0 indicates an increased probability for being found on the surface (Emini *et al.,* 1985). The detailed information and the schematic illustration of the 63 biotinylated synthetic peptides are shown in Table 3.3 and Figure 3.3. All synthetic peptides were dissolved in dimethyl sulfoxide (DMSO) to obtain a final concentration of 15 μg/ml.

3.4.4.2 Virion-based ELISA and sera isotyping

Polystyrene 96-well Maxisorp Nunc-immuno plates (Thermo Scientific, Denmark) were coated with 10 μg/ml of purified EV-A71 and incubated at 37℃ for 1 hour with gentle rocking. The plates were washed with 0.05% PBST and subsequently blocked with 3% bovine serum albumin (BSA) diluted in 0.05% PBST for 1 hour. Pooled human sera were pre-treated with RIDA RF-Absorbens to obtain IgM specific antibody prior to primary antibody incubation. The plates were washed and pooled human sera were then diluted at 1:100 to 1:8000 in 1% BSA-0.05% PBST and incubated for 1 hour at 37℃.

The plates were washed and incubated for 1 hour with 1:5000 diluted HRP-conjugated polyclonal rabbit anti-human IgM (KPL, USA), 1:5000 diluted HRP-conjugated polyclonal rabbit anti-human IgG (Dakocytomation, Denmark) or 1:500 diluted HRP-conjugated isotype IgG1 (Molecular Probe, USA), IgG2 (Invitrogen, USA), IgG3 (Invitrogen, USA), and IgG4 antibodies (Molecular Probe, USA). Readout was detected with TMB microwell peroxidase substrate (KPL, USA) and terminated with 1 M phosphoric acid after 10 minutes. Absorbance was measured at 450 nm with a reference filter of 630 nm. The OD values were plotted as means ± standard deviation (SD).

3.4.4.3 Peptide-based ELISA

All synthetic peptides were screened in triplicate and analysed by indirect ELISA. Briefly, streptavidin high binding capacity coated plates (Pierce Biotechnology, USA) were first washed with 0.05% PBST and blocked with 3% BSA diluted in 0.05% PBST for 1 hour. The plates were washed and subsequently coated with synthetic peptides diluted at 1:1000 in 0.05% PBST. The plates were incubated at room temperature for 1 hour with gentle rocking. Pooled human sera were pre-treated with RIDA RF-Absorbens to obtain IgM specific antibody. The plates were then washed with 0.05% PBST before incubating with 1:500 diluted pooled human sera with 1% BSA-0.05% PBST for 1 hour. The plates were washed, then incubated with the 1:5000 diluted HRP-conjugated polyclonal rabbit anti-human IgM (KPL, USA) or polyclonal rabbit anti-human IgG (1:5000) antibodies for 1 hour. For visualization, 100 µl of TMB microwell peroxidase susbstrate (KPL, USA) was added to each well and incubated for 10 minutes. The OD was measured at 450 nm with a reference filter of 630 nm after termination with 1 M phosphoric acid. The cut-off value was calculated as mean OD of the negative controls. If the mean OD of negative controls was lower than 0.105, the value was

considered to be 0.105. Data was presented as S/CO values, with a value <2.1 scored as negative, a value of 2.1-4.9 scored as weakly positive, and a value ≥5 scored as strongly positive.

3.4.4.4 Three-dimensional structure and sequence analysis

The crystal structure of EV-A71 was retrieved from Protein Data Bank (PDB) (identifiers 3VBS) and visualized using the UCSF Chimera software version 1.10.1 (Pettersen *et al*., 2004). For sequence analysis, sequences from different enteroviruses were downloaded from GenBank and were aligned using the Geneious R6 (Biomatters Ltd., Auckland, New Zealand).

Table 3.3: List of the 63 synthetic biotinylated peptides

Name	Sequence	Location	Region	Prediction / Reference
PEP1	STQRSGSHENSNSAT	6-20	VP4	Predicted by EMINI in this study
PEP2	TEGSTINYTTINYYK	20-34	VP4	Predicted by EMINI in this study
PEP3	YTTINYYKDSYAATA	27-41	VP4	Predicted by EMINI in this study
PEP4	AGKQSLKQDPDKFAN	41-55	VP4	Predicted by EMINI in this study
PEP5	LTIGNSTITTQEAAN	85-99	VP2	Predicted by EMINI in this study VP2-6 (Gao *et al.*, 2012)
PEP6	VDKPTRPDVSVNRFY	119-133	VP2	Predicted by EMINI in this study
PEP7	DVSVNRFYTLDTKLW	126-140	VP2	VP2-21 (Gao *et al.*, 2012)
PEP8	YTLDTKLWEKSSKGW	133-147	VP2	Predicted by EMINI in this study
PEP9	QGALLVAILPEYVIG	188-202	VP2	VP2-40 (Gao *et al.*, 2012)
PEP10	TVAGGTGTEDSHPPY	203-217	VP2	Predicted by EMINI in this study VP2-27 (Liu *et al.*, 2011) VP2-28 (Liu *et al.*, 2011)
PEP11	GTEDSHPPYKQTQPG	209-223	VP2	Predicted by EMINI in this study VP2-29 (Liu *et al.*, 2011)
PEP12	PYKQTQPGADGFELQ	216-230	VP2	Predicted by EMINI in this study VP2-50 (Gao *et al.*, 2012)
PEP13	VTQGFPTEPKPGTNQ	321-335	VP2-VP3	Predicted by EMINI in this study
PEP14	IHIPGEVRNLLELCQ	357-371	VP3	VP3-10 (Gao *et al.*, 2012) VP3-12 (Gao *et al.*, 2012)
PEP15	RNLLELCQVETILEV	364-378	VP3	VP3-15 (Gao *et al.*, 2012)
PEP16	RFPVSAQAGKGELCA	393-407	VP3	VP3-24 (Gao *et al.*, 2012)
PEP17	FRADPGRDGPWQSTM	409-423	VP3	Predicted by EMINI in this study
PEP18	PGGPLPKDRATAMLG	461-475	VP3	Predicted by EMINI in this study
PEP19	WISNTHYRAHARDGV	494-508	VP3	Predicted by EMINI in this study
PEP20	QTASIQGDRVADVIE	560-574	VP3-VP1	Predicted by EMINI in this study VP1-01 (Liu *et al.*, 2011)
PEP21	PTGQNTQVSSHRLDT	592-606	VP1	Predicted by EMINI in this study
PEP22	VSSHRLDTGEVPALQ	599-613	VP1	VP1-14 (Gao *et al.*, 2012)
PEP23	TGEVPALQAAEIGAS	606-620	VP1	VP1-15 (Gao *et al.*, 2012)
PEP24	VLNSHSTAETTLDSF	634-648	VP1	Predicted by EMINI in this study
PEP25	PLEGTTNPNGYANWD	661-675	VP1	Predicted by EMINI in this study BC loop VP1-31 (Gao *et al.*, 2012)
PEP26	ITGYAQMRRKVELFT	678-692	VP1	Predicted by EMINI in this study
PEP27	PTGEVVPQLLQYMFV	707-721	VP1	Predicted by EMINI in this study DE loop
PEP28	VPPGAPKPESRESLA	721-735	VP1	Predicted by EMINI in this study SP55 (Foo *et al.*, 2007b) VP1-54 (Gao *et al.*, 2012)

Table 3.3, continued.

Name	Sequence	Location	Region	Prediction / Reference
PEP29	YPTFGEHKQEKDLEY	773-787	VP1	Predicted by EMINI in this study SP70 (Foo *et al.*, 2007b) VP1-71 (Gao *et al.*, 2012) VP1-42 (Liu *et al.*, 2011) VP1-43 (Liu *et al.*, 2011)
PEP30	VGSSKSKYPLVVRIY	803-817	VP1	HI loop
PEP31	PRPMRNQNYLFKANP	828-842	VP1	Predicted by EMINI in this study
PEP32	NYLFKANPNYAGNSI	835-849	VP1	Predicted by EMINI in this study
PEP33	VYYCNSKRKHYPVSF	924-938	2A	Predicted by EMINI in this study
PEP34	YVEASEYYPARYQSH	945-959	2A	Predicted by EMINI in this study
PEP35	NLEQSAASQEDLEAM	1173-1187	2C	Predicted by EMINI in this study
PEP36	KRMNNYMQFKSKHRI	1217-1231	2C	Predicted by EMINI in this study
PEP37	LPPDPDHFDGYKQQV	1268-1282	2C	Predicted by EMINI in this study
PEP38	DAIRRRFYMDCDIEV	1347-1361	2C	Predicted by EMINI in this study
PEP39	YMDCDIEVTDSYKTD	1354-1368	2C	Predicted by EMINI in this study
PEP40	KLCSENNTANFKRCS	1379-1393	2C	Predicted by EMINI in this study
PEP41	LRDRKSKVRYSVDTV	1403-1417	2C	Predicted by EMINI in this study
PEP42	VVSELIREYNSRSAI	1417-1431	2C	Predicted by EMINI in this study
PEP43	GPPKFRPIRISLEEK	1441-1455	3A	Predicted by EMINI in this study
PEP44	IPETPTNVERHLNRA	1484-1498	3A	Predicted by EMINI in this study
PEP45	LRRNIRQVQTDQGHF	1559-1573	3C	Predicted by EMINI in this study
PEP46	RHSQPGKTIWVEHKL	1587-1601	3C	Predicted by EMINI in this study
PEP47	VTLDTNEKFRDITKF	1623-1637	3C	Predicted by EMINI in this study
PEP48	NLSGKPTHRTMMYNF	1674-1688	3C	Predicted by EMINI in this study
PEP49	GRQGFCAGLKRSYFA	1714-1728	3C	Predicted by EMINI in this study
PEP50	VKPNKETGRLNINGP	1737-1751	3D	Predicted by EMINI in this study
PEP51	GRLNINGPTRTKLEP	1744-1758	3D	Predicted by EMINI in this study
PEP52	AVLTSKDPRLEVDFE	1772-1786	3D	Predicted by EMINI in this study
PEP53	EPDEYVTQAALHYAN	1800-1814	3D	Predicted by EMINI in this study
PEP54	NQLKQLDINTSKMSM	1814-1828	3D	Predicted by EMINI in this study
PEP55	IKKRDILDPTTRDVS	1856-1870	3D	Predicted by EMINI in this study
PEP56	SKMKFYMDKYGLDLP	1870-1884	3D	Predicted by EMINI in this study
PEP57	PYSTYVKDELRSLDK	1884-1898	3D	Predicted by EMINI in this study
PEP58	DELRSLDKIKKGKSR	1891-1905	3D	Predicted by EMINI in this study
PEP59	INHTHHVYRNKTYCV	2000-2014	3D	Predicted by EMINI in this study
PEP60	LELAKTGKEYGLTMT	2073-2087	3D	Predicted by EMINI in this study
PEP61	ESIRWTKDARNTQDH	2131-2145	3D	Predicted by EMINI in this study
PEP62	LAWHNGKDEYEKFVS	2152-2166	3D	Predicted by EMINI in this study
PEP63	AIPNFENLRRNWLEL	2178-2192	3D	Predicted by EMINI in this study

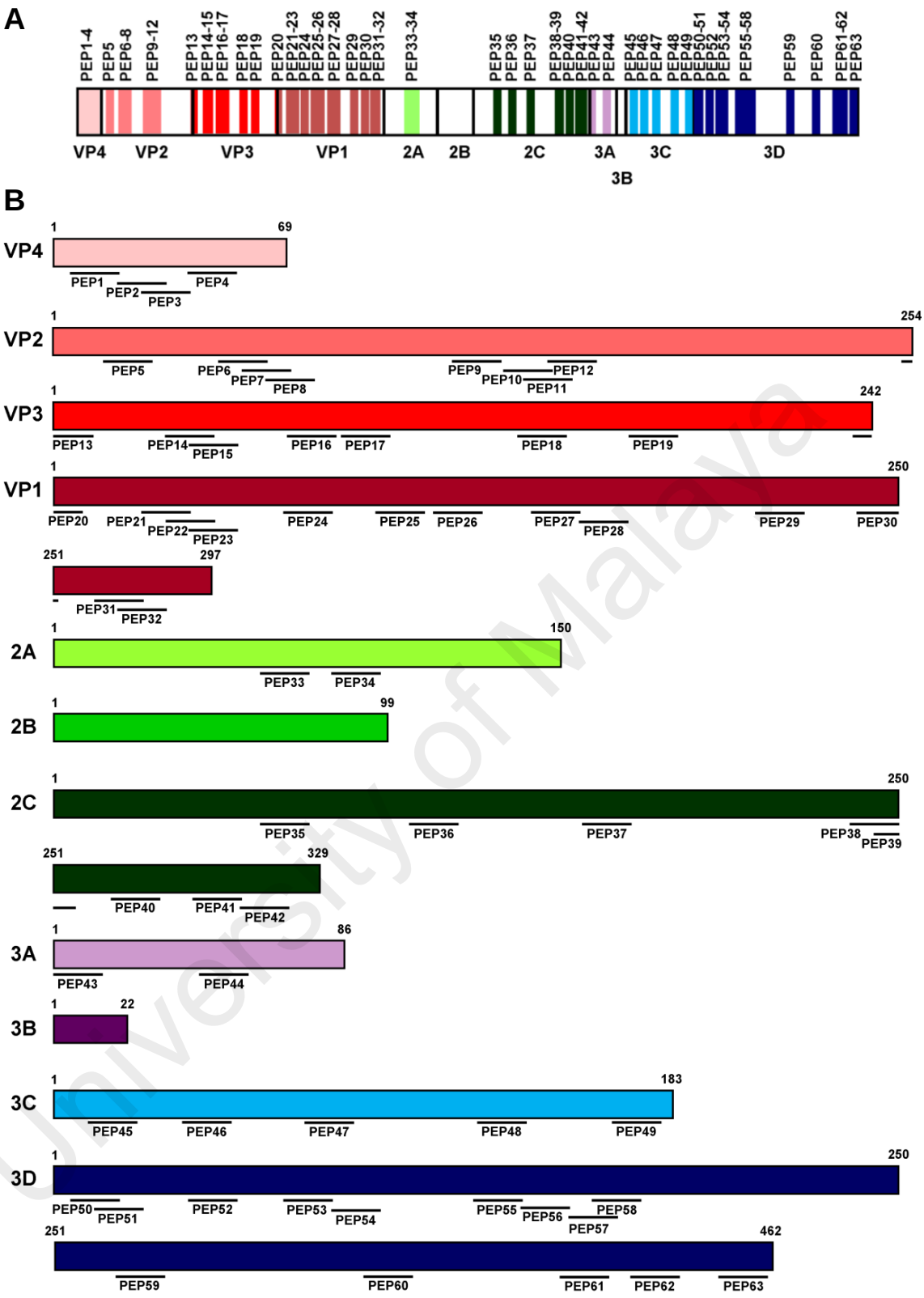

Figure 3.3: Schematic illustration of 63 synthetic biotinylated peptides. The distribution of the peptides is shown in the EV-A71 whole genome (A) and in each EV-A71 gene (B).

3.5 Determination of cellular responses in HFMD patients with specific reference to enterovirus A71

3.5.1 Study subjects

A total of 56 individuals were recruited for the intracellular cytokine staining analysis. Children clinically diagnosed as HFMD were enrolled, and were further divided into EV-A71-infected children (n=7) and CV-A6-infected children (n=7). Children from outpatient clinic with no infection in the last two weeks and neutralization titers <8 were categorized as seronegative children (n=8). All the adult subjects displayed no symptoms of HFMD during the sampling period. Healthy adult subjects were further divided into two categories: seropositive (n=22; neutralization titer ≥1:8) and seronegative (n=11; neutralization titer <1:8). All child participants were recruited through UMMC, Kuala Lumpur, whereas healthy adult subjects were volunteers from the Department of Medical Microbiology and the Department of Pathology, University of Malaya. This study was approved by the UMMC Medical Ethics Committee (reference number: 932.17).

3.5.2 Peripheral blood mononuclear cells isolation and cryopreservation

PBMCs were isolated from whole blood by density gradient centrifugation. Blood samples were diluted with the Roswell Park Memorial Institute 1640 medium (RPMI-1640) containing 2 mM EDTA. A volume of 20 ml of diluted blood sample was layered over 7 ml of Ficoll-Paque PLUS (GE Healthcare, Sweden) in a 50 ml conical tube. The conical tube was centrifuged at 970 x g for 22 minutes at 22℃ in a swinging-bucket rotor without brakes. The upper layer of plasma was removed and the buffy coat containing PBMCs over the Ficoll layer was transferred to a new conical tube, as shown

in Figure 3.4. The PBMCs were washed with 30 ml of RPMI-1640 with 2 mM EDTA and centrifuged at 650 x g for 10 minutes at 4 ℃. The supernatant was removed and the washing steps were repeated with centrifugation at 450 x g and 300 x g for 10 minutes each at 4 ℃. The supernatant was removed and 5 ml of RPMI-1640 supplemented with 10% FBS was added. Cell count was performed and the PBMCs were cryopreserved with freezing medium (FBS with 10% DMSO).

3.5.3 Intracellular cytokine staining

PBMCs were seeded in a 6-well plate at a density of 1 x 10^6 cells/well and rested for 2 days at 37 ℃ in 5% CO_2. PMBCs were then stimulated with sucrose cushion purified EV-A71 at a multiplicity of infection (MOI) of 1 for 24 hours supplemented with 50 IU/ml of rIL-2 (Sigma Aldrich, Germany). The cell culture was stimulated with 10 µg/ml of phytohemagglutinin (PHA; Sigma Aldrich, Germany) positive control. The stimulated PBMCs were subsequently incubated for an additional 3 hours with Brefeldin A (Sigma Aldrich, Germany) at a final concentration of 10 µg/ml. The cells were harvested and washed twice with staining buffer (PBS supplemented with 2% FBS). The cells were then stained with fluorescent mouse anti-human monoclonal antibodies specific for CD3-APC (clone UCHT1), CD4-PerCP-Cy5.5 (clone RPA-T4) and CD8-PE (clone HIT8a) as surface markers for 30 minutes at 4 ℃. Later, the cells were washed before fixation and permeabilization with BD Cytofix/Cytoperm Fixation/Permeabilization Kit (BD Bioscience, USA) for 30 minutes at 4 ℃. The cells were washed with BD perm/wash buffer and stained with IFN-γ FITC antibody (clone 4S.B3) for 30 minutes at 4 ℃. To analyze the function of granzyme B, perforin and CD57 in HFMD patient samples, the PBMCs were stained with antibodies specific for CD3-PerCP-Cy5.5 (clone SK7), CD8-APC (clone SK1) and CD57-FITC (clone HNK-1)

as surface markers, and then intracellularly stained with perforin-AlexaFluor 647 (clone δG9) and granzyme B-PE (clone GB11). All antibodies were from BD Bioscience, USA. All fluorescent lymphocytes were analyzed using a FACSCanto II flow cytometer (BD Biosciences, USA). Approximately 30,000 events were acquired for each sample. Acquisition was performed with BD FACSDiva software v6.1.3 (BD Biosciences, USA). Data were analyzed using the FlowJo software version 9.3.1 (Tree Star, San Carlos, CA).

3.6 Statistical analysis

Clinical data of EV-A71 and CV-A6 patients were analysed using IBM SPSS statistics 22.0 (IBM, New York, USA), and the categorical variables were compared using Fisher's exact test or chi-square test. The sensitivity, specificity, positive predictive value (PPV), and negative predictive value (NPV) of EV-A71 IgM-capture ELISA and EV-A71 IgM GICA were calculated, and compared using Fisher's exact test. The S/CO values of EV-A71 IgM-capture ELISA for EV-A71-positive sera and false-positive samples were compared using the Mann-Whitney U test or one-way ANOVA with the Kruskal-Wallis test. The EV-A71-specific IgM and IgG antibody detection with individual serum were compared using one-way ANOVA with the Kruskal-Wallis test. The expression levels of $CD3^+$ IFN-γ^+, $CD4^+$ IFN-γ^+, $CD8^+$ IFN-γ^+, $CD8^+$ granzyme B^+, $CD8^+$ $perforin^+$ and $CD8^+$ $CD57^+$ were compared using the Mann-Whitney U test.

Cohen's kappa (κ) was used to estimate inter-assay concordance between EV-A71 IgM capture ELISA and EV-A71 GICA, with a value ranging between 0 (no agreement) to 1 (complete agreement). Correlation analysis among granzyme B, perforin and/or CD57 was performed using Spearman rank correlation analysis.

All of the graphs were plotted and statistical analyses were performed using GraphPad Prism version 5.0 (GraphPad software, La Jolla, CA). Statistical significance was calculated using appropriate statistical tests (Fisher's exact test, chi-square test, Mann-Whitney U test, one-way ANOVA with the Kruskal-Wallis test, Cohen's kappa or Spearman rank correlation analysis). A p value of <0.05 was considered as statistically significant.

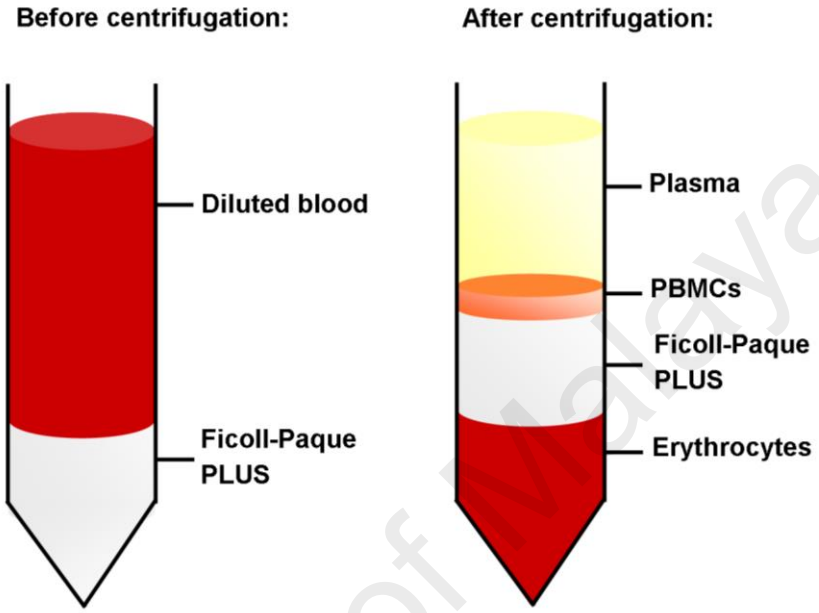

Figure 3.4: Schematic illustration of PBMCs isolation. Diluted blood sample was layered over Ficoll-Paque PLUS in a 50 ml conical tube. After centrifugation, blood sample was separated into few layers as the following components from the top: plasma, PBMCs (lymphocytes and monocytes), Ficoll-Paque PLUS and erythrocytes.

CHAPTER 4

RESULTS

4.1 Enterovirus identification in HFMD patients

4.1.1 Enterovirus identification

To determine the humoral and cellular immune responses in HFMD patients, well-characterized sera are required. From May 2012 to September 2013, enteroviruses were detected in 25 out of 42 (59.5%) throat swab specimens collected from children with suspected HFMD who attended at UMMC, Kuala Lumpur. Based on the results of sequencing the 5' UTR gene, the predominant serotypes were EV-A71 (n=12; 48%) and CV-A6 (n=12; 48%), followed by CV-A16 (n=1; 4%). This confirms that multiple enteroviruses co-circulate endemically.

4.1.2 Epidemiology and clinical manifestations

The complete demographic and clinical data of 11 EV-A71 and 11 CV-A6 patients were available for comparison (Table 4.1). The EV-A71-infected children (mean, 3.3 years) were significantly older than the CV-A6-infected patients (mean, 2.1 years; p=0.001). There was a non-significant trend towards hospitalization for CV-A6 patients, with 4 patients admitted for 0.5 ± 0.82 days, while none of the EV-A71-infected patients required hospital admission. Both sets of patients had the classical symptoms of HFMD including mouth/throat ulcers and/or hand/feet lesions. There were no significant differences in the clinical presentations. Only one patient was confirmed as CV-A16-infected patient in this study, and hence was not included in the analysis.

Table 4.1: The demographic and clinical characteristics of patients with EV-A71 and CV-A6 infection

	EV-A71 (n=11)		CV-A6 (n=11)		
	n	**%**	**n**	**%**	**p value**
Demographic					
Male: female ratio	1:1.8		2.7:1		0.198
Ethnicity:					0.495
(a) Malay	9	81.8	8	72.7	
(b) Chinese	1	9.1	-	-	
(c) Indian	1	9.1	2	18.2	
(d) Others	-	-	1	9.1	
Mean age ± SD at enrolment (years)	3.29 ± 0.85		2.08 ± 2.29		**0.001***
Clinical manifestations					
Length of history:					0.650
(a) 1 – 2 days	7	63.6	5	45.5	
(b) 3 – 4 days	3	27.3	5	45.5	
Hospitalized	0	0	4	36.4	0.090
Fever	8	72.7	10	90.9	0.586
Mouth/throat ulcers	11	100	9	81.8	0.476
Hand lesions:					0.442
(a) Palms	8	72.7	7	63.6	
(b) Dorsum and palms	2	18.2	-	-	
(c) No lesions	1	9.1	1	9.1	
Foot lesions	6	54.5	9	81.8	0.361

* Significant difference

4.1.3 Phylogenetic analyses

To identify the enterovirus serotype, the partial 5' UTR gene (positions 127 to 553) for each isolate was sequenced and aligned with relevant sequences available in the Genbank. Phylogenetic analysis of 5' UTR showed that the isolates were grouped into EV-A71 (n=11), CV-A16 (n=1) and CV-A6 (n=10) (Figure 4.1), similar to the BLAST result. Three isolates could not be sequenced, and were not included in the phylogenetic analysis. Based on the 5' UTR phylogenetic tree, EV-A71 was divided into 2 groups, where the first group is belonged to genotype C, while the another group with EV-A71 isolates from this study is belonged to genotype B (Figure 4.1). The segregation is probably due to recombination among enteroviruses.

Next, the VP4 gene for EV-A71 isolates, and VP1 gene for CV-A16 and CV-A6 isolates were sequenced for genotyping. EV-A71 VP4 sequences from the present study (n=12) were aligned with other previously published EV-A71 sequences from Malaysia. Based on the VP4 phylogenetic tree, isolates from this study were solely grouped in a distinct cluster within subgenotype B5 (Figure 4.2). Similarly, the sequence of CV-A16 isolate from this study (n=1) was aligned with other previously published CV-A16 sequences from Malaysia. Based on the VP1 phylogenetic tree, CV-A16 isolate was grouped into subgenotype B2b (Figure 4.3). This shows the EV-A71 B5 strains and CV-A16 B2b strains continue to evolve since its emergence in Malaysia in 2000 and 2003, respectively.

There are limited CV-A6 sequences available, hence only those from China, France, Japan, Spain and Taiwan were used for comparison. The phylogenetic tree of CV-A6 based on these 168 partial VP1 sequences (Figure 4.4) showed the same topology with the CV-A6 phylogenetic trees constructed by He *et al.* (2013). Based on this genotyping, CV-A6 is grouped into four major clusters, denoted as B, C and D, with genotypes C

and D further divided into genotypes C1, C2, D1 and D2. Five Malaysian sequences in present study were clustered into genotype D1 while seven sequences were clustered into genotype D2. Within both clusters, Malaysian sequences in present study were closely related to isolates from Seri Kembangan, Malaysia and China. Co-circulation of multiple clusters was observed in countries like Malaysia, China, and France. Globally, genotype B circulated from 1992-2004 and was replaced by genotypes C1 and C2, which were found between 1999-2011; in turn, these were replaced by genotypes D1 and D2, the dominant genotypes in all the recent outbreaks in Taiwan, Spain, France, China and Malaysia (Figure 4.4). This study demonstrates a high diversity of the circulating CV-A6 genotypes which possibly promoted the rapid spread of CV-A6 globally in recent years.

4.1.4 Evolutionary rates

To understand the evolutionary dynamics of EV-A71, CV-A16 and CV-A6, a Bayesian uncorrelated lognormal relaxed molecular clock model was used to estimate the evolutionary rate of these enteroviruses. In EV-A71, the evolutionary rate of VP4 gene is 7.8×10^{-3} (highest posterior density, HPD, $6.0\text{-}9.6 \times 10^{-3}$) substitutions per site per year. The VP1 gene evolutionary rates of CV-A16 and CV-A6 were 4.8×10^{-3} (HPD, $3.8\text{-}5.8 \times 10^{-3}$), and 6.8×10^{-3} (HPD, $5.6\text{-}8.3 \times 10^{-3}$) substitutions per site per year, respectively.

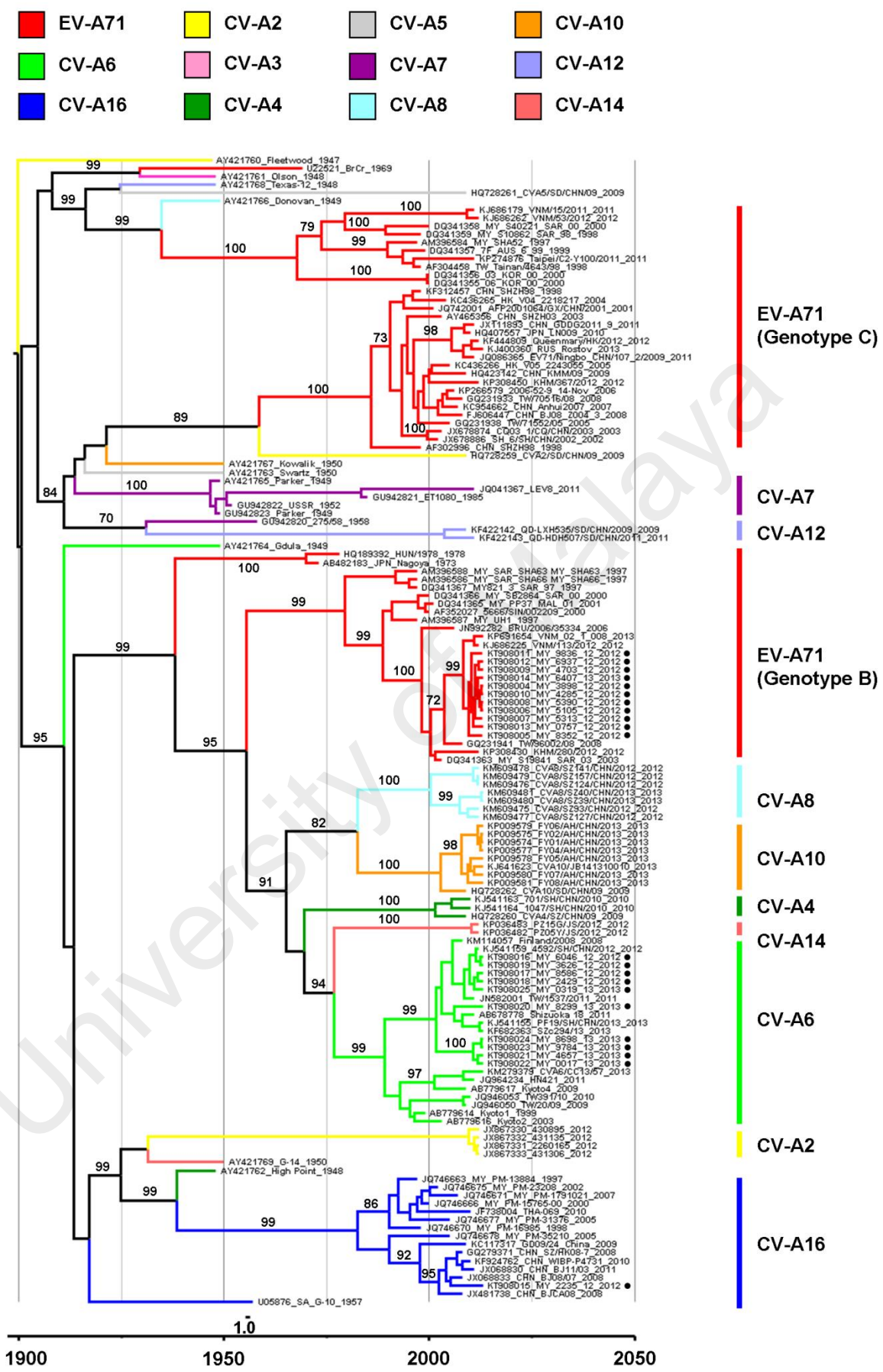

Figure 4.1: Phylogenetic analysis of enteroviruses based on partial 5' UTR gene sequences (434 bp). The phylogenetic tree was constructed using the Bayesian MCMC method implemented in BEAST with a TIM2EF+I+G nucleotide substitution model. Only bootstrap values over 70% are shown. The dots (●) indicate sequences from the present study.

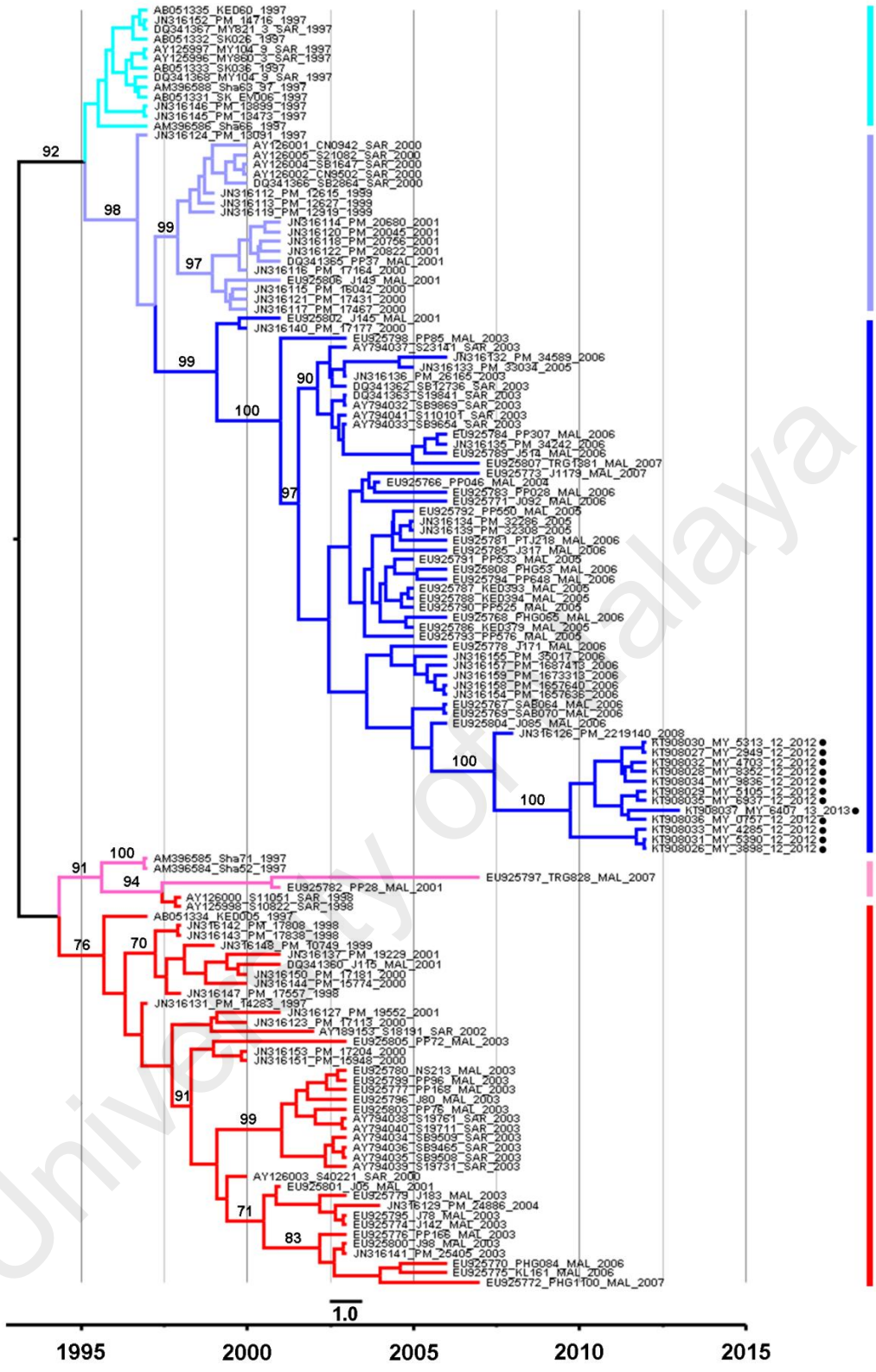

Figure 4.2: Phylogenetic analysis of EV-A71 based on VP4 gene sequences (207 bp). The phylogenetic tree was constructed using the Bayesian MCMC method implemented in BEAST with a HKY+G nucleotide substitution model. Only bootstrap values over 70% are shown. The dots (●) indicate EV-A71 strains from the present study.

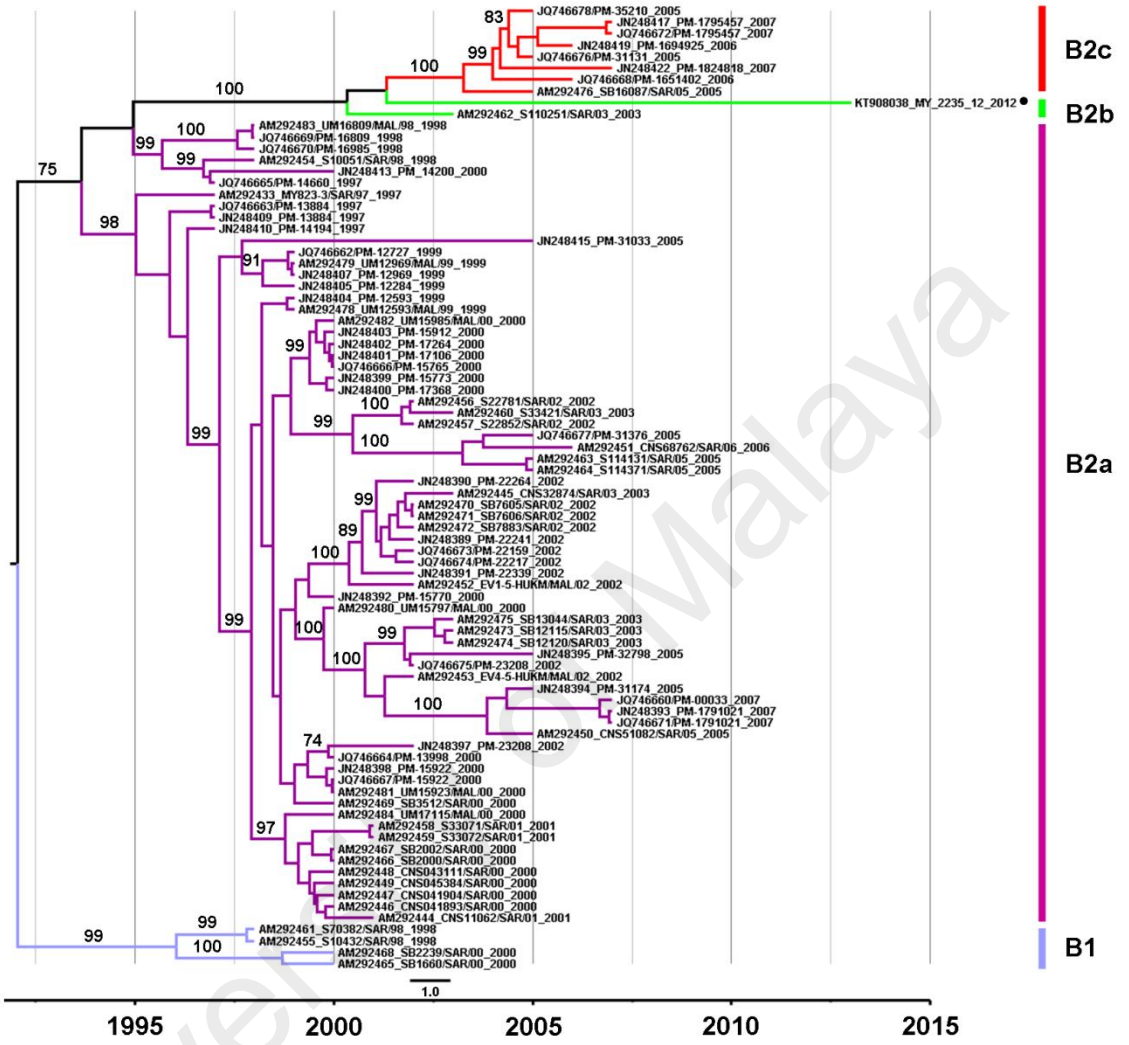

Figure 4.3: Phylogenetic analysis of CV-A16 based on VP1 gene sequences (891 bp). The phylogenetic tree was constructed using the Bayesian MCMC method implemented in BEAST with a TIM2+I+G nucleotide substitution model. Only bootstrap values over 70% are shown. The dot (●) indicates the CV-A16 strain from the present study.

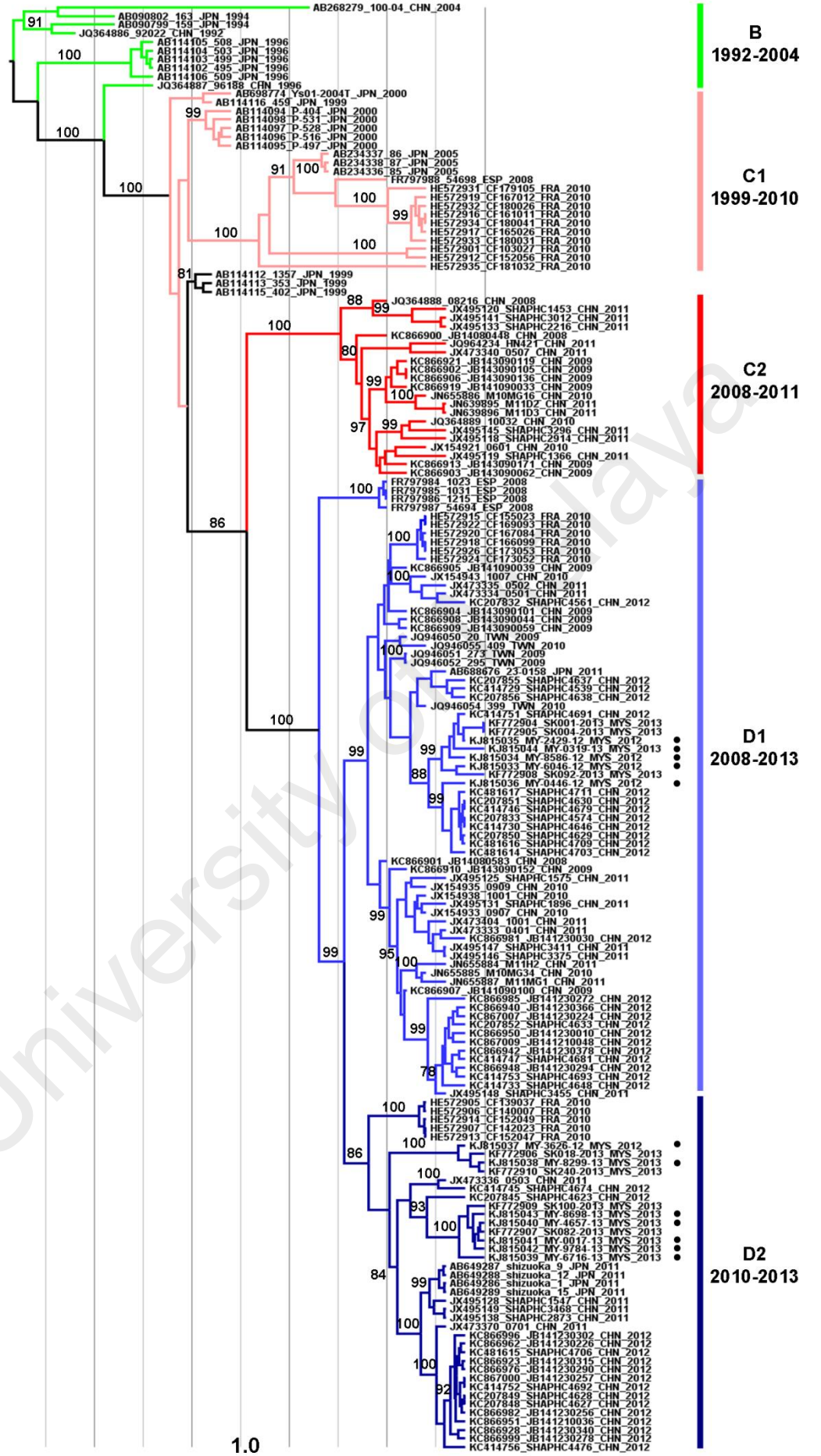

Figure 4.4: Phylogenetic analysis of CV-A6 based on partial VP1 gene sequences (657 bp). The phylogenetic tree was constructed using the Bayesian MCMC method implemented in BEAST with a K80+G nucleotide substitution model. Only bootstrap values over 70% are shown. The sequences were divided into five clusters: genotypes B, C1, C2, D1 and D2. The dots (●) indicate the CV-A6 strain from the present study.

4.2 Antibody detection in HFMD patients

Well-characterized sera are required to determine the adaptive immune responses in HFMD patients. In the present study, the levels of anti-EV-A71 IgM and IgG, and neutralization titers against EV-A71 in patients clinically diagnosed as HFMD were determined. Subsequently, we characterized the sera into three categories: acute, early convalescent and late convalescent to investigate the humoral and cellular immune responses at different stages of HFMD.

4.2.1 Anti-EV-A71 IgM antibody detection

4.2.1.1 Grouping of serum samples

A total of 89 HFMD sera (36 sera from panel A and 53 sera from panel B) and 47 non-HFMD sera (panel C) were used for IgM detection (Table 4.2). Of these, 37 HFMD sera were from EV-A71-positive patients (confirmed by RT-PCR or culture), and 24 sera were from patients positive for non-EV-A71 enteroviruses, which consisted of CV-A4 (n=1), CV-A6 (n=10), CV-A16 (n=2), CV-B (n=1), echovirus 7 (n=6), rhinovirus (n=1) and untyped enteroviruses (n=3). The remaining HFMD sera were enterovirus RT-PCR-/culture-negative (n=28).

4.2.1.2 Performance characteristics of IgM-capture ELISA and IgM GICA

Two commercially available IgM diagnostic kits, EV-A71 IgM-capture ELISA and EV-A71 IgM GICA were used. Both diagnostic kits had previously only been assessed in China (Xu *et al.*, 2010, Yu *et al.*, 2012, Wang *et al.*, 2015b, Zhang *et al.*, 2016). It is

critical to evaluate assays in different geographical settings, where there may be potential differences in circulating EV-A71 genotype and patient immune responses.

Overall, sensitivity and specificity rates were moderately good. The sensitivity rates for ELISA and GICA were 78.4% and 75.7%, respectively, and specificity rates were 89.9% and 85.9%, respectively (Table 4.3). Negative predictive value (NPV) rates were >90%, but positive predictive value (PPV) rates were moderate for ELISA (74.4%) and GICA (66.7%). Performances of the assays were also determined just for the HFMD cases, as this is the most likely group to be tested for EV-A71 IgM. Specificity (ELISA, 80.8% and GICA, 76.9%) and NPV (ELISA, 84.0% and GICA, 81.6%) decreased, while PPV remained similar. There were no significant differences in sensitivity, specificity, PPV and NPV rates between the two assays.

Concordance between the results of the two assays for each category of sera is shown in Table 4.4. The overall concordance was 91.1%, with a κ value of 0.805. The concordance for testing the HFMD sera (panels A and B) was 92.1%, with a κ value of 0.841. The concordance for testing EV-A71-positive sera was 97.3%, with a κ value of 0.924 indicating almost perfect agreement, whereas the concordance for testing EV-A71 negative control subjects was 91.9%, with a κ value of 0.622.

4.2.1.3 False positive rates of IgM-capture ELISA and IgM GICA

Next, the false positive rates in sera obtained from patients who tested negative for EV-A71 were compared. In HFMD sera, anti-EV-A71 IgM was detected in 10/52 (19.2%) and 12/52 (23.1%) with IgM-capture ELISA and IgM GICA, respectively. Of those with confirmed enterovirus (other than EV-A71) infection, anti-EV-A71 IgM was detected in 3/24 (12.5%) and 4/24 (16.7%) with IgM-capture ELISA and IgM GICA,

respectively (Table 4.5). These false positives were detected in patients infected with echovirus 7 (n=2) and CV-A16 (n=1) in the IgM-capture ELISA assay, whereas the false positives in the IgM-GICA assay were seen in patients with echovirus 7 (n=1), CV-A16 (n=1) and CV-A6 (n=2). Two samples (one each with echovirus 7 and CV-A16) were positive with both assays. In enterovirus RT-PCR-/culture-negative sera, anti-EV-A71 IgM was detected in 7/28 (25.0%) and 8/28 (28.6%) with IgM-capture ELISA and IgM GICA, respectively. For the non-HFMD sera, only the IgM GICA recorded false positives, in 2/47 (4.3%) samples.

Overall, the mean S/CO value (0.76 ± 2.37) of the false-positive samples was significantly lower than the mean S/CO value of 4.70 ± 3.91 for the EV-A71-positive sera (Figure 4.5). Furthermore, the mean S/CO values of EV-A71-positive sera was also significantly higher than the mean S/CO values of non-EV-A71 enterovirus-positive sera, enterovirus RT-PCR-/culture-negative sera and non-HFMD sera, at 1.29 ± 3.27, 1.38 ± 3.15 and 0.11 ± 0.14, respectively.

4.2.2 Anti-EV-A71 IgG antibody detection

EV-A71-specific IgG antibody in serum specimens was also determined by immunoblotting analysis. Due to insufficient volume of remaining samples, 70 out of 89 HFMD sera were tested for anti-EV-A71 IgG detection (Appendix V). Of these, anti-EV-A71 IgG was detected in 54/70 (77.1%). Anti-EV-A71 IgG was detected in 31/35 (88.6%) of EV-A71-positive patients, 9/12 (75.0%) of non-EV-A71 enterovirus-positive patients, and 60.9% (14/23) of enterovirus RT-PCR-/culture-negative patients.

Table 4.2: Classification of serum samples used for the evaluation of EV-A71 commercial diagnostic kits

Group	Panel A 2000 outbreak	Panel B 2012-2013 outbreak	Panel C non-HFMD controls	Total
EV-A71[a]	24	13	N/A	37
Non-EV-A71 enterovirus[a,b]	12	12	N/A	24
Enterovirus RT-PCR-/culture negative[a]	N/A	28	N/A	28
Non-HFMD	N/A	N/A	47	47
Total	36	53	47	136

[a] tested on throat swabs, vesicle swabs and/or rectal swabs from the same patient; all patients in panels A and B had suspected HFMD

[b] CV-A4 (n=1), CV-A6 (n=10), CV-A16 (n=2), CV-B (n=1), echovirus 7 (n=6), rhinovirus (n=1), untyped enteroviruses (n=3).

N/A, not applicable

Table 4.3: Comparative performances of the EV-A71 IgM-capture ELISA and EV-A71 IgM GICA in serum samples

		EV-A71 (n=37)		Non-EV-A71		Sensitivity, % [95% CI]	Specificity, % [95% CI]	PPV, % [95% CI]	NPV, % [95% CI]
		IgM positive	IgM negative	IgM positive	IgM negative				
Overall analysis[a]	**EV-A71 IgM-capture ELISA**	29	8	10	89	78.4 (29/37) [62.6–88.9]	89.9 (89/99) [82.2-94.6]	74.4 (29/39) [58.8-85.6]	91.8 (89/97) [84.4-96.0]
	EV-A71 IgM-GICA	28	9	14	85	75.7 (28/37) [59.7-86.8]	85.9 (85/99) [77.5-91.5]	66.7 (28/42) [51.5-79.1]	90.4 (85/94) [82.6-95.1]
Analysis of HFMD cases[b]	**EV-A71 IgM-capture ELISA**	29	8	10	42	78.4 (29/37) [62.6–88.9]	80.8 (42/52) [67.9-89.4]	74.4 (29/39) [58.8-85.6]	84.0 (42/50) [71.2-91.9]
	EV-A71 IgM-GICA	28	9	12	40	75.7 (28/37) [59.7-86.8]	76.9 (40/52) [63.7-86.4]	70.0 (28/40) [54.5-82.0]	81.6 (40/49) [68.4-90.3]

[a] non-EV-A71 cases comprising non-EV-A71 enterovirus, enterovirus RT-PCR-/culture-negative, and non-HFMD cases (n=99) for overall analysis

[b] non-EV-A71 cases comprising non-EV-A71 enterovirus and enterovirus RT-PCR-/culture-negative cases (n=52), all of whom had suspected HFMD

Table 4.4: Concordance between EV-A71 IgM-capture ELISA and EV-A71 IgM GICA

EV-A71 IgM-capture ELISA		EV-A71 IgM GICA								
		EV-A71		**Non-EV-A71 enterovirus**		**Enterovirus RT-PCR-/culture-negative**		**Non-HFMD**		
		+	-	+	-	+	-	+	-	**Total**
EV-A71	+	28	1							29
	-	0	8							8
Non-EV-A71 enteroviruses	+			2	1					3
	-			2	19					21
Enterovirus RT-PCR-/ culture-negative	+					6	1			7
	-					2	19			21
Non-HFMD	+							0	0	0
	-							2	45	47
	Total	28	9	4	20	8	20	2	45	136

Table 4.5: Specificity and cross-reactivity of IgM anti-EV-A71 in subjects testing negative for EV-A71

		EV-A71 IgM-capture ELISA		EV-A71 IgM-GICA	
	Total no.	**IgM positive**	**Specificity, % (95% CI)**	**IgM positive**	**Specificity, % (95% CI)**
Non-EV-A71 enterovirus	24	3	87.5 (68.2-96.5)	4	83.3 (63.5-93.9)
Enterovirus RT-PCR/culture-negative	28	7	75.0 (56.4-87.6)	8	71.4 (52.8-84.9)
Non-HFMD	47	0	100 (91.0-100)	2	95.7 (85.0-99.6)

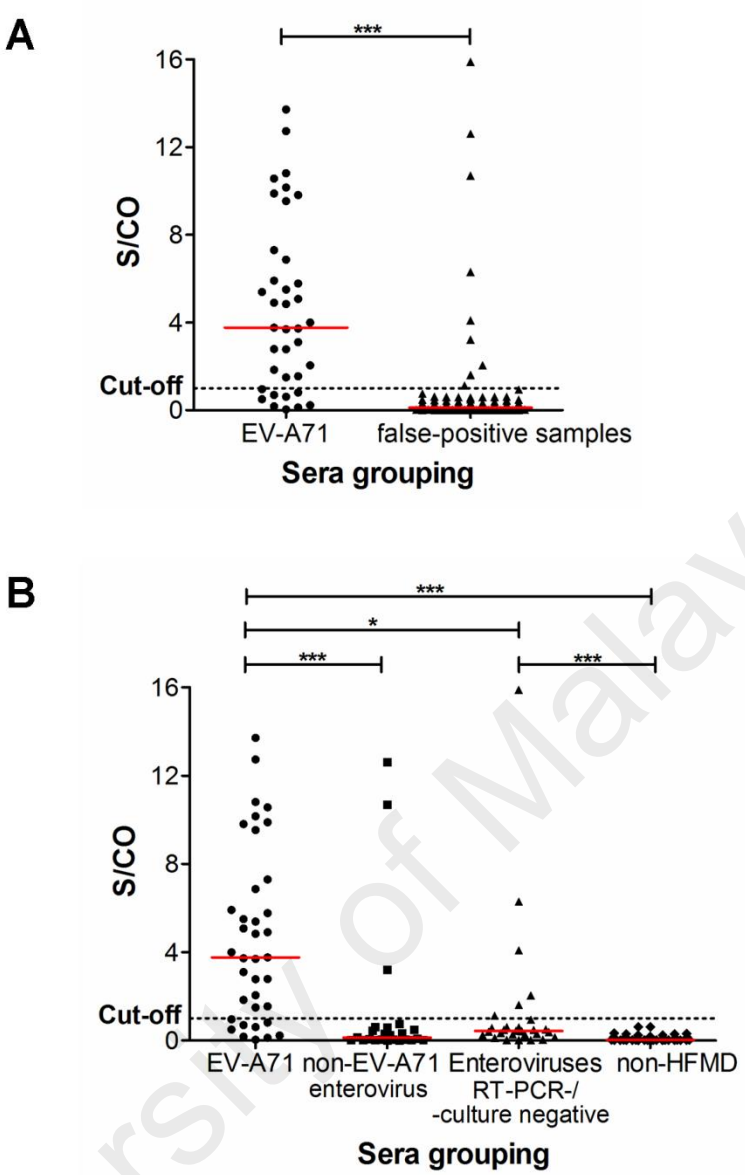

Figure 4.5: Signal/cut-off (S/CO) values for EV-A71 IgM-capture ELISA. (A) Comparison of S/CO values for EV-A71-positive sera and overall false-positive samples. (B) Comparison of S/CO values for EV-A71-positive sera and other groups of false-positive sera. Red solid lines represent medians and dotted straight lines represent the cut-off value (S/CO value: 1). Values above the cut-off value were scored as positive. Mann-Whitney U test and one-way ANOVA with Kruskal-Wallis test were used for statistical analysis (*P<0.05, ***P<0.001).

4.2.3 Neutralization titers

Serum specimens were considered seropositive if the neutralizing titer was ≥1:8. Of the 70 HFMD sera tested for both EV-A71 IgM and IgG, 11 were not tested for neutralization test as the sera obtained were limited. Overall, 52/59 (88.1%) of HFMD sera were found to be seropositive. In the EV-A71 positive sera, 24/29 (82.8%) were seropositive, and 16/24 (66.7%) sera had neutralization titers ≥32. Interestingly, 9/10 (90.0%) of non-EV-A71 enterovirus sera and 19/20 (95.0%) of enterovirus RT-PCR-/culture-negative sera were seropositive.

4.2.4 Summary of antibody profiles

The complete profile of IgM and IgG antibodies, and neutralization titers for 89 HFMD sera is shown in Appendix V. Only sera from patients with PCR- or culture-confirmed EV-A71 were selected for subsequent experiments to characterize immune responses to EV-A71 and identification of immunogenic proteins. The antibody profiles for the EV-A71 positive sera are shown in Figure 4.6. The selected samples were then divided into 3 groups. Sera positive for EV-A71-specific IgM but negative for EV-A71-specific IgG, and with neutralization titers <8 were grouped as IgM^+IgG^- (n=2). This group is likely to comprise the acute infection samples, as IgM is present but IgG has not yet been produced at detectable levels. IgM^+IgG^+ sera (n=15) were those that were positive for EV-A71-specific IgM and IgG, with neutralization titers of ≥32, and these represent early convalescent infection, when IgG has become detectable. IgM^-IgG^+ sera (n=6) were those which were negative for EV-A71-specific IgM but positive for EV-A71-specific IgG, with neutralization titers ≥8, which represent the late convalescent stage of infection.

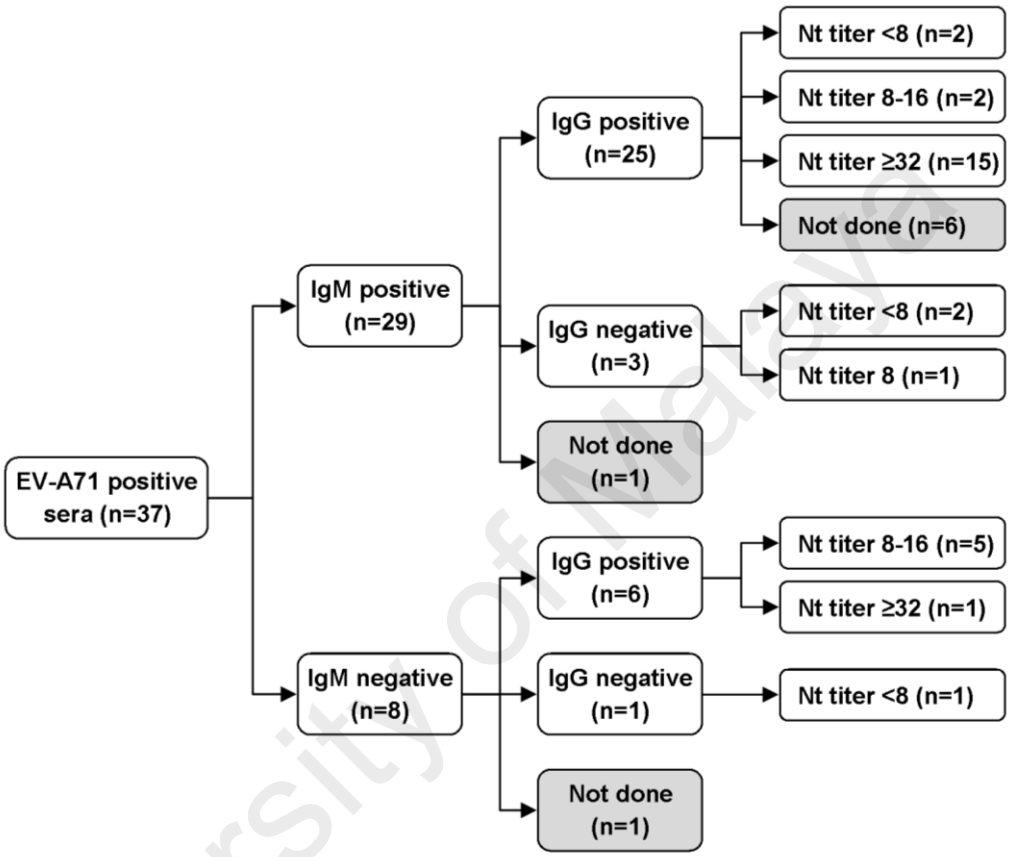

Figure 4.6: Antibody profiles for EV-A71-infected patient sera. Serum IgM and IgG antibodies, and neutralization (Nt) titers were characterized for patients with PCR- or culture-confirmed EV-A71 infections.

4.3 Identification of antigenic proteins and peptides

4.3.1 Transfection and protein expression of EGFP-expressing EV-A71 genes

Individual expression plasmids encoding each structural (VP1-4) and non-structural (2A-C, 3A-D) gene of the EV-A71 UH1/PM/1997 proteome were generated. An additional cassette with domain linker, StrepTag II, FLAG Tag and 8X His-Tag functions was included in pEGFP-cassette-VP1, -VP2, -VP3, -VP4, -3C and -3D expression plasmids. The domain linker is a short peptide sequence composed of flexible residues such as glycine and serine to allow the recombinant proteins to rotate independently from the C-terminus EGFP. StrepTag II and 8X-His Tag were also inserted for protein purification, while FLAG Tag allows detection with an anti-FLAG monoclonal antibody (mAb).

After transient transfection in HEK293 cells, all recombinant EV-A71 EGFP proteins were successfully expressed, except recombinant EV-A71 2A protein (Figure 4.7). To resolve this problem, recombinant EV-A71 2A protein was expressed in a bacterial expression system with pET-52b(+)-2A expression plasmids. EV-A71 virions were purified by sucrose cushion purification and lysates were prepared under reducing conditions. EV-A71 viral proteins were then stained with Coomassie brilliant blue R-250 and immunoblot analysis was performed with mAb 3323 (Millipore, USA) and mAb 979 (Millipore, USA) (Figure 4.8A). Both EV-A71-specific mAb detected VP0 (36 kDa) and VP2 (28 kDa) proteins, and mAb 979 further detected P1 proteins (95 kDa), VP4+VP2+VP3 proteins (62 kDa) and another protein of approximately 25 kDa that could be the proteolytic product of P1 protein. All recombinant EV-A71 EGFP proteins were purified and confirmed by immunoblotting with anti-GFP antibody (Figure 4.8B), whereas EV-A71 2A proteins were assessed by immunoblotting with

Coomassie brilliant blue R-250 staining (Figure 4.8C). In summary, all recombinant proteins were successfully expressed.

4.3.2 Identification of antigenic protein

4.3.2.1 Antigen recognition by EV-A71-infected patient sera

Sera characterized in section 4.2 were used. EV-A71-specific IgM antibody (from IgM^+ IgG^- sera and IgM^+ IgG^+ sera) recognized all structural proteins (VP1 to VP4) and non-structural proteins 2A, 3C and 3D (Figure 4.9A and B). EV-A71-specific IgG antibody (from IgM^+ IgG^+ sera and IgM^- IgG^+ sera) recognized all structural and non-structural proteins (Figure 4.9C and D). As a parallel control, all these patient sera recognized VP0 protein and an unidentified protein at ≈25 kDa in the EV-A71 virion proteins.

4.3.2.2 Antigen recognition by sera from mice immunized with inactivated EV-A71

Antibodies from sera collected from mice immunized with inactivated EV-A71 (kind gift from Kien-Chai Ong from University Malaya) recognized multiple bands in the EV-A71 virion proteins (Figure 4.10). The mouse sera also recognized all structural and non-structural proteins, similar to EV-A71-infected patient sera. This suggests that the immune profile generated from the inactivated EV-A71 mimicked the natural infection.

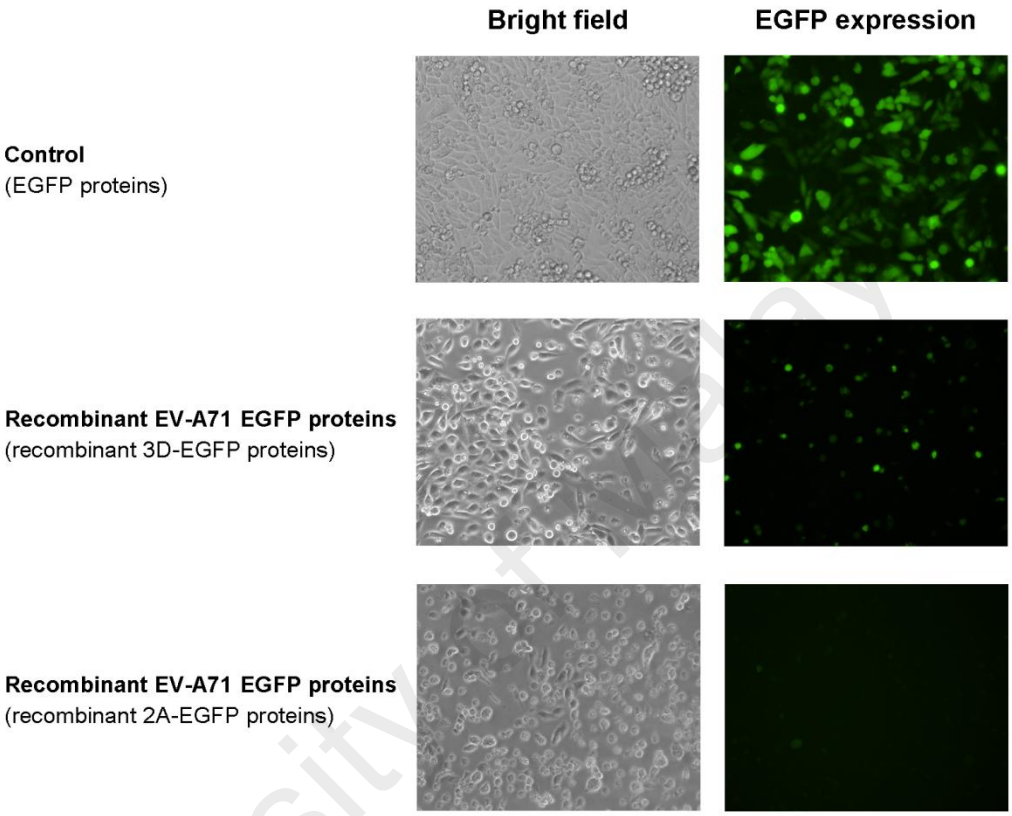

Figure 4.7: EGFP expression of recombinant EV-A71-EGFP proteins. HEK-293 cells were transiently transfected with structural and non-structural EV-A71 gene-pEGFP plasmids and EGFP expression was observed 48 hours post-infection. The EGFP signal was detected using a fluorescence microscope at an excitation wavelength of 488 nm.

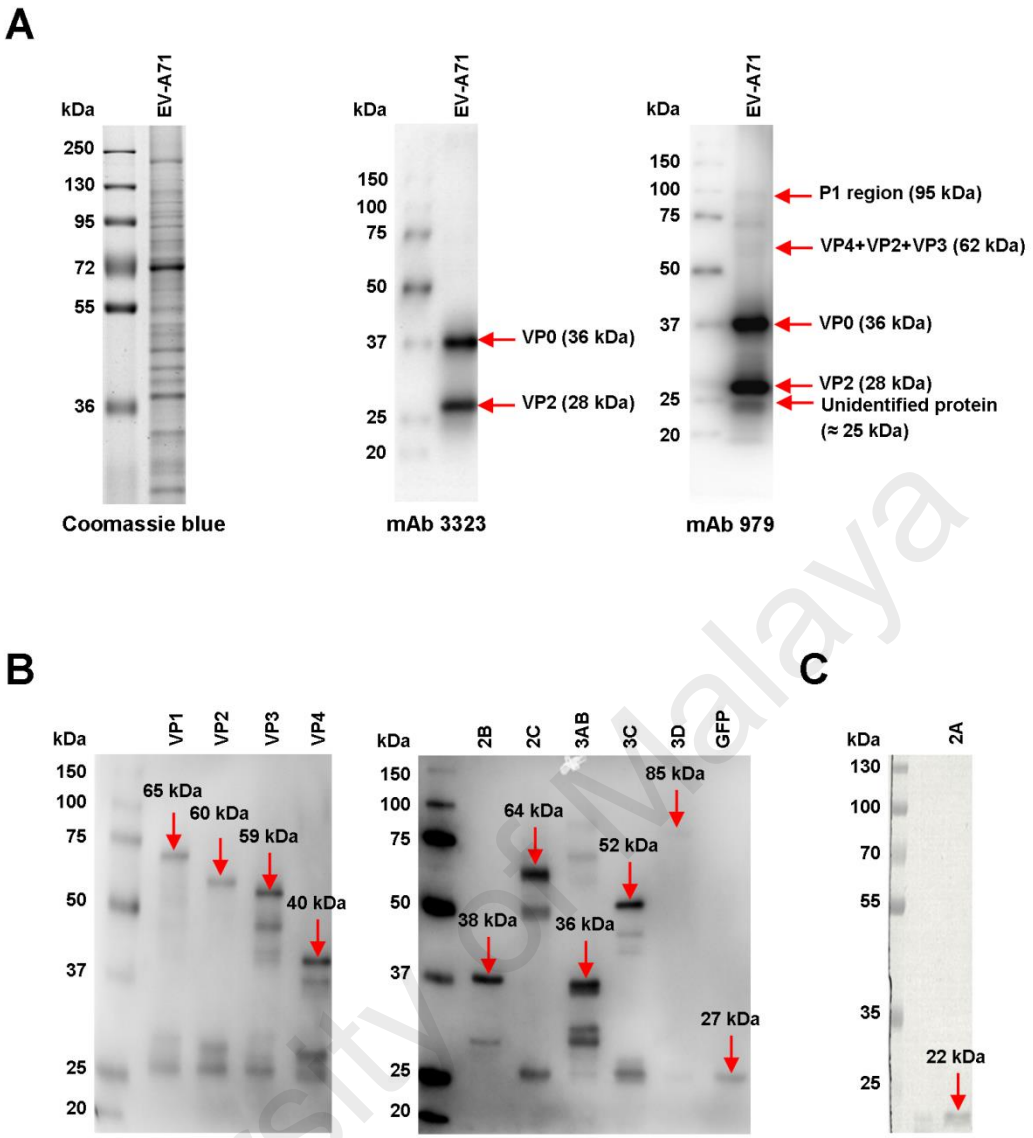

Figure 4.8: Detection of EV-A71 virion proteins and recombinant EV-A71-EGFP proteins. (A) EV-A71 virion lysates were subjected to SDS-PAGE gel electrophoresis with Coomassie brilliant blue R-250 staining or immunodetection with EV-A71-specific mAb 3323 (Millipore, USA) and mAb 979 (Millipore, USA), followed by secondary anti-mouse IgG-HRP. (B) Recombinant EV-A71-EGFP proteins (structural and non-structural proteins) were subjected to SDS-PAGE gel electrophoresis and probed with anti-GFP-HRP. (C) Recombinant EV-A71 2A proteins were subjected to SDS-PAGE gel electrophoresis and stained with Coomassie brilliant blue R-250. The expected band for each individual recombinant protein is indicated by red solid arrows and the protein size is shown.

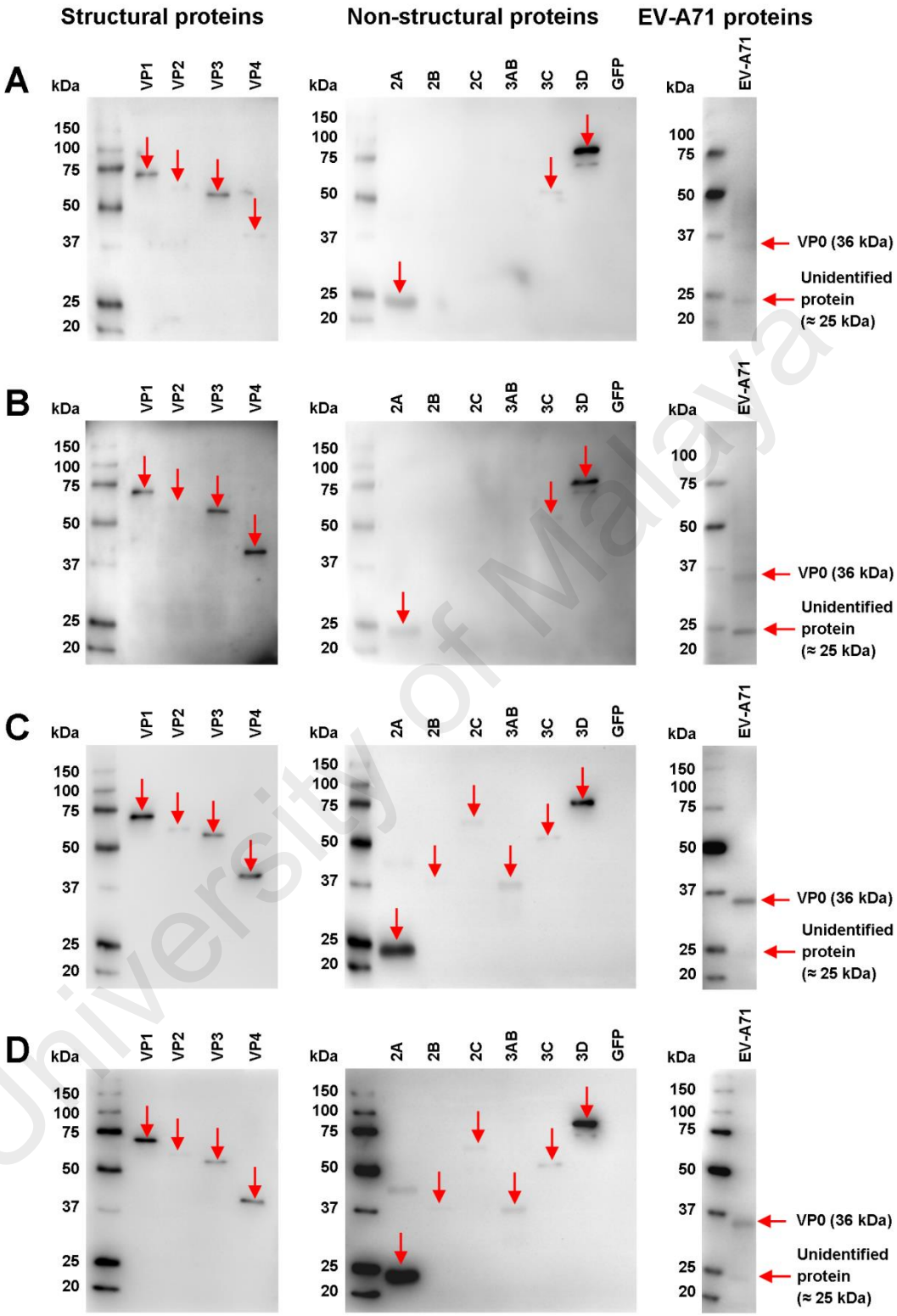

Figure 4.9: Antigenic profiles of the human anti-EV-A71 antibodies. The amount of EV-A71 structural and non-structural protein cell lysates loaded into SDS-PAGE gel electrophoresis was normalized with anti-GFP-HRP since the presence of inhibitory factors affected accurate quantitation of total proteins. The EV-A71 protein cell lysates and EV-A71 virion lysates were subjected to SDS-PAGE gel electrophoresis and probed with pooled human sera at a dilution of 1:300. (A) $IgM^{+}IgG^{-}$ sera (n=2) and (B) $IgM^{+}IgG^{+}$ sera (n=12) were used for EV-A71-specific IgM antibody detection. (C) $IgM^{+}IgG^{+}$ sera (n=12) and (D) $IgM^{-}IgG^{+}$ (n=5) sera were used for EV-A71-specific IgG antibody detection. The immunoblot was developed with Clarity Western ECL substrate and detected by chemiluminescence. The antigens recognized by EV-A71-infected patient sera are indicated by red solid arrows.

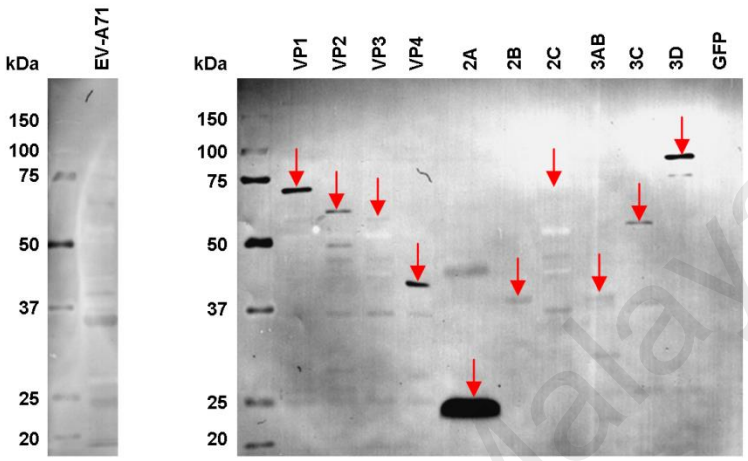

Figure 4.10: Antigenic profiles of the mouse anti-EV-A71 antibodies. The amount of EV-A71 structural and non-structural protein cell lysates loaded into SDS-PAGE gel electrophoresis was normalized with anti-GFP-HRP. The EV-A71 protein cell lysates and EV-A71 virion lysates were subjected to SDS-PAGE gel electrophoresis and probed with mouse sera immunized with inactivated EV-A71 at a dilution of 1:100, followed by secondary anti-mouse IgG-HRP. The immunoblot was developed with DAB substrate in stable peroxide substrate solution. The antigens recognized by EV-A71-infected patient sera are indicated by red solid arrows.

4.3.3 Identification of antigenic peptides

4.3.3.1 Isotyping of EV-A71-specific antibodies

Sera were tested individually with purified EV-A71 virion-based ELISA, and only those with high absorbance values were selected for this analysis. The selected EV-A71-infected sera were categorized into $IgM^{+}IgG^{+}$ (n=5) and $IgM^{-}IgG^{+}$ (n=3) sera. Healthy adult sera (n=5) with neutralization titers ≥16 and non-HFMD children sera (n=4) were also included in the analysis.

The amount of IgM and IgG present in EV-A71-infected patient sera were quantified by the purified EV-A71 virion-based ELISA. $IgM^{+}IgG^{+}$ sera had good antibody responses for EV-A71-specific IgM antibody, even at high dilution (Figure 4.11A). All human sera showed weak IgG antibody responses at higher dilution (Figure 4.11B). Therefore, the human pooled sera were optimized at dilutions of 1:2000 and 1:500 for EV-A71-specific IgM and IgG antibodies detection, respectively, in the following experiments. IgG1 subclass was the predominant isotype in the EV-A71-infected patient sera and adult sera (Figure 4.12). A stronger IgG3 subclass response was observed in EV-A71-infected children ($IgM^{+}IgG^{+}$ and $IgM^{-}IgG^{+}$ samples), but not in adults. No patterns were observed in negative control sera.

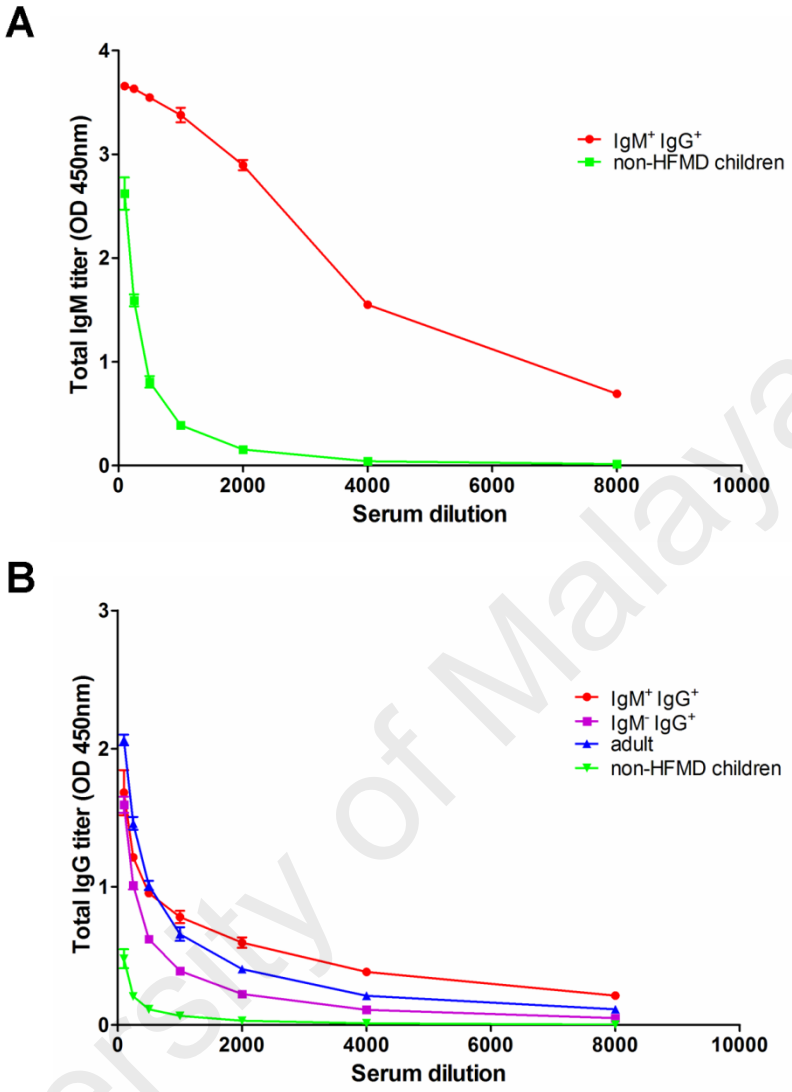

Figure 4.11: Measurement of EV-A71-specific antibodies. (A) EV-A71-specific IgM antibody titers and (B) EV-A71-specific IgG antibody titers were determined by virion-based ELISAs. EV-A71-infected patient pooled sera were assayed by serial dilution and subjected to virion-based ELISA. Non-HFMD children sera were used as negative controls. Each point represents mean ± SD of 3 replicates.

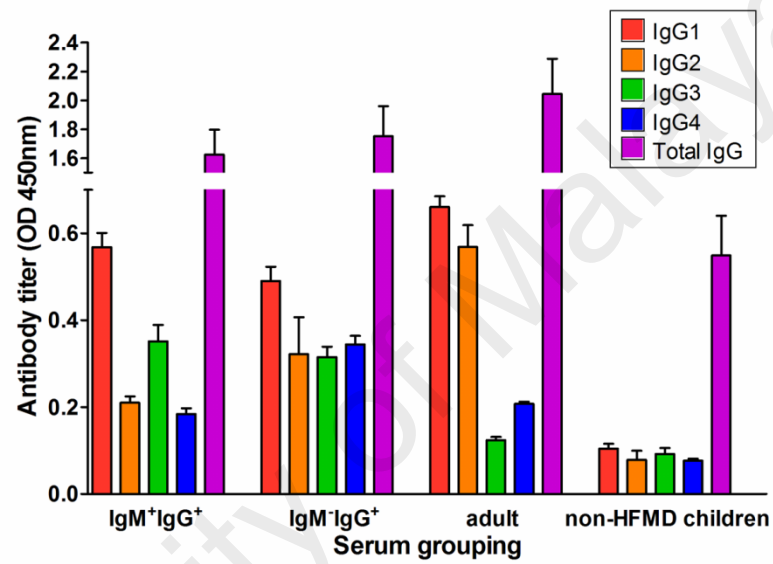

Figure 4.12: Isotyping of EV-A71 specific antibodies. EV-A71-specific IgG isotype titers in pooled sera were determined at dilutions of 1:100 using specific secondary antibodies. Data are presented as means ± SD of 3 replicates.

4.3.3.2 Mapping of EV-A71 specific peptides

A total of 63 peptides were studied as potential EV-A71 B-cell epitopes, based on prediction using EMINI surface accessibility scale or previous publications (Table 3.3). Peptide-based ELISAs using these 63 biotinylated peptides were initially performed with pooled sera using an optimized plasma dilution of 1:2000 and 1:500 for IgM and IgG antibodies detection, respectively. Interestingly, a majority of the peptides were recognized as EV-A71-specific IgM linear epitopes at S/CO above 2.1 (Figure 4.13A). $IgM^{+}IgG^{+}$ sera recognized eight EV-A71-specific IgG linear epitopes covering VP1, VP3, VP4, 2A, 3C and 3D proteins. Two dominant linear epitopes were recognized, PEP47 and PEP62 (Figure 4.13B). $IgM^{-}IgG^{+}$ sera showed similar EV-A71-specific IgG epitope profiles as adult sera, with eight and thirteen linear epitopes recognized, respectively. Both sets of sera strongly recognized PEP23 as the dominant linear epitope, and adult sera also recognized PEP30 as additional dominant linear epitope (Figure 4.13C and D). Both PEP23 and PEP30 are located at VP1 protein.

All identified B-cell linear epitopes are summarized in Figure 4.14. For the EV-A71-specific IgM linear epitopes, only dominant linear epitopes (S/CO $\geq$5) were selected for further analysis. Results were expressed as the percentage of antibody recognition within the whole EV-A71 proteome. A total of 22 EV-A71-specific IgM dominant linear epitopes were identified and the average percentage of peptide recognition by the sera was very similar (range 3.47% to 6.23%). Eight EV-A71-specific IgG linear epitopes were recognized by $IgM^{+}IgG^{+}$ pooled sera, the most strongly recognized being the PEP62 on the 3D protein and PEP47 on the 3C protein, at 31.49% and 17.35% of total antibody recognition, respectively. $IgM^{-}IgG^{+}$ sera and adult sera displayed similar antibody recognition profiles, recognizing eight and thirteen IgG linear epitopes, respectively. Both pooled sera had strongest detection signals in the VP1 protein, with

PEP23 identified as the dominant linear epitope, with 26.82% (IgM^-IgG^+ sera) and 26.29% (adult sera) of the total antibody recognition. Adult sera further recognized PEP30 (located in the VP1 protein) as another dominant linear epitope, at 10.41% of antibody recognition. No recognizable linear epitopes were found in the VP3 protein for both pooled sera. PEP23, PEP33 and PEP49, located within the VP1, 2A and 3C proteins, respectively, were recognized by EV-A71-specific IgG antibodies from all 3 groups of sera. Of these commonly recognized epitopes, PEP23 was identified as the dominant linear epitope, at 9.85, 26.82 and 26.29% of antibody recognition by IgM^+IgG^+, IgM^-IgG^+ and adult pooled sera, respectively, followed by PEP33 (7.53, 13.88 and 8.93) and PEP49 (6.87, 8.90 and 4.67%).

4.3.3.3 Seroprevalence of IgM and IgG to specific peptides

Of the 22 EV-A71-specific IgM dominant linear epitopes, 13 peptides were IgM-specific epitopes. These peptide sequences were subsequently aligned to the corresponding sequences from 12 different enteroviruses (EV-A71, CV-A2 to CV-A8, CV-A10, CV-A12, CV-A14 and CV-A16). Epitopes with conserved sequences (Appendix VI) were removed as these would likely cross-react with antibodies from other enteroviruses. The remaining five epitopes, for which EV-A71 sequences varied from other enteroviruses (Figure 4.15), were selected for study of seroprevalence in HFMD-infected patients. These were PEP12, PEP19, PEP21, PEP25 and PEP27.

To further validate the specificity of the selected IgM epitopes as suitable early detection targets, serum samples from patients infected with EV-A71 (n=22) and non-HFMD children (n=10) were screened. All IgM linear epitopes showed good responses for EV-A71-infected patient sera, particularly for PEP27, which had the highest mean OD values of 0.85 ± 0.47 (Figure 4.16A). The OD values of EV-A71-infected patient

sera were significantly higher than non-HFMD children sera for PEP12, PEP19, and PEP27, suggesting that these IgM epitopes are suitable for distinguishing EV-A71 and non-HFMD patients. To determine if the antibodies from patients infected with other enteroviruses cross-reacted with EV-A71 IgM epitopes, peptide-based ELISA was further performed using 12 serum samples from patients infected with non-EV-A71 enteroviruses. Serum samples from patients infected with non-EV-A71 enteroviruses, namely CV-A4, CV-A6, CV-A16, echovirus 7 and untyped enteroviruses, showed cross-reactivity to PEP12, PEP19 and PEP25. This cross-reactivity suggests that these IgM epitope recognitions are not EV-A71-specific. Significant differences between the OD values of EV-A71-infected and non-EV-A71-infected patient sera were observed in PEP21 and PEP27, suggesting that these IgM epitopes are EV-A71 specific. Overall, PEP27 is the best EV-A71-specific IgM epitope among the five IgM epitopes.

For the EV-A71-specific IgG epitopes, PEP23 was selected for individual serum testing, as it is the dominant linear epitope that was commonly recognized by the three sets of sera in the previous section. All individual serum selected was positive for EV-A71-specific IgG. No statistical differences were observed, as shown in Figure 4.17A. These results also suggest the EV-A71 IgG epitope PEP23 may be highly cross-reactive.

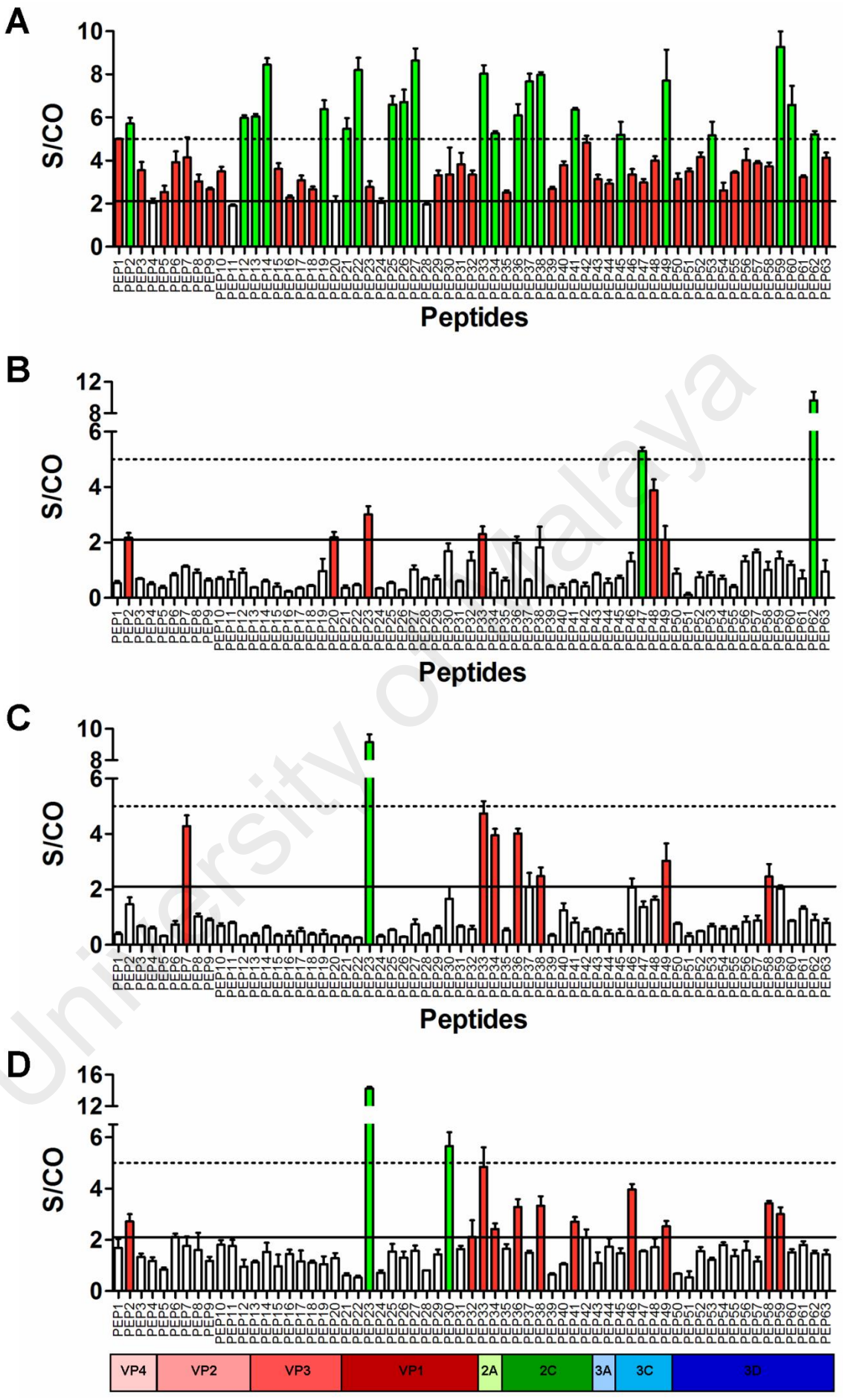

Figure 4.13: Mapping of EV-A71 B-cell epitopes within the EV-A71 proteome. Pooled human sera, at an optimized dilution of 1:2000 (IgM) and 1:500 (IgG), were subjected to peptide-based ELISA. (A) $IgM^{+}IgG^{+}$ sera (n=5) were used for EV-A71-specific IgM antibody detection. (B) $IgM^{+}IgG^{+}$ sera (n=5), (C) $IgM^{-}IgG^{+}$ (n=3) sera, and (D) adult sera (n=5) were used for EV-A71-specific IgG antibody detection. Non-HFMD children sera (n=4) were used as negative controls. Data are presented as mean ± SD of 3 replicates. Values above the solid black line (S/CO=2.1) were scored as weakly positive and values above the dotted line (S/CO=5) were scored as strongly positive reactions. Red bars represent weakly positive human anti-EV-A71 epitopes and green bars represent strongly positive human anti-EV-A71 epitopes.

A

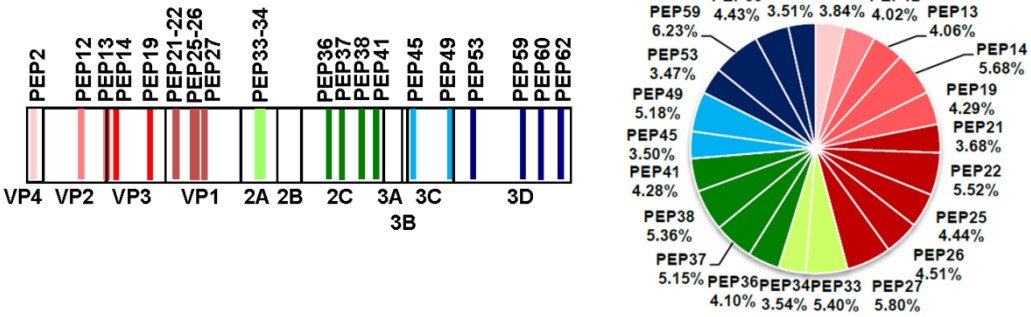

B

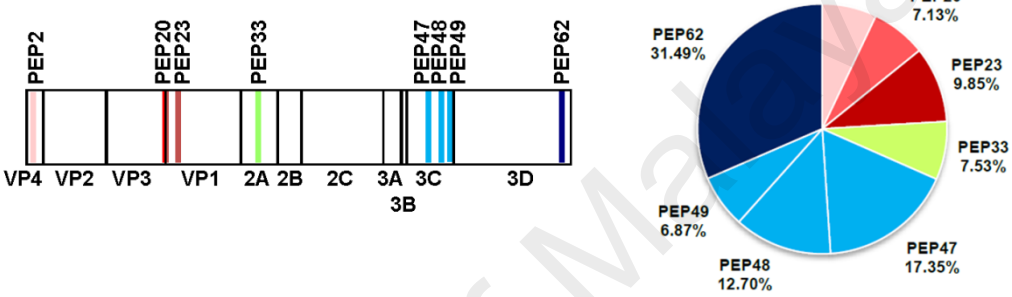

C

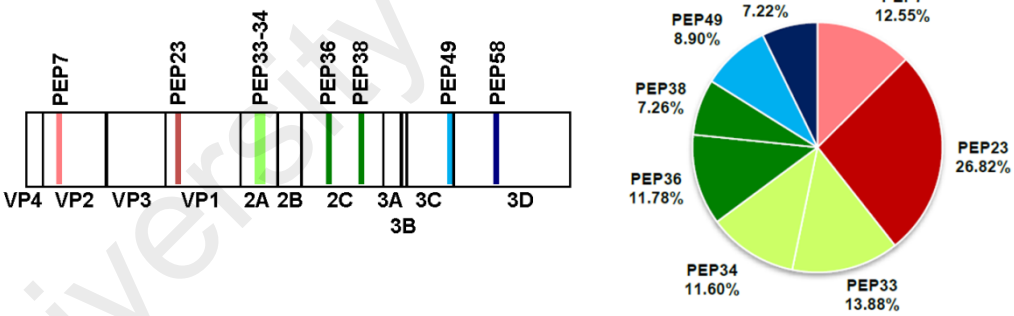

D

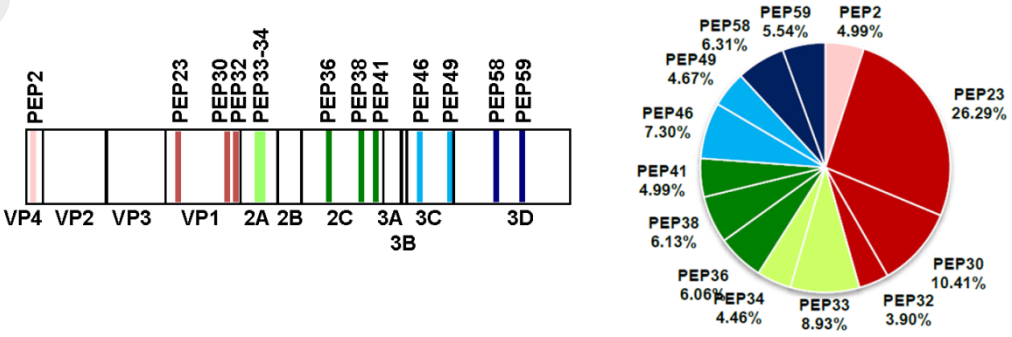

Figure 4.14: Analysis of anti-EV-A71 antibodies recognizing linear B-cell epitopes. (A) IgM antibody determinants identified from $IgM^{+}IgG^{+}$ sera. IgG antibody determinants identified from (B) $IgM^{+}IgG^{+}$ sera, (C) $IgM^{-}IgG^{+}$ sera, and (D) adult sera. Regions of amino acid sequences corresponding to the identified linear B-cell epitopes are indicated in the schematic diagrams of the EV-A71 genome. The percentage of antibody recognition contributed by each individual EV-A71 epitope is indicated in the pie charts, and was calculated according to the following equation: % antibody recognition = 100 x (OD values from individual peptide group/sum of the OD values from all peptide groups). Peptides are colour-coded according to the respective viral proteins.

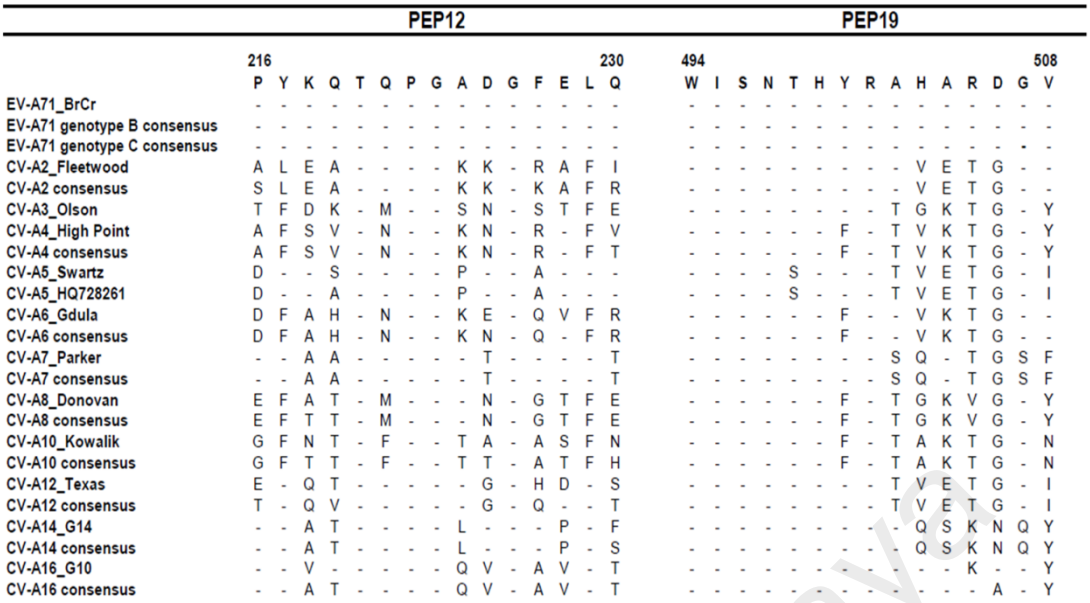

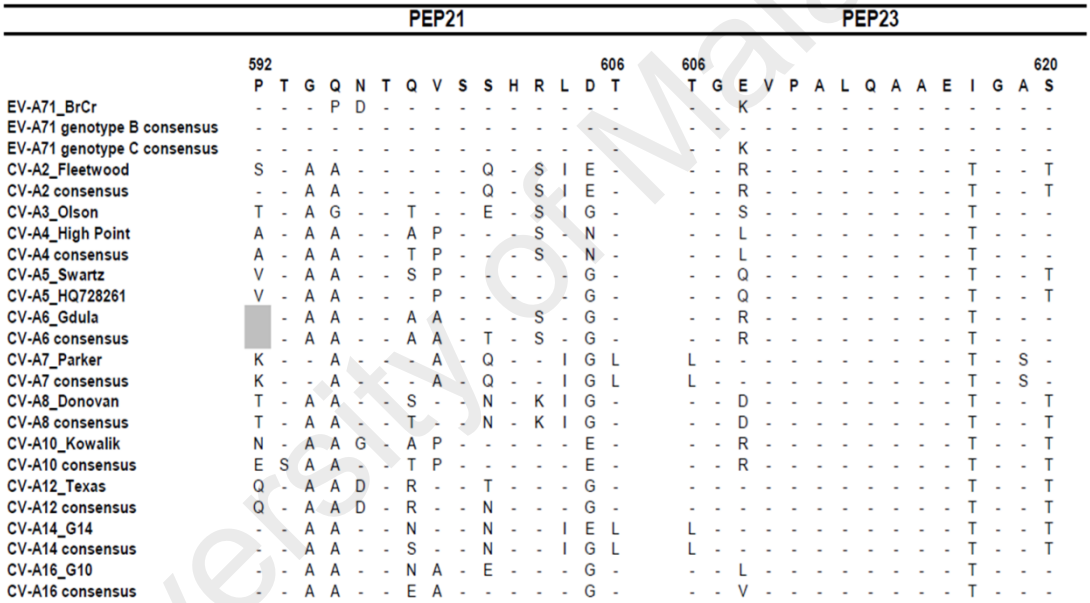

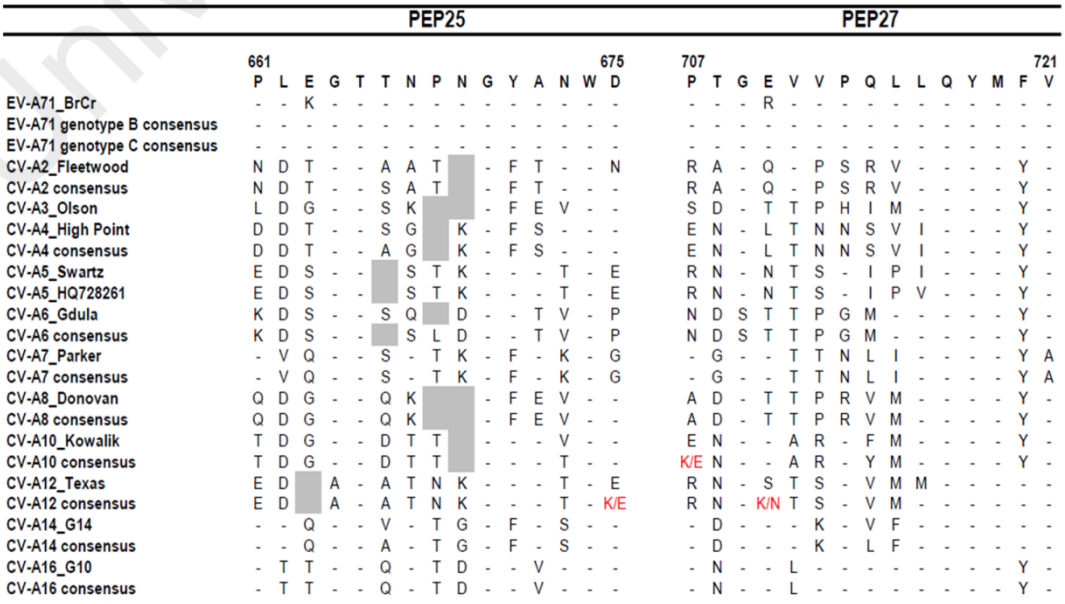

Figure 4.15: Amino acid sequence alignment of peptides with enteroviruses. The selected peptides (PEP12, PEP19, PEP21, PEP23, PEP25 and PEP27) were aligned to the corresponding sequences from 12 enterovirus prototype and consensus sequences (EV-A71, CV-A2 to CV-A8, CV-A10, CV-A12, CV-A14 and CV-A16). Conserved amino acids are indicated by a '–' and alignment gaps are shown in grey. The consensus sequences represent the current circulating strains while BrCr, Fleetwood, Olson, High Point, Swartz, Gdula, Parker, Donovan, Kowalik, Texas, G14 and G10 are prototype virus strains.

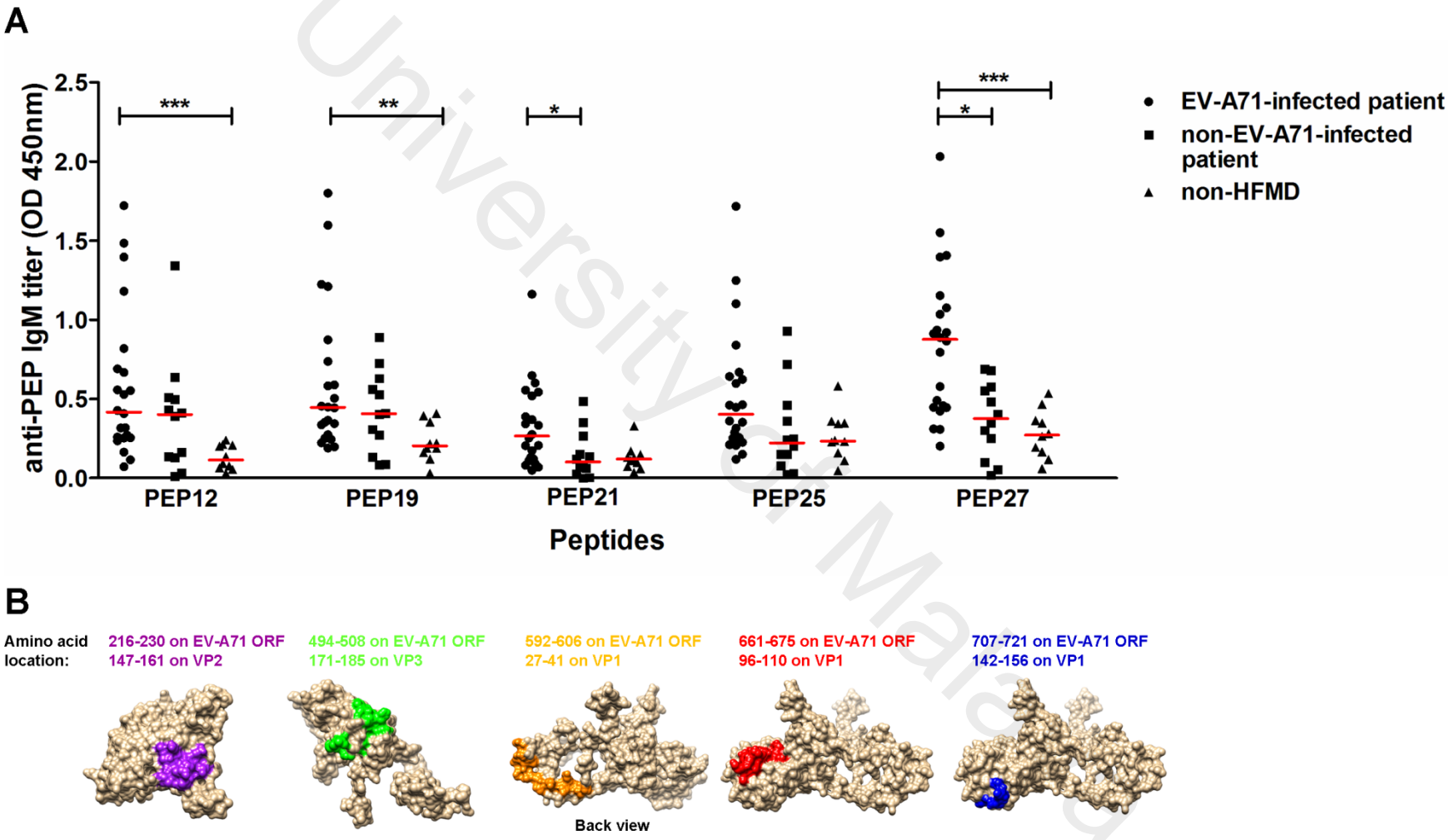

Figure 4.16: EV-A71-specific IgM antibody determinants. (A) EV-A71-specific IgM antibody detection in sera (n=44) at a dilution of 1:2000 was determined by peptide-based ELISA. Sera were categorized into EV-A71-infected patients (n=22), non-EV-A71 enterovirus-infected patients (n=12) and non-HFMD patients (n=10). Red solid line represents median. One-way ANOVA with Kruskal-Wallis test was used for statistical analysis (*P<0.05, **P<0.01, ***P<0.001). (B) Schematic representation of locations of IgM antibody determinants in VP1, VP2 and VP3 proteins, based on structural data retrieved from PDB records (identifier 3VBS).

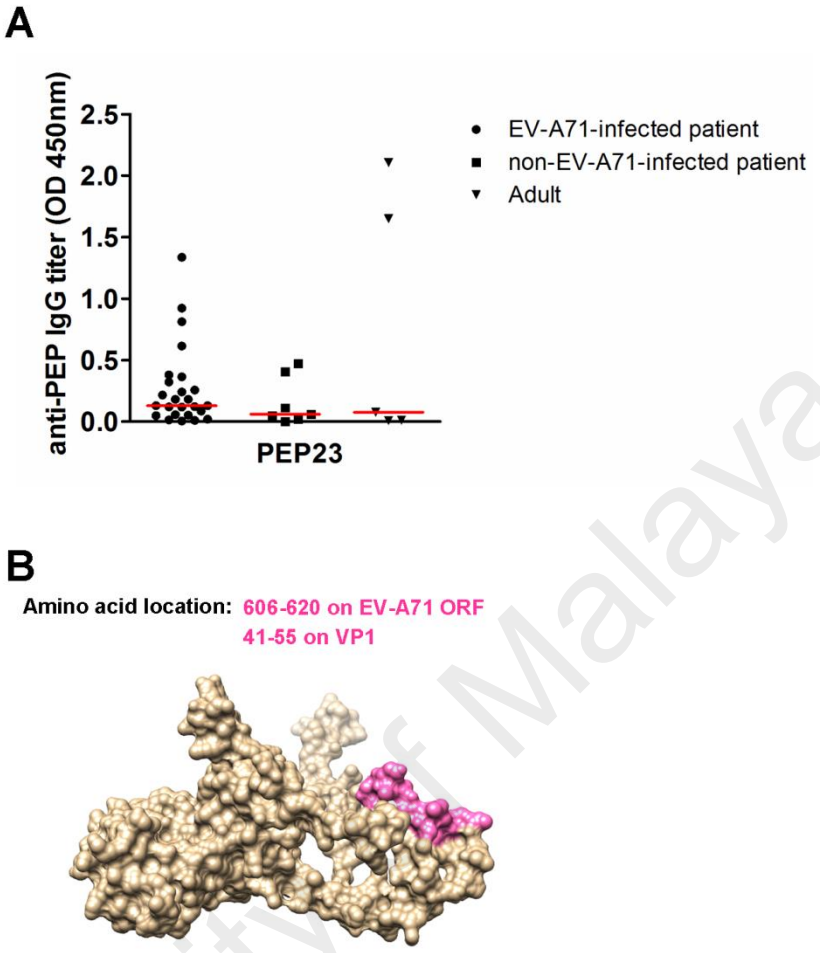

Figure 4.17: EV-A71-specific IgG antibody determinant. (A) EV-A71-specific IgG antibody detection in sera (n=38) at a dilution of 1:500 was determined by peptide-based ELISA. Sera were categorized into EV-A71-infected patients (n=25), non-EV-A71 enterovirus-infected patients (n=8) and healthy adults (n=5). Red solid line represents median. One-way ANOVA with Kruskal-Wallis test was used for statistical analysis. (B) Schematic representation of the location of the PEP23 in the VP1 protein, based on structural data retrieved from PDB records (identifier 3VBS).

4.3.3.4 Structural localization of the antigenic peptides

Epitope-containing sequences were next mapped onto the available three-dimensional crystal structures of the VP1, VP2 and VP3 proteins (PDB identifier: 3VBS). For the EV-A71-specific IgM epitopes, PEP12 is located in the solvent-exposed region of VP2, whereas PEP19 is partially embedded in the VP3 protein (Figure 4.16B). Similar analyses for the VP1 protein revealed that PEP21 and PEP25 are located in the solvent-exposed region, while PEP27 is partially concealed in the folder protein (Figure 4.16B). The EV-A71-specific IgG epitope PEP23 is prominently exposed on the surface of the virus (Figure 4.17B).

4.4 Determination of T-cell responses to EV-A71 in HFMD patients

4.4.1 Study subjects

Of a total of 56 individuals recruited for the intracellular cytokine staining analysis, 14 were RT-PCR confirmed enterovirus-infected patients, with EV-A71-infected (n=7) and CV-A6-infected children (n=7). The remaining eight children showed no infection in the last two weeks and had neutralization titers <8, and were categorized as seronegative children. Healthy adults were further divided into seropositive (n=22; neutralization titers ≥8) and seronegative adults (n=11; neutralization titer <8) based on neutralization test. PBMCs were extracted and stimulated with EV-A71 as mentioned in the section 3.5.3.

4.4.2 IFN-γ analysis

IFN-γ is a pro-inflammatory Th1 cytokine that plays an important role in both innate and adaptive immunity, especially against viral infections. Besides, IFN-γ can also be secreted by helper cytotoxic T cells ($CD8^+$ T cells) and NK cells in response to antigens. Here, the frequency of IFN-γ-expressing $CD4^+$ and $CD8^+$ T cells during EV-A71 infection was investigated. The differential expression of IFN-γ was gated on the T-cell subsets as shown in Figure 4.18A. A different gating pattern but similar strategy was applied to samples from children and adults, as lymphocytes of children increase in size after virus stimulation (lymphoblasts). Results with the positive control PHA-stimulated samples (Appendix VII), confirmed that $CD8^+$ T cells of HFMD patients and adult donors could robustly express IFN-γ upon stimulation.

Firstly, IFN-γ expression by the T-cell subsets in EV-A71-infected and CV-A6-infected patients were compared, and were found to show similar T cell responses (Figure 4.18B). There were no significant differences observed in infected and healthy children (data not shown) due to the low number of samples, and hence both samples were combined for subsequent analysis. Overall, a higher frequency of IFN-γ-expressing $CD4^+$ T cells was observed in children, and a higher frequency of IFN-γ-expressing $CD8^+$ T cells was seen in adults (Figure 4.18B).

4.4.3 Granzyme B, perforin and CD57 in $CD8^+$ T cells

Next, the levels of granzyme B and perforin were studied, as these molecules are known to induce caspase-independent cell-death, allowing $CD8^+$ T cells to kill virus-infected cells. The expression of the terminal differentiation marker, CD57 on $CD8^+$ T cells, which indicates replicative senescence, was also analyzed. The expressions of granzyme

B, perforin and CD57 were gated on the $CD8^+$ T cells, as shown in Figure 4.19A. Similarly, a different gating pattern but similar strategy was applied to samples of children and adults. Results with the positive control PHA-stimulated samples (Appendix VIII), confirmed that $CD8^+$ T cells of HFMD patients and adult donors could robustly express the T-cell markers following stimulation.

Granzyme B and perforin were expressed in both children and adults (Figure 4.19B). Similar expression of $CD57^+$ $CD8^+$ T cells was observed in children and adults. The expression of CD57 cells suggests that immunosenescence, which is common in chronic infections, may also play a role in EV-A71 T-cell immunity. No significant differences were observed in the expression of granzyme B, perforin and CD57 on $CD8^+$ T cells in adults and children. Next, we compared the expression levels of different markers on $CD8^+$ T cells within the same group of samples (Figure 4.19C). Overall, higher granzyme B compared to perforin was expressed in $CD8^+$ T cells in both children and adults. The frequency of $CD57^+$ $CD8^+$ T cells positively correlated with granzyme B^+ $CD8^+$ T cells ($r=0.7940$; $P<0.0001$) (Figure 4.19D). The expressions of perforin, granzyme B and CD57 on $CD8^+$ T cells all correlated significantly with each other.

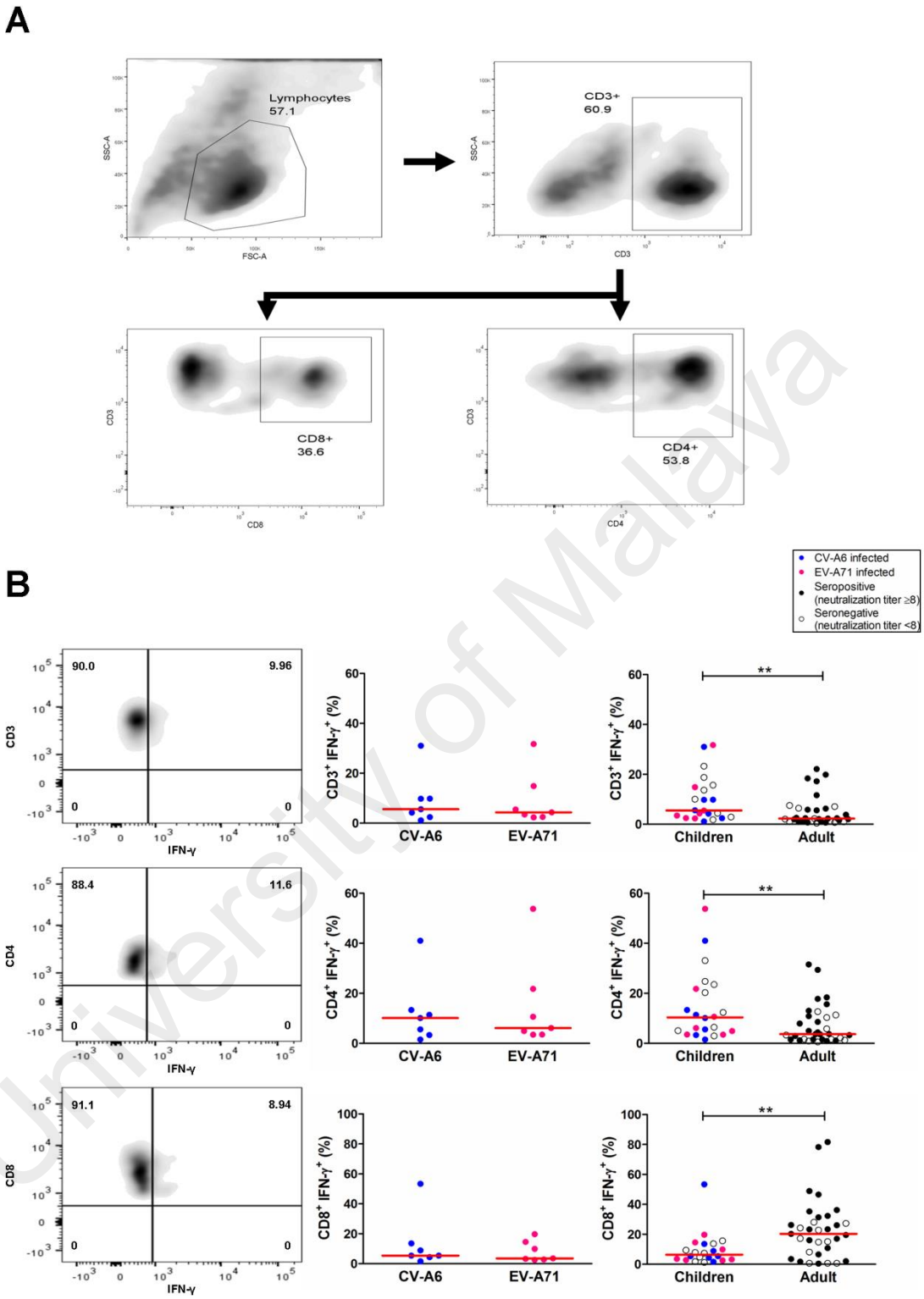

Figure 4.18: IFN-γ expression by T-cell subsets following stimulation with EV-A71 in the study population. (A) Depiction of the gating strategy used to identify T cells in the study. Lymphocytes were selected on the basis of forward-(FSC) and side-scatter (SSC) characteristics. T cells were defined using the expression of CD3. Next, T cells were segregated to $CD4^+$ helper and $CD8^+$ cytotoxic T cells. (B) The left plots show the gating strategy for expression of IFN-γ by T-cell subsets. The scatter plots on the right show the frequencies of $CD3^+$ IFN-γ^+, $CD4^+$ IFN-γ^+ and $CD8^+$ IFN-γ^+ T cells in EV-A71-infected and CV-A6-infected patients, and in children and adult samples. Each symbol represents an individual, and for each plot the median is represented by the horizontal red line. Differences between any two groups were calculated using the Mann-Whitney test (*P<0.05, **P<0.01, ***P<0.001).

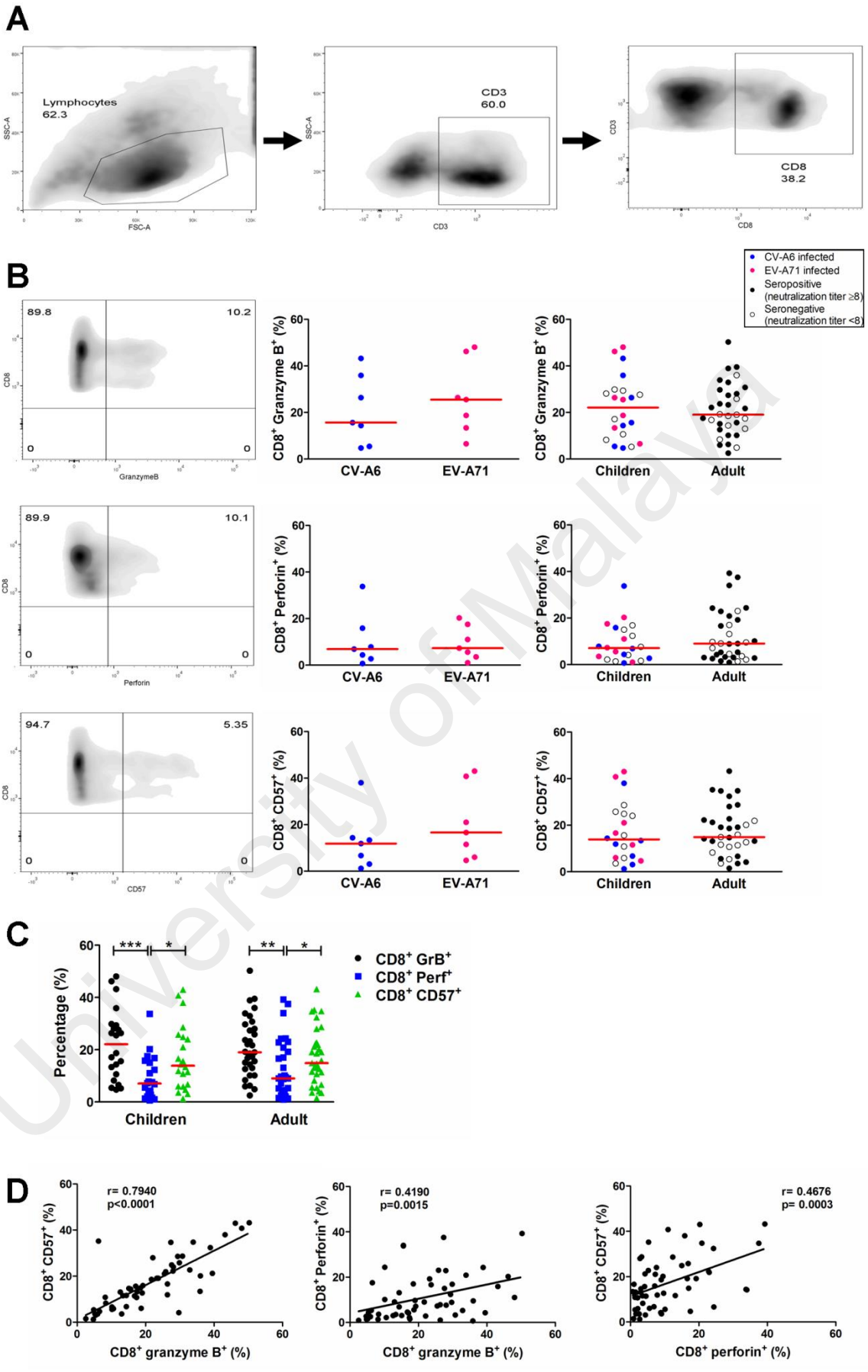

Figure 4.19: Expression level of different markers by $CD8^+$ T cells following stimulation with EV-A71 in the study population. (A) Depiction of the gating strategy used to identify $CD8^+$ T cells. Lymphocytes were selected on the basis of forward (FSC) and side-scatter (SSC) characteristics. T cells were defined by CD3 expression and later plotted for $CD8^+$ T cells. (B) The left plots show the representative gating strategy for expression of different markers by $CD8^+$ T cells. The scatter plots on the right show the frequencies of $CD8^+$ T cells expressing granzyme B, perforin and CD57 in EV-A71-infected and CV-A6-infected patients, and in children and adult samples. (C) The percentages of expression of different markers in CD8+ T cells. Each symbol represents an individual, and for each plot the median is represented by the horizontal red line. Differences between any two groups were calculated using the Mann-Whitney test (*P<0.05, **P<0.01, ***P<0.001). (D) Relationship between CD57 and granzyme B expressions, between CD57 and perforin expressions, and between granzyme B and perforin expressions in $CD8^+$ T cells. Correlation analysis was performed using Spearman rank correlation analysis.

CHAPTER 5

DISCUSSION

5.1 Enterovirus identification in HFMD patients

Prior to 2012, EV-A71 and CV-A16 were the main causative agents of HFMD in Malaysia (Chan *et al.*, 2012). However, CV-A6 has recently emerged to be the main cause of unusual HFMD outbreaks in Europe (Osterback *et al.*, 2009, Mirand *et al.*, 2012) and Asia (Wu *et al.*, 2010, Lu *et al.*, 2012, Fujimoto *et al.*, 2012), and is often found co-circulating with other enteroviruses. In this study, three human enteroviruses, EV-A71, CV-A16 and CV-A6 were found to co-circulate in Malaysia. With the co-circulation of various enteroviruses and the potential for viral co-infection and recombination, enteroviruses other than EV-A71 and CV-A16 also have the propensity to cause HFMD outbreaks (Yoke-Fun and AbuBakar, 2006, Chan and AbuBakar, 2004).

In the present study, there were no significant differences in clinical manifestations between CV-A6 and EV-A71 patients. A few studies have reported that CV-A6 was more commonly associated with herpangina than HFMD (Lo *et al.*, 2011, Mirand *et al.*, 2012, Chen *et al.*, 2012), and that CV-A6 causes more severe and widespread skin manifestations, involving sites such as knees, elbows, trunk and neck (Puenpa *et al.*, 2013, Kobayashi *et al.*, 2013). The rash in CV-A6 may be vesiculobullous and form scabs (Feder *et al.*, 2014). Onychomadesis, or painless nail shedding, has been reported as a hallmark for CV-A6-infected HFMD patients 1-2 months after the onset of disease (Osterback *et al.*, 2009, Fujimoto *et al.*, 2012, Kobayashi *et al.*, 2013, Wei *et al.*, 2011). This observation could not be confirmed in the current study as no patient follow-up was performed. However, CV-A6 patients were younger than EV-A71 patients, similar to other studies (Lu *et al.*, 2012, He *et al.*, 2013).

Highly conserved 5' UTR is used for broad-range detection of enteroviruses (Hyypia *et al.*, 1989, de Vries *et al.*, 2008, Zhou *et al.*, 2014). In the present study, EV-A71, CV-A16 and CV-A6 were identified based on 5' UTR phylogenetic analysis. The results suggest that 5' UTR is suitable for initial identification of enteroviruses during HFMD outbreaks, as co-circulation of various enteroviruses occurs frequently. As 5' UTR is a hotspot for recombination, specific capsid genes such as VP1 and VP4/VP2 were required to further confirm genotypes.

EV-A71 subgenotype B5 and CV-A16 subgenotype B2 have been the genotypes circulating in Malaysia since 2000 and 2003, respectively (Chan *et al.*, 2012). In this study, EV-A71 and CV-A16 isolates were still from subgenotypes B5 and B2b, respectively, similar to previous reports (Chua and Kasri, 2011, Ling *et al.*, 2014, Yusof *et al.*, 2014). This suggests that persistence of previous circulating EV-A71 and CV-A16 genotypes in Malaysia. For CV-A6, Malaysian sequences obtained in the current study were clustered into genotypes D1 and D2, and were closely related to isolates from Seri Kembangan, Malaysia and China.

Many estimated substitution rates have been published for enteroviruses, especially for the VP1 region. The VP1 of CV-A6 is 915 bp, but only 897 bp in both EV-A71 and CV-A16. He *et al.* (2013) used 234 CV-A6 isolates and 31 reference sequences of 269 bp lengths in their analysis, whereas 12 CV-A16 isolates and 156 reference sequences of 657 bp lengths were used in the present study for evolutionary rate estimation analysis. In this study, the CV-A6 evolutionary rate of VP1 gene was estimated at 6.8 x 10^{-3} substitutions per site per year, which is higher than the previously reported rate of 4.4-4.5 x 10^{-3} (He *et al.*, 2013). The greater lengths of VP1 sequences used in this study are more phylogenetically informative and likely to provide a better estimate. The CV-A16 evolutionary rate of 4.8 x 10^{-3} substitutions per site per year is also higher than the

reported rate of 4.0-4.1 x 10^{-3} (He *et al.*, 2013). However, the EV-A71 evolutionary rate of 7.8 x 10^{-3} in this study was not comparable with the reported rate of 4.2-4.5 x 10^{-3} (Tee *et al.*, 2010), as different capsid genes were used for analysis. Overall, the CV-A6 evolutionary rate was found to be higher than the evolutionary rate of CV-A16. This higher evolutionary rate could lead to beneficial mutations that increase infectivity or enable escape from immune responses, which may explain the recent increase of CV-A6 HFMD outbreaks observed, and explain the replacement of CV-A16 as the second most common causative agent of HFMD in Malaysia.

In summary, EV-A71, CV-A16 and CV-A6 were detected from patients clinically diagnosed with HFMD in Kuala Lumpur, Malaysia. This study also demonstrates that CV-A6 is emerging as a new and important cause of epidemic HFMD in Malaysia, in addition to EV-A71 and CV-A16. In the subsequent work, the patient sera collected during this 2012-2013 HFMD outbreaks were used to investigate the humoral and cellular immune responses against EV-A71.

5.2 EV-A71 antibody detection in HFMD patients

Well-characterized sera are required to determine humoral and cellular immune responses to EV-A71 in HFMD patients. Anti-EV-A71 antibody responses were determined for serum samples collected during the 2000 and 2012-2013 HFMD outbreaks with two commercial available diagnostic kits, EV-A71 IgM-capture ELISA and IgM GICA, which had previously been evaluated only in China. It is important to evaluate the performances of these two commercial assays in different geographical settings where the circulating EV-A71 genotypes and patient immune responses may differ.

In Malaysia, HFMD is endemic and outbreaks of EV-A71 infection occur every 2-3 years. Early social distancing resulted in reduced HFMD cases in Sarawak, Malaysia in 2006 (Solomon *et al.,* 2010). Therefore, early diagnosis of EV-A71 could enable early interventions to curb the spread of infection and appropriately observe patients for complications. While PCR will detect the virus at the earliest time, IgM has also been shown to be a good early indicator for EV-A71 infection, as it may be detectable as early as 1 day of illness, peaks on day 5 (Zhao *et al.*, 2011), and is detectable for up to 94 days (Wang *et al.*, 2004b). Serological detection of IgM would be suitable for most laboratories which do not have PCR or viral culture facilities, but are more likely to have ELISA. More importantly, the rapid and more convenient GICA assay showed comparable performance to the ELISA-based assay, suggesting that it can be used in clinics or rural settings with no laboratory facilities.

There are very few commercial EV-A71 IgM diagnostic kits available. EV-A71 IgM-capture ELISA and IgM GICA assays were compared in Malaysian patients, and sensitivity rates (78.4% and 75.7%, respectively) were lower than the 93.6% and 94.1% (IgM-capture ELISA), and 93.3% and 97.6% (IgM-GICA) reported earlier in China (Xu *et al.*, 2010, Yu *et al.*, 2012, Wang *et al.*, 2015b, Zhang *et al.*, 2016). One possible reason might be the varying detection of antibodies resulting from different circulating EV-A71 genotypes found in Malaysia and China. In Malaysia, subgenotypes B4, B5 and C1 circulated in 2000, and only subgenotype B5 has been present after 2005, whereas the current predominant EV-A71 in China is subgenotype C4 (Chan *et al.*, 2012). The purified EV-A71 antigen used in the diagnostic kits was subgenotype C4, which may explain the higher sensitivity reported in the China studies.

When testing serum from children with HFMD, the assays showed specificity rates of 80.8% and 76.9% for the IgM-capture ELISA and IgM GICA, respectively. These

specificity rates were lower than the 88.6% (IgM-capture ELISA) and 94.7% (IgM GICA) reported by Xu *et al.* (2010) and Zhang *et al.* (2016), but higher than the 69.6% reported for the IgM-capture ELISA by Yu *et al.* (2012) and the 50% for the IgM GICA reported by Wang *et al.* (2015b). The PPV rates of 74.4% (ELISA) and 70.0% (GICA) were moderate, although these rates would have been affected by the lower prevalence of EV-A71 in the HFMD outbreak in 2012-2013 (panel B), which had relatively more cases due to CV-A6. The false positives are likely due to detection of IgM which recognize common epitopes among enteroviruses (Xu *et al.*, 2010, Yu *et al.*, 2012). Increasing the cut-off values according to locally-determined background seropositive rates may improve specificity and PPV.

PCR is known to be the most sensitive diagnostic assay for EV-A71 (Ooi *et al.*, 2010); yet, in the present study, IgM was detected in 25.0% (ELISA) and 28.6% (GICA) of serum samples from patients with negative enterovirus RT-PCR. One possibility is the presence of low levels of virus RNA, which may be resolved by the use of real-time RT-PCR rather than the less sensitive conventional RT-PCR used in the present study. In addition, RT-PCR in this study is only limited to amplification of 5'UTR, so targeting other gene regions such as VP4/VP2 and VP1 should be considered.

One of the limitations of the present study is that the timing of disease onset is not known, and cannot be correlated with the IgM response. However, the value in this study is the use of samples from patients with confirmed enterovirus infection, in a different geographical location with different circulating enteroviruses to other previously reported evaluations, which were limited to China. The circulation of different serotypes of EV-A71 in Malaysia likely explains the lower test sensitivities seen here. Both EV-A71 IgM-capture ELISA and EV-A71 IgM GICA had comparable performance characteristics and concordance, despite the fact that point-of-care tests are

generally felt to be inferior to ELISA-based assays. Therefore, the IgM GICA can be used in clinics or rural settings with no laboratory or ELISA facilities. Both diagnostic kits may be useful and convenient for the screening for EV-A71 infection during HFMD outbreaks in Malaysia, but confirmation (of patients with both positive and negative IgM results) with either culture or RT-PCR remains essential.

The sera from HFMD children were then used to determine the anti-EV-A71 IgG level and neutralization titers against EV-A71. Overall, 89 HFMD sera were tested and 37 of them were samples from children confirmed to have EV-A71 by PCR or culture. These 37 sera were further divided into three categories: acute infection (EV-A71 $IgM^{+}IgG^{-}$), early convalescent infection (EVA-71 $IgM^{+}IgG^{+}$) and late convalescent stage (EV-A71 $IgM^{-}IgG^{+}$). There are a few possible explanations for the $IgM^{-}IgG^{+}$ status in a patient with PCR- or culture-confirmed EV-A71 in the late convalescent stage, such as (1) persistent infection (with persistent shedding), (2) reinfection, or (3) false negative IgM results. In hepatitis B, IgG with the absence of IgM may be present in persistent chronic and resolved infections (World Health Organization, accessed February 7, 2016). Likewise, long term shedding of EV-A71 may result in low or transient IgM detection. The longest duration of EV-A71 shedding in throat swabs and fecal specimens of HFMD patients was 30 days and 54 days, respectively (Han *et al.*, 2010). Furthermore, EV-A71 shedding correlated with disease severity (Li *et al.*, 2013). Several studies demonstrated that rubella-specific IgM is generally absent or present at a low level transiently in reinfection cases, whereas the IgG response is highly elevated (Morgan-Capner *et al.*, 1985, Hamkar *et al.*, 2009). False negative IgM results could be one of the conceivable explanations. Different circulating EV-A71 genotypes in Malaysia might vary the detection of IgM antibodies. Based on all the tests performed, these sera were subsequently selected for identification of immunogenic proteins and peptides.

5.3 Identification of antigenic proteins and peptides

Understanding the immune responses against EV-A71 is important for the development of diagnostic tools and potential vaccine candidates. In the present study, the first comprehensive analysis of antibody responses against structural and non-structural proteins of EV-A71 was performed. Using EV-A71-infected patient serum samples from the HFMD outbreaks in Malaysia, all viral structural proteins (VP1-VP4) were found to be the targets for EV-A71-specific IgM and IgG antibodies. EV-A71-specific IgM antibody also recognized viral non-structural proteins 2A, 3C and 3D, whereas EV-A71-specific IgG antibody recognized all the non-structural proteins. Further investigation will be required to identify the most appropriate antigen to distinguish the infection stages of the EV-A71 patient. Serum antibodies from mice immunized with inactivated EV-A71 showed similar results to patient sera, suggesting that the immune profile generated from the inactivated vaccine mimicked the nature infection. In foot-and-mouth disease, non-structural proteins were used as a diagnostic antigen in ELISA to distinguish infected animals from vaccinated animals due to its high immunogenicity (Ma *et al.*, 2011). Infected animals produced antibodies against both structural and non-structural proteins, whereas vaccinated animals only developed antibodies against structural proteins since the inactivated vaccine had no replicating virus (Clavijo *et al.*, 2004). Among all the non-structural proteins, 3ABC was shown to be the most appropriate antigen to distinguish infection from vaccination (Bergmann *et al.*, 2003, Sorensen *et al.*, 2005, Bronsvoort *et al.*, 2006). Similarly, when the EV-A71 vaccine is available, non-structural proteins 2A, 3C and 3D recognized by IgM, and 2A, 2B, 2C, 3AB, 3C and 3D which are recognized by IgG antibody from EV-A71-infected patient sera, could be used as potential diagnostic antigens to differentiate vaccinated from naturally infected individuals. Further investigation will be required to determine which protein should be used for diagnostic antigens.

Different roles of human IgG subclasses in neutralization and antibody-dependent enhancement activities were well documented in dengue and West Nile virus studies (Hofmeister *et al.*, 2011, Rodrigo *et al.*, 2009). In EV-A71, IgG1 subclass demonstrated the strongest neutralizing ability and is found in human intravenous immunoglobulin (Cao *et al.*, 2013). In the present study, IgG1 subclass was identified as the predominant isotype in EV-A71-infected patient sera. It has been shown that IgG3 subclass did not have neutralizing activity but enhanced EV-A71 infection *in vitro* (Cao *et al.*, 2010). Interestingly, a stronger IgG3 subclass response was observed in EV-A71-infected children, but not in adults, and this could imply poorer neutralizing antibody protection in children compared to adults.

IgM response detection is important for early diagnosis of infectious diseases. Therefore, a total of 63 biotinylated peptides were synthesized to determine EV-A71-specifc IgM linear epitopes using peptide-based ELISAs. Linear epitopes instead of discontinuous epitopes were the focus since they are more easily identifiable in a medium-throughput approach (Kam *et al.*, 2012). Interestingly, 92.0% (58/63) of the peptides were recognized by IgM antibody from EV-A71-infected patient sera. All previously reported EV-A71 human IgM epitopes were also positive in the current study. Overall, 22 dominant human anti-EV-A71 IgM linear epitopes were identified, suggesting that anti-EV-A71 IgM responses against multiple epitopes are induced during EV-A71 infection (Gao *et al.*, 2012). The dominant linear epitopes with signal/cut-off levels of ≥5 were PEP12, PEP14 and PEP22, which were mapped at similar locations as the human IgM epitopes VP2-50, VP3-10, VP3-12 and VP1-14 reported by Gao *et al.* (2012). To determine the seroprevalence of IgM against these EV-A71 epitopes, five unique epitopes with least similarity to other enteroviruses were screened with individual serum testing by using peptide-based ELISAs. Non-HFMD children sera were used to eliminate the non-specific epitopes, and these samples are likely to be from patients

without active EV-A71 infection based on the negative results obtained from EV-A71 IgM-capture ELISA and EV-A71 GICA, and neutralization titers of <8. The OD values of EV-A71-infected patient sera tested against PEP12, PEP19 and PEP27 were significantly higher than the OD values of non-HFMD children sera, suggested that these IgM epitopes are enterovirus-specific epitopes. To further validate these IgM epitopes are EV-A71-specific, serum samples from patient infected with non-EV-A71 enteroviruses were used. Cross-reactivity was observed in PEP12 and PEP19, suggesting that these epitope recognitions are not EV-A71-specific. The high cross-reactivity is likely due to previous exposure to other enteroviruses, which can't be rule out. However, since children can be infected with HFMD multiple times, it is not likely that the cross-reactivity will result in cross-immunoprotection against enteroviruses. Significant differences between the OD values of EV-A71-infected and non-EV-A71-infected patient sera were observed in PEP27, suggesting that this epitope is EV-A71 specific. Overall, PEP27 (amino acids 707-721) mapped at VP1 is the best candidate for an EV-A71-specific IgM epitope. However, the OD values of PEP27 in non-HFMD children sera was higher than the remaining four IgM epitopes, suggesting that the cut-off could be improved. High population immunity to EV-A71 has been reported in Malaysian children, with EV-A71 seropositive rates in non-HFMD urban children increasing gradually from 47.1% at 1-3 years to 75.0% at 13-17 years (NikNadia *et al.*, 2016), suggesting that truly non-HFMD sera are required to establish the cut-off. PEP27 was found to be mapped at a similar location as the reported $CD4^+$ T-cell epitopes SP2 and VP1-20 (Foo *et al.*, 2008, Tan *et al.*, 2013), suggesting that PEP27 is a EV-A71 potential B-cell and T-cell epitope.

Different human IgG epitopes were recognized by patient serum samples from early and late convalescence. Using EV-A71-infected patient sera from early convalescence (IgM^+IgG^+), we observed that PEP47 and PEP62, located at non-structural proteins 3C

and 3D, respectively, were identified as dominant anti-EV-A71 IgG linear epitopes. $IgM^{-}IgG^{+}$ sera (late convalescent) showed similar EV-A71-specific IgG epitope profiles as adult sera, as both sera strongly recognized PEP23 as the dominant IgG linear epitope, and adult sera also recognized PEP30 as an additional dominant linear epitope. Surprisingly, all the previously reported anti-EV-A71 IgG epitopes identified in rabbit and murine sera (in our panel of 63 peptides) were not recognized by EV-A71-infected patient sera, except PEP20, which mapped to a similar location as the reported VP1-01 epitope (Liu *et al.*,2011). The synthetic peptide SP70, located at amino acids 208-222 in VP1, was identified as a neutralizing and protective EV-A71-specific B-cell epitope (Foo *et al.*, 2007a, Foo *et al.*, 2007b). Several studies have demonstrated that neutralizing mAbs generated by EV-A71-immunized mice can recognize SP70 (Li *et al.*, 2009, Deng *et al.*, 2015, Chang *et al.*, 2011, Lim *et al.*, 2012). In addition, VP2-28 (amino acids 136-150 in VP2) was also proven as a cross-neutralization epitope and is recognized by commercial mAb 979 and mAbs generated by immunized mice (Liu *et al.*, 2011, Kiener *et al.*, 2012, Xu *et al.*, 2014). In the present study, EV-A71-infected human sera in early convalescent and late convalescent stage failed to recognize the EV-A71-specific neutralizing epitopes SP70 and VP2-28, represented by PEP29 and PEP10, respectively. This finding suggests that human sera may target different immunogenic epitopes compared with sera from immunized mice. Interestingly, PEP23 (amino acids 606-620) was recognized by all anti-EV-A71 IgG antibodies from patient and adult sera. This PEP23 was the previously reported human IgG epitope, namely VP1-15 (Gao *et al.*, 2012). This long-lasting immune response of anti-EV-A71 IgG antibody against PEP23 makes it an attractive candidate for seroepidemiology studies. However, cross-reactivity was observed in PEP23, suggest that this epitope may not EV-A71 specific. Further improvement such as the use of longer peptides or multiple

peptides may reduce the cross-reactivity in PEP23. Further development of a good peptide ELISA will be valuable for the evaluation of EV-A71 vaccine immunogenicity.

In summary, comparison of the distribution of immune-reactive IgM and IgG linear epitopes showed that PEP27 (amino acids 142-156 in VP1) was identified as EV-A71 IgM-specific immunodominant epitope, while PEP23 (amino acids 41-55 in VP1) was identified as IgG cross-reactive immunodominant epitope. This study revealed that the structural protein VP1 is the main immunodominant site targeted by anti-EV-A71 IgG and IgM antibodies.

5.4 Determination of T-cell responses in HFMD patients

T cells are known to play an important role in immune protection against viral infection. Some studies demonstrated that cellular rather than humoral immunity is correlated with clinical outcome of EV-A71 infection (Chang *et al.*, 2006). IFN-γ is important in innate and adaptive immune responses, and can be secreted by $CD4^+$ T cells, $CD8^+$ T cells and NK cells in response to antigenic stimuli. High levels of IFN-γ have been reported in clinical HFMD (Li *et al.*, 2014), whereas low expressions of IFN-γ and other cytokines have been detected in HFMD patients with pulmonary edema, suggesting an inverse correlation between antigen-specific T-cell responses and disease severity (Chang *et al.*, 2006, Yang *et al.*, 2001).

In the present study, the potential role of IFN-γ expressing $CD4^+$ and $CD8^+$ T cells across the patient groups was analyzed. The number of EV-A71 patients was small, and hence comparisons were also made with CV-A6 patients and adults who were previously infected with EV-A71. Enterovirus-induced T-cell responses were reported to be cross-reactive between different enteroviruses (Beck and Tracy, 1989, Mahon *et*

al., 1992, Cello *et al.*, 1996). Our results showed that EV-A71-infected and CV-A6-infected children showed similar T-cell responses when stimulated by EV-A71, suggesting that the induced T-cell responses are cross-reactive. Different immune profiles were observed in children and adults. A higher frequency of IFN-γ expressing $CD4^+$ T cells was observed in children, while a higher frequency of IFN-γ expressing $CD8^+$ T cells was observed in adults. This appears to indicate that $CD4^+$ T cells are involved in responses to primary infections, which mostly occur in children, while $CD8^+$ T-cell responses in adults likely reflect immune memory. The thymus is the central lymphoid organ responsible for the generation of T lymphocytes. The thymus begins to undergo atrophy with age, and hence the development of new T cells in the thymus slows down in adults, and T cell numbers are maintained through division of mature T cells outside of the central lymphoid organs (Janeway *et al.*, 2001). In response to infection, children will generate $CD4^+$ T cells from the new T cell clones in the thymus and activate antibody production during primary infection. Previously exposed adults will largely expand $CD8^+$ T cell clones from pre-existing peripheral T cells due to thymic atrophy. Nonetheless, further confirmation may still be required to measure memory T cell responses from children and adults.

Cytolytic enzymes such as granzyme A and B are critical to anti-viral immune responses by activation of cell death through caspase-dependent and caspase-independent mechanisms (Trapani *et al.*, 1998). Inactive granzyme B and perforin are packed within granules of cytotoxic T cells, NK cells and NKT cells (Cullen *et al.*, 2010). The efficiency of apoptosis in targeted cells is increased when granzymes are released in the presence of the pore-forming toxin perforin. Granzymes require the presence of perforin to induce apoptosis in target cells, and thus regulating perforin may obliterate the need for a tight control of the granzymes (Kagi *et al.*, 1994). Others have shown that granzyme B-deficient mice induced apoptosis in target cells more slowly

than wild-type mice (Heusel *et al.*, 1994), and that perforin-deficient mice were highly susceptible to viral infections (Kagi *et al.*, 1994). In the present study, granzyme B and perforin were expressed both in children and adults in response to EV-A71 antigen. Discordant expression patterns between granzymes and perforin are common in chronic viral infections such as Epstein-Barr virus, HIV, cytomegalovirus and smallpox (Appay *et al.*, 2000, Chen *et al.*, 2001, Zhang *et al.*, 2003, Rock *et al.*, 2005). Notably, the circulating EV-A71-specific $CD8^+$ T cells expressed significantly higher levels of granzyme B than perforin in both children and adults, suggest that these effector molecules are differentially regulated and a proportion of EV-A71-specific $CD8^+$ T cells may not be directly cytotoxic.

Cytolytic enzymes have also been linked to cellular maturity, especially senescence of immune cells. CD57 expression is a critical marker for replicative senescence/clonal exhaustion. In HIV infection, $CD57^+$ T lymphocytes have been correlated with disease progression (Le Priol *et al.*, 2006). Furthermore, expression of CD57 has also been correlated with concurrent expression of granzyme A, B and perforin (Chattopadhyay *et al.*, 2009). In the current study, a similar profile of expression of $CD57^+$ $CD8^+$ T cells was observed in both children and adults. This suggests that immunosenescence common in chronic viral infections may also play a role in EV-A71 T-cell immune responses. Furthermore, the frequency of $CD57^+$ $CD8^+$ T cells positively correlates with the expression of granzyme B and perforin on $CD8^+$ T cells, suggesting that CD57 might be a marker associated with high cytolytic potential (Chattopadhyay *et al.*, 2009).

In summary, experiments performed in the current investigation represent a preliminary analysis of IFN-γ expression in $CD4^+$ and $CD8^+$ T cells and the association of granzyme B, perforin and CD57 in EV-A71 infection.

CHAPTER 6

CONCLUSION

This study identified three human enteroviruses, EV-A71, CV-A16 and CV-A6, co-circulating during the 2012-2013 HFMD outbreaks. The highly conserved 5' UTR is suitable for broad-range identification of enteroviruses, while specific capsid genes such as VP1 and VP4/VP2 are required for genotyping. Serological test of the sera collected during HFMD outbreaks suggested that the commercial EV-A71 IgM-capture ELISA and IgM GICA assays had comparable performance, thus both diagnostic kits are suitable for early diagnosis of HFMD caused by EV-A71 in Malaysia. Structural proteins (VP1-VP4) and non-structural proteins 2A, 3C and 3D were targeted by anti-EV-A71 IgM and IgG antibodies in the human sera, whereas non-structural proteins 2B, 2C and 3AB were solely detected by IgG antibodies. The screening of 63 biotinylated peptides representing predicted and previously characterized epitopes led to the discovery of 22 IgM and 4 IgG dominant linear epitopes. PEP27 (VP1 142-156) and PEP23 (VP1 41-55) were further identified as EV-A71 IgM-specific and IgG cross-reactive immunodominant epitopes, respectively. In the study of the role of T-cell immunity, intracellular cytokine staining showed that IFN-γ expressing $CD4^+$ T cells were predominant in children, whereas a higher frequency of IFN-γ expressing $CD8^+$ T cells was observed in adults. Discordant expression of granzyme B and perforin was observed, implying a proportion of EV-A71-specific $CD8^+$ T cells may not be directly cytotoxic. Overall, the findings from this study provide an insight into the role of humoral and cellular immunity against EV-A71 infection.

REFERENCES

AbuBakar S, Chee HY, Al-Kobaisi MF, Xiaoshan J, Chua KB, Lam SK. Identification of enterovirus 71 isolates from an outbreak of hand, foot and mouth disease (HFMD) with fatal cases of encephalomyelitis in Malaysia. Virus Research. 1999; 61(1): 1-9.

AbuBakar S, Sam IC, Yusof J, Lim MK, Misbah S, Matrahim N, Hooi PS. Enterovirus 71 outbreak, Brunei. Emerging Infectious Diseases. 2009; 15(1): 79-82.

Adams MJ, King AM, Carsten EB. Ratification vote on taxonomic proposals to the International Committee on Taxonomy of Viruses (2013). Archives of Virology. 2013; 158(9): 2023-30.

Adams MJ, Lefkowitz EJ, King AM, Bamford DH, Breitbart M, Davison AJ, Ghabrial SA, Gorbalenya AE, Knowles NJ, Krell P, Lavigne R, Prangishvili D, Sanfaçon H, Siddell SG, Simmonds P, Carstens EB. Ratification vote on taxonomic proposals to the International Committee on Taxonomy of Viruses (2015). Archives of Virology. 2015; 160(7): 1837-50.

Ang LW, Koh BK, Chan KP, Chua LT, James L, Goh KT. Epidemiology and control of hand, foot and mouth disease in Singapore, 2001-2007. Annals of the Academy of Medicine Singapore. 2009; 38(2): 106-12.

Ang LW, Phoon MC, Wu Y, Cutter J, James L, Chow VT. The changing seroepidemiology of enterovirus 71 infection among children and adolescents in Singapore. BMC Infectious Diseases. 2011; 11: 270.

Appay V, Nixon DF, Donahoe SM, Gillespie GM, Dong T, King A, Ogg GS, Spiegel HM, Conlon C, Spina CA, Havlir DV, Richman DD, Waters A, Easterbrook P, McMichael AJ, Rowland-Jones SL. HIV-specific CD8(+) T cells produce antiviral cytokines but are impaired in cytolytic function. Journal of Experimental Medicine. 2000; 192(1): 63-75.

Arita M, Nagata N, Iwata N, Ami Y, Suzaki Y, Mizuta K, Iwasaki T, Sata T, Wakita T, Shimizu H. An attenuated strain of enterovirus 71 belonging to genotype a showed a broad spectrum of antigenicity with attenuated neurovirulence in cynomolgus monkeys. Journal of Virology. 2007; 81(17): 9386-95.

Arola A, Kalimo H, Ruuskanen O, Hyypia T. Experimental myocarditis induced by two different coxsackievirus B3 variants: aspects of pathogenesis and comparison of diagnostic methods. Journal of Medical Virology. 1995; 47(3): 251-9.

Astrup BS, Johnsen IBG, Engsbro AL. The role of coxsackievirus A16 in a case of sudden unexplained death in an infant - A SUDI case. Forensic Science International. 2016; 259: e9-e13.

Beck MA, Tracy SM. Murine cell-mediated immune response recognizes an enterovirus group-specific antigen(s). Journal of Virology. 1989; 63(10): 4148-56.

Bek EJ, Hussain KM, Phuektes P, Kok CC, Gao Q, Cai F, Gao Z, McMinn PC. Formalin-inactivated vaccine provokes cross-protective immunity in a mouse model of human enterovirus 71 infection. Vaccine. 2011; 29(29-30): 4829-38.

Biondillo DE, Konicek SA, Iwamoto GK. Interferon-gamma regulation of interleukin 6 in monocytic cells. American Journal of Physiology. 1994; 267(5 Pt 1): L564-8.

Blomberg J, Lycke E, Ahlfors K, Johnsson T, Wolontis S, Von Zeipel G. Letter: New enterovirus type associated with epidemic of aseptic meningitis and-or hand, foot, and mouth disease. Lancet. 1974; 2(7872): 112.

Blomqvist S, Klemola P, Kaijalainen S, Paananen A, Simonen ML, Vuorinen T, Roivainen M. Co-circulation of coxsackieviruses A6 and A10 in hand, foot and mouth disease outbreak in Finland. Journal of Clinical Virology. 2010; 48(1): 49-54.

Brenchley JM, Karandikar, NJ, Betts, MR, Ambrozak, DR, Hill, BJ, Crotty, LE, Casazza JP, Kuruppu J, Migueles SA, Connors M, Roederer M, Douek, DC, Koup, RA. Expression of CD57 defines replicative senescence and antigen-induced apoptotic death of CD8+ T cells. Blood. 2003; 101(7): 2711-20.

Bronsvoort BM, Toft N, Bergmann IE, Sorensen KJ, Anderson J, Malirat V, Tanya VN, Morgan KL. Evaluation of three 3ABC ELISAs for foot-and-mouth disease non-structural antibodies using latent class analysis. BMC Veterinary Research. 2006; 2: 30.

Brown BA, Oberste MS, Alexander JP Jr, Kennett ML, Pallansch MA. Molecular epidemiology and evolution of enterovirus 71 strains isolated from 1970 to 1998. Journal of Virology. 1999; 73(12): 9969-75.

Brown BA, Pallansch MA. Complete nucleotide sequence of enterovirus 71 is distinct from poliovirus. Virus research. 1995; 39(2-3): 195-205.

Cao R, Han J, Deng Y, Yu M, Qin E, Qin C. Presence of high-titer neutralizing antibodies against enterovirus 71 in intravenous immunoglobulin manufactured from Chinese donors. Clinical Infectious Diseases. 2010; 50(1): 125-6.

Cao RY, Dong DY, Liu RJ, Han JF, Wang GC, Zhao H, Li XF, Deng YQ, Zhu SY, Wang XY, Lin F, Zhang FJ, Chen W, Qin ED, Qin CF. Human IgG subclasses against enterovirus type 71: neutralization versus antibody dependent enhancement of infection. PLoS One. 2013; 8(5): e64024.

Cardosa MJ, Krishnan S, Tio PH, Perera D, Wong SC. Isolation of subgenus B adenovirus during a fatal outbreak of enterovirus 71-associated hand, foot, and mouth disease in Sibu, Sarawak. Lancet. 1999; 354(9183): 987-91.

Cardosa MJ, Perera D, Brown BA, Cheon D, Chan HM, Chan KP, Cho H, Mcminn P. Molecular epidemiology of human enterovirus 71 strains and recent outbreaks in the Asia-Pacific region: comparative analysis of the VP1 and VP4 genes. Emerging Infectious Diseases. 2003; 9(4): 461-8.

Cello J, Samuelson A, Stalhandske P, Svennerholm B, Jeansson S, Forsgren M. Identification of group-common linear epitopes in structural and nonstructural proteins of enteroviruses by using synthetic peptides. Journal of Clinical Microbiology. 1993; 31(4): 911-6.

Cello J, Strannegard O, Svennerholm B. A study of the cellular immune response to enteroviruses in humans: identification of cross-reactive T cell epitopes on the structural proteins of enteroviruses. Journal of General Virology. 1996; 77(Pt 9): 2097-108.

Chan KP, Goh KT, Chong CY, Teo ES, Lau G, Ling AE. Epidemic hand, foot and mouth disease caused by human enterovirus 71, Singapore. Emerging Infectious Diseases. 2003; 9(1): 78-85.

Chan YF, Abubakar S. Recombinant human enterovirus 71 in hand, foot and mouth disease patients. Emerging Infectious Diseases. 2004; 10(8): 1468-70.

Chan YF, Sam IC, Wee KL, AbuBakar S. Enterovirus 71 in Malaysia: a decade later. Neurology Asia. 2011; 16(1): 1-15.

Chan YF, Wee KL, Chiam CW, Khor CS, Chan SY, Amalina WM, Sam IC. Comparative genetic analysis of VP4, VP1 and 3D gene regions of enterovirus 71 and coxsackievirus A16 circulating in Malaysia between 1997-2008. Tropical Biomedicine. 2012; 29(3): 451-66.

Chang GH, Luo YJ, Wu XY, Si BY, Lin L, Zhu QY. Monoclonal antibody induced with inactived EV71-Hn2 virus protects mice against lethal EV71-Hn2 virus infection. Virology Journal. 2010; 7: 106.

Chang HW, Liu CC, Lin MH, Ho HM, Yang YT, Chow YH, Chong P, Sia C. Generation of murine monoclonal antibodies which cross-neutralize human enterovirus genogroup B isolates. Journal of Virological Methods. 2011; 173(2): 189-95.

Chang LY, Hsiung CA, Lu CY, Lin TY, Huang FY, Lai YH, Chiang YP, Chiang BL, Lee CY, Huang LM. Status of cellular rather than humoral immunity is correlated with clinical outcome of enterovirus 71. Pediatric Research. 2006; 60(4): 466-71.

Chang LY, King CC, Hsu KH, Ning HC, Tsao KC, Li CC, Huang YC, Shih SR, Chiou ST, Chen PY, Chang HJ, Lin TY. Risk factors of enterovirus 71 infection and associated hand, foot, and mouth disease/herpangina in children during an epidemic in Taiwan. Pediatrics. 2002; 109(6): e88.

Chang LY, Lin TY, Hsu KH, Huang YC, Lin KL, Hsueh C, Shih SR, Ning HC, Hwang MS, Wang HS, Lee CY. Clinical features and risk factors of pulmonary oedema after enterovirus-71-related hand, foot, and mouth disease. Lancet. 1999; 354(9191): 1682-6.

Chattopadhyay PK, Betts MR, Price DA, Gostick E, Horton H, Roederer M, De Rosa SC. The cytolytic enzymes granyzme A, granzyme B, and perforin: expression patterns, cell distribution, and their relationship to cell maturity and bright CD57 expression. Journal of Leukocyte Biology. 2009; 85(1): 88-97.

Chen G, Shankar P, Lange C, Valdez H, Skolnik PR, Wu L, Manjunath N, Lieberman J. CD8 T cells specific for human immunodeficiency virus, Epstein-Barr virus, and cytomegalovirus lack molecules for homing to lymphoid sites of infection. Blood. 2001; 98(1): 156-64.

Chen TC, Weng KF, Chang SC, Lin JY, Huang PN, Shih SR. Development of antiviral agents for enteroviruses. Journal of Antimicrobial Chemotherapy. 2008; 62(6): 1169-73.

Chen YC, Yu CK, Wang YF, Liu CC, Su IJ, Lei HY. A murine oral enterovirus 71 infection model with central nervous system involvement. Journal of General Virology. 2004; 85(Pt 1): 69-77.

Chen YJ, Chang SC, Tsao KC, Shih SR, Yang SL, Lin TY, Huang YC. Comparative genomic analysis of coxsackievirus A6 strains of different clinical disease entities. PLoS One. 2012; 7(12): e52432.

Chiu CH, Chu C, He CC, Lin TY. Protection of neonatal mice from lethal enterovirus 71 infection by maternal immunization with attenuated Salmonella enterica serovar Typhimurium expressing VP1 of enterovirus 71. Microbes and Infection. 2006; 8(7): 1671-8.

Ch'ng WC, Saw WT, Yusoff K, Shafee N. Immunogenicity of a truncated enterovirus 71 VP1 protein fused to a Newcastle disease virus nucleocapsid protein fragment in mice. Acta Virologica. 2011; 55(3): 227-33.

Chua BH, Phuektes P, Sanders SA, Nicholls PK, Mcminn PC. The molecular basis of mouse adaptation by human enterovirus 71. Journal of General Virology. 2008; 89(Pt 7): 1622-32.

Chua KB, Chua BH, Lee CS, Chem YK, Ismail N, Kiyu A, Kumarasamy V. Genetic diversity of enterovirus 71 isolated from cases of hand, foot and mouth disease in the 1997, 2000 and 2005 outbreaks, Peninsular Malaysia. Malaysian Journal of Pathology. 2007; 29(2): 69-78.

Chua KB, Kasri AR. Hand foot and mouth disease due to enterovirus 71 in Malaysia. Virologica Sinica. 2011; 26(4): 221-8.

Chumakov M, Voroshilova M, Shindarov L, Lavrova I, Gracheva L, Koroleva G, Vasilenko S, Brodvarova I, Nikolova M, Gyurova S, Gacheva M, Mitov G, Ninov N, Tsylka E, Robinson I, Frolova M, Bashkirtsev V, Martiyanova L, Rodin V. Enterovirus 71 isolated from cases of epidemic poliomyelitis-like disease in Bulgaria. Archives of Virology. 1979; 60(3-4): 329-40.

Clavijo A, Wright P, Kitching P. Developments in diagnostic techniques for differentiating infection from vaccination in foot-and-mouth disease. Veterinary Journal. 2004; 167(1): 9-22.

Cullen SP, Brunet M, Martin SJ. Granzymes in cancer and immunity. Cell Death and Differentiation. 2010; 17(4): 616-23.

Dang S, Gao N, Li Y, Li M, Wang X, Jia X, Zhai S, Zhang X, Liu J, Deng H, Dong T. Dominant CD4-dependent RNA-dependent RNA polymerase-specific T-cell responses in children acutely infected with human enterovirus 71 and healthy adult controls. Immunology. 2014; 142(1): 89-100.

de Vries M, Pyrc K, Berkhout R, Vermeulen-Oost W, Dijkman R, Jebbink MF, Bruisten S, Berkhout B, van der Hoek L. Human parechovirus type 1, 3, 4, 5, and 6 detection in picornavirus cultures. Journal of Clinical Microbiology. 2008; 46(2): 759-62.

Deng YQ, Ma J, Xu LJ, Li YX, Zhao H, Han JF, Tao J, Li XF, Zhu SY, Qin E, Qin CF. Generation and characterization of a protective mouse monoclonal antibody against human enterovirus 71. Applied Microbiology and Biotechnology. 2015; 99(18): 7663-71.

Dong C, Liu L, Zhao H, Wang J, Liao Y, Zhang X, Na R, Liang Y, Wang L, Li Q. Immunoprotection elicited by an enterovirus type 71 experimental inactivated vaccine in mice and rhesus monkeys. Vaccine. 2011; 29(37): 6269-75.

Downing C, Ramirez-Fort MK, Doan HQ, Benoist F, Oberste MS, Khan F, Tyring SK. Coxsackievirus A6 associated hand, foot and mouth disease in adults: clinical presentation and review of the literature. Journal of Clinical Virology. 2014; 60(4): 381-6.

Drummond AJ, Rambaut A. BEAST: Bayesian evolutionary analysis by sampling trees. BMC Evolutionary Biology. 2007; 7: 214.

Emini EA, Hughes JV, Perlow DS, Boger J. Induction of hepatitis A virus-neutralizing antibody by a virus-specific synthetic peptide. Journal of Virology. 1985; 55(3): 836-9.

Feder HM Jr, Bennett N, Modlin JF. Atypical hand, foot, and mouth disease: a vesiculobullous eruption caused by coxsackievirus A6. Lancet Infectious Disease. 2014; 14(1): 83-6.

Flett K, Youngster I, Huang J, Mcadam A, Sandora TJ, Rennick M, Smole S, Rogers SL, Nix WA, Oberste MS, Gellis S, Ahmed AA. Hand, foot, and mouth disease caused by coxsackievirus A6. Emerging Infectious Diseases. 2012; 18(10): 1702-4.

Fonseca MC, Sarmiento L, Resik S, Martinez Y, Hung LH, Morier L, Pinon A, Valdez O, Kouri V, Gonzalez G. Coxsackievirus A6 and enterovirus 71 causing hand, foot and mouth disease in Cuba, 2011-2013. Archives of Virology. 2014; 159(9): 2451-5.

Foo DG, Alonso S, Chow VT, Poh CL. Passive protection against lethal enterovirus 71 infection in newborn mice by neutralizing antibodies elicited by a synthetic peptide. Microbes and Infection. 2007a; 9(11): 1299-306.

Foo DG, Alonso S, Phoon MC, Ramachandran NP, Chow VT, Poh CL. Identification of neutralizing linear epitopes from the VP1 capsid protein of enterovirus 71 using synthetic peptides. Virus Research. 2007b; 125(1): 61-8.

Foo DG, Macary PA, Alonso S, Poh CL. Identification of human CD4 T-cell epitopes on the VP1 capsid protein of enterovirus 71. Viral Immunology. 2008; 21(2): 215-24.

Fu D, Li CR, He YX, Zu Y, Cao DZ, Wang GB, Deng JK, Wang HP. Changes of immune function in patients with enterovirus 71 infection. Zhonghua Er Ke Za Zhi. 2009; 47(11): 829-34. (Article in Chinese)

Fujii K, Nagata N, Sato Y, Ong KC, Wong KT, Yamayoshi S, Shimanuki M, Shitara H, Taya C, Koike S. Transgenic mouse model for the study of enterovirus 71 neuropathogenesis. Proceedings of the National Academy of Sciences of the United States of America. 2013; 110(36): 14753-8.

Fujimoto T, Iizuka S, Enomoto M, Abe K, Yamashita K, Hanaoka N, Okabe N, Yoshida H, Yasui Y, Kobayashi M, Fujii Y, Tanaka H, Yamamoto M, Shimizu H. Hand, foot, and mouth disease caused by coxsackievirus A6, Japan, 2011. Emerging Infectious Diseases.2012; 18(2): 337-9.

Gao F, Wang YP, Mao QY, Yao X, Liu S, Li FX, Zhu FC, Yang JY, Liang ZL, Lu FM, Wang JZ. Enterovirus 71 viral capsid protein linear epitopes: identification and characterization. Virology Journal. 2012; 9: 26.

Geller TJ, Condie D. A case of protracted coxsackievirus meningoencephalitis in a marginally immunodeficient child treated successfully with intravenous immunoglobulin. Journal of the Neurological Sciences. 1995; 129(2): 131-3.

Gilbert GL, Dickson KE, Waters MJ, Kennett ML, Land SA, Sneddon M. Outbreak of enterovirus 71 infection in Victoria, Australia, with a high incidence of neurologic involvement. Pediatric Infectious Disease Journal. 1988; 7(7): 484-8.

Goto K, Sanefuji M, Kusuhara K, Nishimura Y, Shimizu H, Kira R, Torisu H, Hara T. Rhombencephalitis and coxsackievirus A16. Emerging Infectious Diseases. 2009; 15(10): 1689-91.

Hagiwara A, Tagaya I, Yoneyama T. Epidemic of hand, foot and mouth disease associated with enterovirus 71 infection. Intervirology. 1978; 9(1): 60-3.

Hamilton MS, Jackson MA, Abel D. Clinical utility of polymerase chain reaction testing for enteroviral meningitis. Pediatric Infectious Disease Journal. 1999; 18(6): 533-7.

Hamkar R, Jalilvand S, Abdolbaghi MH, Jelyani KN, Esteghamati A, Hagh-Goo A, Mohktari-Azad T, Nategh R. Distinguishing between primary infection and reinfection with rubella vaccine virus by IgG avidity assay in pregnant women. Eastern Mediterranean Health Journal. 2009; 15(1): 94-103.

Han J, Ma XJ, Wan JF, Liu YH, Han YL, Chen C, Tian C, Gao C, Wang M, Dong XP. Long persistence of EV71 specific nucleotides in respiratory and feces samples of the patients with hand-foot-mouth disease after recovery. BMC Infectious Diseases. 2010; 10: 178.

Hashimoto I, Hagiwara A, Kodama H. Neurovirulence in cynomolgus monkeys of enterovirus 71 isolated from a patient with hand, foot and mouth disease. Archives of Virology. 1978; 56(3): 257-61.

Hashimoto I, Hagiwara A. Pathogenicity of a poliomyelitis-like disease in monkeys infected orally with enterovirus 71: a model for human infection. Neuropathology and Applied Neurobiology. 1982; 8(2): 149-56.

He DL, Xia NS, Xu FH, Cheng T, Weng ZX, Ge SX, Chen YX, Chen ZM. Enterovirus 71 neutralized epitope polypeptide and application thereof CN102690327 A. 2012. Available from: http://www. google.com/patents/CN102690327A?cl=en. Accessed February 7, 2016.

He YQ, Chen L, Xu WB, Yang H, Wang HZ, Zong WP, Xian HX, Chen HL, Yao XJ, Hu ZL, Luo M, Zhang HL, Ma HW, Cheng JQ, Feng QJ, Zhao DJ. Emergence, circulation, and spatiotemporal phylogenetic analysis of coxsackievirus A6- and coxsackievirus A10-associated hand, foot, and mouth disease infections from 2008 to 2012 in Shenzhen, China. Journal of Clinical Microbiology. 2013; 51(11): 3560-6.

Heusel JW, Wesselschmidt RL, Shresta S, Russell JH, Ley TJ. Cytotoxic lymphocytes require granzyme B for the rapid induction of DNA fragmentation and apoptosis in allogeneic target cells. Cell. 1994; 76(6): 977-87.

Ho M, Chen ER, Hsu KH, Twu SJ, Chen KT, Tsai SF, Wang JR, Shih SR. An epidemic of enterovirus 71 infection in Taiwan. Taiwan nterovirus Epidemic Working Group. New England Journal of Medicine. 1999; 341(13): 929-35.

Hober D, Sane F, Riedweg K, Moumna I, Goffard A, Choteau L, Alidjinou EK, Desailloud R. Viruses and type 1 diabetes: focus on the enteroviruses. In Escher AP, Li A, editors. Type 1 diabetes. Croatia: Intech; 2013. P 25-69.

Hofmeister Y, Planitzer CB, Farcet MR, Teschner W, Butterweck HA, Weber A, Holzer GW, Kreil TR. Human IgG subclasses: in vitro neutralization of and in vivo protection against West Nile virus. Journal of Virology. 2011; 85(4): 1896-9.

Hosoya M, Kawasaki Y, Sato M, Honzumi K, Kato A, Hiroshima T, Ishiko H, Suzuki H. Genetic diversity of enterovirus 71 associated with hand, foot and mouth disease epidemics in Japan from 1983 to 2003. Pediatric Infectious Disease Journal. 2006; 25(8): 691-4.

Huang CC, Liu CC, Chang YC, Chen CY, Wang ST, Yeh TF. Neurologic complications in children with enterovirus 71 infection. New England Journal of Medicine. 1999; 341(13): 936-42.

Huang KY, Lin JJ, Chiu CH, Yang S, Tsao KC, Huang YC, Lin TY. A potent virus-specific antibody-secreting cell response to acute enterovirus 71 infection in children. Journal of Infectious Diseases. 2015; 212(5): 808-17.

Huang SW, Hsu YW, Smith DJ, Kiang D, Tsai HP, Lin KH, Wang SM, Liu CC, Su IJ, Wang JR. Reemergence of enterovirus 71 in 2008 in taiwan: dynamics of genetic and antigenic evolution from 1998 to 2008. Journal of Clinical Microbiology. 2009; 47(11): 3653-62.

Huang YC, Lin TY, Lin YJ, Lien RI, Chou YH. Prophylaxis of intravenous immunoglobulin and acyclovir in perinatal varicella. European Journal of Pediatrics. 2001; 160(2): 91-4.

Huang YP, Lin TL, Kuo CY, Lin MW, Yao CY, Liao HW, Hsu LC, Yang CF, Yang JY, Chen PJ, Wu HS. The circulation of subgenogroups B5 and C5 of enterovirus 71 in Taiwan from 2006 to 2007. Virus Research. 2008; 137(2): 206-12.

Hyypia T, Auvinen P, Maaronen M. Polymerase chain reaction for human picornaviruses. Journal of General Virology. 1989; 70(Pt 12): 3261-8.

Janeway CA Jr, Travers P, Walport M, Schlomchik M, editors. Immunobiology: The immune system in health and disease. 5th ed. New York: Garland Science; 2001.

Ji H, Li L, Liu Y, Ge H, Wang X, Hu J, Wu B, Fu J, Zhang Z, Chen X, Zhang M, Ding Q, Xu W, Tang F, Zhou M, Wang H, Zhu F. Seroepidemiology of human enterovirus71 and coxsackievirusA16 in Jiangsu province, China. Virology Journal. 2012; 9: 248.

Jolles S, Sewell WA, Misbah SA. Clinical uses of intravenous immunoglobulin. Clinical and Experimental Immunology. 2005; 142(1): 1-11.

Kagi D, Ledermann B, Burki K, Seiler P, Odermatt B, Olsen KJ, Podack ER, Zinkernagel RM, Hengartner H. Cytotoxicity mediated by T cells and natural killer cells is greatly impaired in perforin-deficient mice. Nature. 1994; 369(6475): 31-7.

Kam YW, Lee WW, Simarmata D, Harjanto S, Teng TS, Tolou H, Chow A, Lin RT, Leo YS, Renia L, Ng LF. Longitudinal analysis of the human antibody response to chikungunya virus infection: implications for serodiagnosis and vaccine development. Journal of Virology. 2012; 86(23): 13005-15.

Kanda T, Mcmanus JE, Nagai R, Imai S, Suzuki T, Yang D, Mcmanus BM, Kobayashi I. Modification of viral myocarditis in mice by interleukin-6. Circulation Research. 1996; 78(5): 848-56.

Khanh TH, Sabanathan S, Thanh TT, Thoa Le PK, Thuong TC, Hang V, Farrar J, Hien TT, Chau N, Van Doorn HR. Enterovirus 71-associated hand, foot, and mouth disease, Southern Vietnam, 2011. Emerging Infectious Diseases. 2012; 18(12): 2002-5.

Khong WX, Foo DG, Trasti SL, Tan EL, Alonso S. Sustained high levels of interleukin-6 contribute to the pathogenesis of enterovirus 71 in a neonate mouse model. Journal of Virology. 2011; 85(7): 3067-76.

Kiener TK, Jia Q, Lim XF, He F, Meng T, Chow VT, Kwang J. 2012. Characterization and specificity of the linear epitope of the enterovirus 71 VP2 protein. Virology Journal. 2012; 9: 55.

Kiener TK, Jia Q, Meng T, Chow VT, Kwang J. A novel universal neutralizing monoclonal antibody against Enterovirus 71 that targets the highly conserved "knob" region of VP3 protein. PLOS Neglected Tropical Diseases. 2014; 8(5): e2895.

Kimura-Kuroda J, Yasui K. Protection of mice against Japanese encephalitis virus by passive administration with monoclonal antibodies. Journal of Immunology. 1988; 141(10): 3606-10.

Kirsi JJ, North JA, Mckernan PA, Murray BK, Canonico PG, Huggins JW, Srivastava PC, Robins RK. Broad-spectrum antiviral activity of 2-beta-D-ribofuranosylselenazole-4-carboxamide, a new antiviral agent. Antimicrobial Agents and Chemotherapy. 1983; 24(3): 353-61.

Kishimoto C, Crumpacker CS, Abelmann WH. Ribavirin treatment of murine coxsackievirus B3 myocarditis with analyses of lymphocyte subsets. Journal of the American College of Cardiology. 1988; 12(5): 1334-41.

Kobayashi M, Makino T, Hanaoka N, Shimizu H, Enomoto M, Okabe N, Kanou K, Konagaya M, Oishi K, Fujimoto T. Clinical manifestations of coxsackievirus A6 infection associated with a major outbreak of hand, foot, and mouth disease in Japan. Japanese Journal of Infectious Diseases. 2013; 66(3): 260-1.

Ku Z, Shi J, Liu Q, Huang Z. Development of murine monoclonal antibodies with potent neutralization effects on enterovirus 71. Journal of Virological Methods. 2012; 186(1-2): 193-197.

Le Priol Y, Puthier D, Lecureuil C, Combadiere C, Debre P, Nguyen C, Combadiere B. High cytotoxic and specific migratory potencies of senescent CD8+ CD57+ cells in HIV-infected and uninfected individuals. Journal of Immunology. 2006; 177(8): 5145-54.

Lee H, Cifuente JO, Ashley RE, Conway JF, Makhov AM, Tano Y, Shimizu H, Nishimura Y, Hafenstein S. A strain-specific epitope of enterovirus 71 identified by cryo-electron microscopy of the complex with fab from neutralizing antibody. Journal of Virology. 2013; 87(21): 11363-70.

Lee MS, Chiang PS, Luo ST, Huang ML, Liou GY, Tsao KC, Lin TY. Incidence rates of enterovirus 71 infections in young children during a nationwide epidemic in Taiwan, 2008-09. PLOS Neglected Tropical Diseases. 2012; 6(2): e1476.

Legay F, Leveque N, Gacouin A, Tattevin P, Bouet J, Thomas R, Chomelt JJ. Fatal coxsackievirus A16 pneumonitis in adult. Emerging Infectious Diseases. 2007; 13(7): 1084-6.

Li GM, Chiu C, Wrammert J, Mccausland M, Andrews SF, Zheng NY, Lee JH, Huang M, Qu X, Edupuganti S, Mulligan M, Das SR, Yewdell JW, Mehta AK, Wilson PC, Ahmed R. Pandemic H1N1 influenza vaccine induces a recall response in humans that favors broadly cross-reactive memory B cells. Proceedings of the National Academy of Sciences of the United States of America. 2012; 109(23): 9047-52.

Li J, Lin C, Qu M, Li X, Gao Z, Zhang X, Liu Y, Huang Y, Wang X, Jia L, Li X, Liu G, Yan H, Chen L, Wang Q. Excretion of enterovirus 71 in persons infected with hand, foot and mouth disease. Virology Journal. 2013; 10: 31.

Li L, Yin H, An Z, Feng Z. Considerations for developing an immunization strategy with enterovirus 71 vaccine. Vaccine. 2015a; 33(9): 1107-12.

Li MZ, Pang LL, Bai AY, Yu SC, Gong X, Liu N, Cai K, Xie GC, Gao WJ, Jin Y, Duang ZJ. Association of chemotactic chemokine ligand 5 polymorphisms with the rish of developing severe enterovirus 71 infection. American Journal of Tropical Medicine and Hygiene. 2015b; 93(4): 709-13.

Li S, Cai C, Feng J, Li X, Wang Y, Yang J, Chen Z. Peripheral T lymphocyte subset imbalances in children with enterovirus 71-induced hand, foot and mouth disease. Virus Research. 2014; 180: 84-91.

Li X, Mao C, Ma S, Wang X, Sun Z, Yi Y, Guo M, Shen X, Sun L, Bi S. Generation of neutralizing monoclonal antibodies against enterovirus 71 using synthetic peptides. Biochemical and Biophysical Research Communications. 2009; 390(4): 1126-8.

Li ZH, Li CM, Ling P, Shen FH, Chen SH, Liu CC, Yu CK, Chen SH. Ribavirin reduces mortality in enterovirus 71-infected mice by decreasing viral replication. Journal of Infectious Diseases. 2008; 197(6): 854-7.

Liang Z, Mao Q, Gao F, Wang J. Progress on the research and development of human enterovirus 71 (EV71) vaccines. Frontiers in Medicine. 2013; 7(1): 111-21.

Liang Z, Wang J. EV71 vaccine, an invaluable gift for children. Clinical and Translational Immunology. 2014; 3(10): e28.

Lim XF, Jia Q, Chow VT, Kwang J. Characterization of a novel monoclonal antibody reactive against the N-terminal region of enterovirus 71 VP1 capsid protein. Journal of Virological Methods. 2013; 188(1-2): 76-82.

Lim XF, Jia Q, Khong WX, Yan B, Premanand B, Alonso S, Chow VT, Kwang J. Characterization of an isotype-dependent monoclonal antibody against linear neutralizing epitope effective for prophylaxis of enterovirus 71 infection. PLoS One. 2012; 7(1): e29751.

Lin JY, Chen TC, Weng KF, Chang SC, Chen LL, Shih SR. Viral and host proteins involved in picornavirus life cycle. Journal of Biomedical Science. 2009a; 16: 103.

Lin KH, Hwang KP, Ke GM, Wang CF, Ke LY, Hsu YT, Tung YC, Chu PY, Chen BH, Chen HL, Kao CL, Wang JR, Eng HL, Wang SY, Hsu LC, Chen HY. Evolution of EV71 genogroup in Taiwan from 1998 to 2005: an emerging of subgenogroup C4 of EV71. Journal of Medical Virology. 2006; 78(2): 254-62.

Lin TY, Chang LY, Huang YC, Hsu KH, Chiu CH, Yang KD. Different proinflammatory reactions in fatal and non-fatal enterovirus 71 infections: implications for early recognition and therapy. Acta Paediatrica. 2002; 91(6): 632-5.

Lin TY, Hsia SH, Huang YC, Wu CT, Chang LY. Proinflammatory cytokine reactions in enterovirus 71 infections of the central nervous system. Clinical Infectious Diseases. 2003; 36(3): 269-74.

Lin YL, Yu CI, Hu YC, Tsai TJ, Kuo YC, Chi WK, Lin AN, Chiang BL. Enterovirus type 71 neutralizing antibodies in the serum of macaque monkeys immunized with EV71 virus-like particles. Vaccine. 2012; 30(7): 1305-12.

Lin YW, Chang KC, Kao CM, Chang SP, Tung YY, Chen SH. Lymphocyte and antibody responses reduce enterovirus 71 lethality in mice by decreasing tissue viral loads. Journal of Virology. 2009b; 83(13): 6477-83.

Ling BP, Jalilian FA, Harmal NS, Yubbu P, Sekawi Z. Detection and characterization of viruses causing hand, foot and mouth disease from children in Seri Kembangan, Malaysia. Tropical Biomedicine. 2014; 31(4): 654-62.

Linsuwanon P, Puenpa J, Huang SW, Wang YF, Mauleekoonphairoj J, Wang JR, Poovorawan Y. Epidemiology and seroepidemiology of human enterovirus 71 among Thai populations. Journal of Biomedical Science. 2014; 21: 16.

Lipson SM, Walderman R, Costello P, Szabo K. Sensitivity of rhabdomyosarcoma and guinea pig embryo cell cultures to field isolates of difficult-to-cultivate group A coxsackieviruses. Journal of Clinical Microbiology. 1988; 26(7): 1298-303.

Liu CC, Chou AH, Lien SP, Lin HY, Liu SJ, Chang JY, Guo MS, Chow YH, Yang WS, Chang KH, Sia C, Chong P. Identification and characterization of a cross-neutralization epitope of Enterovirus 71. Vaccine. 2011; 29(26): 4362-72.

Liu CC, Tseng HW, Wang SM, Wang JR, Su IJ. An outbreak of enterovirus 71 infection in Taiwan, 1998: epidemiologic and clinical manifestations. Journal of Clinical Virology. 2000; 17(1): 23-30.

Liu JN, Wang W, Duo JY, Hao Y, Ma CM, Li WB, Lin SZ, Gao XZ, Liu XL, Xu YF, Xu WB, Qin C, Zhang LF. Combined peptides of human enterovirus 71 protect against virus infection in mice. Vaccine. 2010; 28(46): 7444-51.

Liu L, Mo Z, Liang Z, Zhang Y, Li R, Ong KC, Wong KT, Yang E, Che Y, Wang J, Dong C, Feng M, Pu J, Wang L, Liao Y, Jiang L, Tan SH, David P, Huang T, Zhou Z, Wang X, Xia J, Guo L, Wang L, Xie Z, Cui W, Mao Q, Liang Y, Zhao H, Na R, Cui P, Shi H, Wang J, Li Q. Immunity and clinical efficacy of an inactivated enterovirus 71 vaccine in healthy Chinese children: a report of further observations. BMC Medicine. 2015; 13: 226.

Liu ML, Lee YP, Wang YF, Lei HY, Liu CC, Wang SM, Su IJ, Wang JR, Yeh TM, Chen SH, Yu CK. Type I interferons protect mice against enterovirus 71 infection. Journal of General Virology. 2005; 86(Pt 12): 3263-9.

Lo SH, Huang YC, Huang CG, Tsao KC, Li WC, Hsieh YC, Chiu CH, Lin TY. Clinical and epidemiologic features of coxsackievirus A6 infection in children in northern Taiwan between 2004 and 2009. Journal of Microbiology, Immunology and Infection. 2011; 44(4): 252-7.

Lott JP, Liu K, Landry ML, Nix WA, Oberste MS, Bolognia J, King B. Atypical hand-foot-and-mouth disease associated with coxsackievirus A6 infection. Journal of the American Academy of Dermatology. 2013; 69(5): 736-41.

Lu QB, Zhang XA, Wo Y, Xu HM, Li XJ, Wang XJ, Ding SJ, Chen XD, He C, Liu LJ, Li H, Yang H, Li TY, Liu W, Cao WC. Circulation of coxsackievirus A10 and A6 in hand-foot-mouth disease in China, 2009-2011. PLoS One. 2012; 7(12): e52073.

Lum LC, Chua KB, Mcminn PC, Goh AY, Muridan R, Sarji SA, Hooi PS, Chua BH, Lam SK. Echovirus 7 associated encephalomyelitis. Journal of Clinical Virology. 2002; 23(3): 153-60.

Lum LC, Wong KT, Lam SK, Chua KB, Goh AY, Lim WL, Ong BB, Paul G, Abubakar S, Lambert M. Fatal enterovirus 71 encephalomyelitis. Journal of Pediatrics. 1998; 133(6): 795-8.

Luo ST, Chiang PS, Chao AS, Liou GY, Lin R, Lin TY, Lee MS. Enterovirus 71 maternal antibodies in infants, Taiwan. Emerging Infectious Diseases. 2009; 15(4): 581-4.

Ma CS, Suryani S, Avery DT, Chan A, Nanan R, Santner-Nanan B, Deenick EK, Tangye SG. Early commitment of naive human CD4(+) T cells to the T follicular helper (T(FH)) cell lineage is induced by IL-12. Immunology and Cell Biology. 2009; 87(8): 590-600.

Ma LN, Zhang J, Chen HT, Zhou JH, Ding YZ, Liu YS. An overview on ELISA techniques for FMD. Virology Journal. 2011; 8: 419.

Mahon BP, Katrak K, Mills KH. Antigenic sequences of poliovirus recognized by T cells: serotype-specific epitopes on VP1 and VP3 and cross-reactive epitopes on VP4 defined by using CD4+ T-cell clones. Journal of Virology. 1992; 66(12): 7012-20.

Man-Li T, Szyporta M, Fang LX, Lwang J. Identification and characterization of a monoclonal antibody recognizing the linear epitope RVADVI on VP1 protein of enterovirus 71. Journal of Medical Virology. 2012; 84(10):1620-7.

Mao Q, Cheng T, Zhu F, Li J, Wang Y, Li Y, Gao F, Yang L, Yao X, Shao J, Xia N, Liang Z, Wang J. The cross-neutralizing activity of enterovirus 71 subgenotype C4 vaccines in healthy chinese infants and children. PLoS One. 2013; 8(11): e79599.

Mao Q, Wang Y, Yao X, Bian L, Wu X, Xu M, Liang Z. Coxsackievirus A16: epidemiology, diagnosis, and vaccine. Human Vaccines and Immunotherapeutics. 2014; 10(2): 360-7.

Marron MP, Raffel LJ, Garchon HJ, Jacob CO, Serrano-Rios M, Martinez Larrad MT, Teng WP, Park Y, Zhang ZX, Goldstein DR, Tao YW, Beaurain G, Bach JF, Huang HS, Luo DF, Zeidler A, Rotter JI, Yang MC, Modilevsky T, Maclaren NK, She JX. Insulin-dependent diabetes mellitus (IDDM) is associated with CTLA4 polymorphisms in multiple ethnic groups. Human Molecular Genetics. 1997; 6(8): 1275-82.

Martinez-Gil L, Bano-Polo M, Redondo N, Sanchez-Martinez S, Nieva JL, Carrasco L, Mingarro I. Membrane integration of poliovirus 2B viroporin. Journal of Virology. 2011; 85(21): 11315-24.

Mcminn PC. An overview of the evolution of enterovirus 71 and its clinical and public health significance. FEMS Microbiology Reviews. 2002; 26(1): 91-107.

Mcminn PC. Recent advances in the molecular epidemiology and control of human enterovirus 71 infection. Current Opinion in Virology. 2012; 2(2): 199-205.

Mirand A, Henquell C, Archimbaud C, Ughetto S, Antona D, Bailly JL, Peigue-Lafeuille H. Outbreak of hand, foot and mouth disease/herpangina associated with coxsackievirus A6 and A10 infections in 2010, France: a large citywide, prospective observational study. Clinical Microbiology and Infection. 2012; 18(5): E110-8.

Montes M, Artieda J, Pineiro LD, Gastesi M, Diez-Nieves I, Cilla G. Hand, foot, and mouth disease outbreak and coxsackievirus A6, northern Spain, 2011. Emerging Infectious Diseases. 2013; 19(4): 676-8.

Morbach H, Eichhorn EM, Liese JG, Girschick HJ. Reference values for B cell subpopulations from infancy to adulthood. Clinical and Experimental Immunology. 2010; 162(2): 271-9.

Morgan-Capner P, Hambling MH, Coleman TJ, Watkins RP, Stern H, Hodgson J, Dulake C, Boswell PA, Booth J, Best JM, Banatvala JE. Detection of rubella-specific IgM in subclinical rubella reinfection in pregnancy. Lancet. 1985; 1(8423): 244-6.

Muir P, Kammerer U, Korn K, Mulders MN, Poyry T, Weissbrich B, Kandolf R, Cleator GM, van Loon AM. Molecular typing of enteroviruses: current status and future requirements. The European Union Concerted Action on Virus Meningitis and Encephalitis. Clinical Microbiology Reviews. 1998; 11(1): 202-27.

Nagy G, Takatsy S, Kukan E, Mihaly I, Domok I. Virological diagnosis of enterovirus type 71 infections: experiences gained during an epidemic of acute CNS diseases in Hungary in 1978. Archives of Virology. 1982; 71(3): 217-27.

Ng DK, Law AK, Cherk SW, Mak KL. First fatal case of enterovirus 71 infection in Hong Kong. Hong Kong Medical Journal. 2001; 7(2): 193-6.

Ng Q, He F, Kwang J. Recent progress towards novel EV71 anti-therapeutics and vaccines. Viruses. 2015; 7(12): 6441-57.

Niknadia N, Sam IC, Khaidir N, Ngui R, Lim YA, Goh XT, Choy SH, Chan YF. Risk factors for enterovirus A71 seropositivity in rural indigenous populations in west Malaysia. PLoS One. 2016; 11(2): e0148767.

Oberste MS, Maher K, Kilpatrick DR, Pallansch MA. Molecular evolution of the human enteroviruses: correlation of serotype with VP1 sequence and application to picornavirus classification. Journal of Virology. 1999; 73(3): 1941-8.

Ong KC, Devi S, Cardosa MJ, Wong KT. Formaldehyde-inactivated whole-virus vaccine protects a murine model of enterovirus 71 encephalomyelitis against disease. Journal of Virology. 2010; 84(1): 661-5.

Ooi MH, Wong SC, Lewthwaite P, Cardosa MJ, Solomon T. Clinical features, diagnosis, and management of enterovirus 71. Lancet Neurology. 2010; 9(11): 1097-105.

Ooi MH, Wong SC, Mohan A, Podin Y, Perera D, Clear D, Del Sel S, Chieng CH, Tio PH, Cardosa MJ, Solomon T. Identification and validation of clinical predictors for the risk of neurological involvement in children with hand, foot, and mouth disease in Sarawak. BMC Infectious Diseases. 2009; 9: 3.

Ooi MH, Wong SC, Podin Y, Akin W, Del Sel S, Mohan A, Chieng CH, Perera D, Clear D, Wong D, Blake E, Cardosa J, Solomon T. Human enterovirus 71 disease in Sarawak, Malaysia: a prospective clinical, virological, and molecular epidemiological study. Clinical Infectious Diseases. 2007; 44(5): 646-56.

Osterback R, Vuorinen T, Linna M, Susi P, Hyypia T, Waris M. Coxsackievirus A6 and hand, foot, and mouth disease, Finland. Emerging Infectious Diseases. 2009; 15(9): 1485-8.

Pettersen EF, Goddard TD, Huang CC, Couch GS, Greenblatt DM, Meng EC, Ferrin TE. UCSF Chimera - a visualization system for exploratory research and analysis. Journal of Computational Chemistry. 2004; 25(13): 1605-12.

Pevear DC, Tull TM, Seipel ME, Groarke JM. Activity of pleconaril against enteroviruses. Antimicrobial Agents and Chemotherapy. 1999; 43(9): 2109-15.

Podin Y, Gias EL, Ong F, Leong YW, Yee SF, Yusof MA, Perera D, Teo B, Wee TY, Yao SC, Yao SK, Kiyu A, Arif MT, Cardosa MJ. Sentinel surveillance for human enterovirus 71 in Sarawak, Malaysia: lessons from the first 7 years. BMC Public Health. 2006; 6: 180.

Posada D. jModelTest: phylogenetic model averaging. Molecular Biology and Evolution. 2008; 25(7): 1253-6.

Puenpa J, Chieochansin T, Linsuwanon P, Korkong S, Thongkomplew S, Vichaiwattana P, Theamboonlers A, Poovorawan Y. Hand, foot, and mouth disease caused by coxsackievirus A6, Thailand, 2012. Emerging Infectious Diseases. 2013; 19(4): 641-3.

Rambaut A. FigTree v1.4.0: Tree figure drawing tool. 2012. Available from: http://tree.bio.ed.ac.uk/software/figtree/. Accessed February 7, 2016.

Renert-Yuval Y, Marva E, Weil M, Shulman LM, Gencylmaz N, Sheffer S, Wolf DG, Molho-Pessach V. Coxsackievirus A6 polymorphic exanthem in Israeli children. Acta Dermato-Venereologica. 2015; Epub ahead of print.

Robinson CC, Willis M, Meagher A, Gieseker KE, Rotbart H, Glode MP. Impact of rapid polymerase chain reaction results on management of pediatric patients with enteroviral meningitis. Pediatric Infectious Disease Journal. 2002; 21(4): 283-6.

Rock MT, Yoder SM, Wright PF, Talbot TR, Edwards KM, Crowe JE Jr. Differential regulation of granzyme and perforin in effector and memory T cells following smallpox immunization. Journal of Immunology. 2005; 174(6): 3757-64.

Rodrigo WW, Block OK, Lane C, Sukupolvi-Petty S, Goncalvez AP, Johnson S, Diamond MS, Lai CJ, Rose RC, Jin X, Schlesinger JJ. Dengue virus neutralization is modulated by IgG antibody subclass and Fcgamma receptor subtype. Virology. 2009; 394(2): 175-82.

Rohll JB, Moon DH, Evans DJ, Almond JW. The 3' untranslated region of picornavirus RNA: features required for efficient genome replication. Journal of Virology. 1995; 69(12): 7835-44.

Ryu WS, Kang B, Hong J, Hwang S, Kim J, Cheon DS. Clinical and etiological characteristics of enterovirus 71-related diseases during a recent 2-year period in Korea. Journal of Clinical Microbiology. 2010; 48(7): 2490-4.

Santti J, Hyypia T, Kinnunen L, Salminen M. Evidence of recombination among enteroviruses. Journal of Virology. 1999; 73(10): 8741-9.

Schmidt NJ, Lennette EH, Ho HH. An apparently new enterovirus isolated from patients with disease of the central nervous system. Journal of Infectious Diseases. 1974; 129(3): 304-9.

Shea YF, Chan CY, Hung IF, Chan KH. Hand, foot and mouth disease in an immunocompetent adult due to coxsackievirus A6. Hong Kong Medical Journal. 2013; 19(3): 262-4.

Shen FH, Tsai CC, Wang LC, Chang KC, Tung YY, Su IJ, Chen SH. Enterovirus 71 infection increases expression of interferon-gamma-inducible protein 10 which protects mice by reducing viral burden in multiple tissues. Journal of General Virology. 2013; 94(Pt 5): 1019-27.

Shih SR, Stollar V, Li ML. Host factors in enterovirus 71 replication. Journal of Virology. 2011; 85(19): 9658-66.

Shindarov LM, Chumakov MP, Voroshilova MK, Bojinov S, Vasilenko SM, Iordanov I, Kirov ID, Kamenov E, Leshchinskaya EV, Mitov G, Robinson IA, Sivchev S, Staikov S. Epidemiological, clinical, and pathomorphological characteristics of epidemic poliomyelitis-like disease caused by enterovirus 71. Journal of Hygiene, Epidemiology, Microbiology and Immunology. 1979; 23(3): 284-95.

Shingler KL, Cifuente JO, Ashley RE, Makhov AM, Conway JF, Hafenstein S. The enterovirus 71 procapsid binds neutralizing antibodies and rescues virus infection in vitro. Journal of Virology. 2015; 89(3): 1900–8.

Sivasamugham LA, Cardosa MJ, Tan WS, Yusoff K. Recombinant newcastle disease virus capsids displaying enterovirus 71 VP1 fragment induce a strong immune response in rabbits. Journal of Medical Virology. 2006; 78(8): 1096-104.

Solomon T, Lewthwaite P, Perera D, Cardosa MJ, Mcminn P, Ooi MH. Virology, epidemiology, pathogenesis, and control of enterovirus 71. Lancet Infectious Disease. 2010; 10(11): 778-90.

Sorensen KJ, de Stricker K, Dyrting KC, Grazioli S, Haas B. Differentiation of foot-and-mouth disease virus infected animals from vaccinated animals using a blocking ELISA based on baculovirus expressed FMDV 3ABC antigen and a 3ABC monoclonal antibody. Archives of Virology. 2005; 150(4): 805-14.

Steil BP, Barton DJ. Cis-active RNA elements (CREs) and picornavirus RNA replication. Virus Research. 2009; 139(2): 240-52.

Stewart CL, Chu EY, Introcaso CE, Schaffer A, James WD. Coxsackievirus A6-induced hand-foot-mouth disease. JAMA Dermatology. 2013; 149(12): 1419-21.

Takaoka A, Yanai H. Interferon signalling network in innate defence. Cellular Microbiology. 2006; 8(6): 907-22.

Tan CS, Cardosa MJ. High-titred neutralizing antibodies to human enterovirus 71 preferentially bind to the N-terminal portion of the capsid protein VP1. Archives of Virology. 2007; 152(6): 1069-73.

Tan CW, Lai JKF, Sam IC, Chan YF. Recent developments in antiviral agents against enterovirus 71 infection. Journal of Biomedical Science. 2014; 21: 14.

Tan S, Tan X, Sun X, Lu G, Chen CC, Yan J, Liu J, Xu W, Gao GF. VP2 dominated CD4+ T cell responses against enterovirus 71 and cross-reactivity against coxsackievirus A16 and polioviruses in a healthy population. Journal of Immunology. 2013; 191(4): 1637-47.

Tan X, Huang X, Zhu S, Chen H, Yu Q, Wang H, Huo X, Zhou J, Wu Y, Yan D, Zhang Y, Wang D, Cui A, An H, Xu W. The persistent circulation of enterovirus 71 in People's Republic of China: causing emerging nationwide epidemics since 2008. PLoS One. 2011; 6(9): e25662.

Tee KK, Lam TT, Chan YF, Bible JM, Kamarulzaman A, Tong CY, Takebe Y, Pybus OG. Evolutionary genetics of human enterovirus 71: origin, population dynamics, natural selection, and seasonal periodicity of the VP1 gene. Journal of Virology. 2010; 84(7): 3339-50.

Thompson SR Sarnow P. Enterovirus 71 contains a type I IRES element that functions when eukaryotic initiation factor eIF4G is cleaved. Virology. 2003; 315(1): 259-66.

Trapani JA, Jans DA, Jans PJ, Smyth MJ, Browne KA, Sutton VR. Efficient nuclear targeting of granzyme B and the nuclear consequences of apoptosis induced by granzyme B and perforin are caspase-dependent, but cell death is caspase-independent. Journal of Biological Chemistry. 1998; 273(43): 27934-8.

Tu PV, Thao NT, Perera D, Huu TK, Tien NT, Thuong TC, How OM, Cardosa MJ, Mcminn PC. Epidemiologic and virologic investigation of hand, foot, and mouth disease, southern Vietnam, 2005. Emerging Infectious Diseases. 2007; 13(11): 1733-41.

Tung WS, Bakar SA, Sekawi Z, Rosli R. 2007. DNA vaccine constructs against enterovirus 71 elicit immune response in mice. Genetic Vaccines and Therapy. 2007; 5: 6.

van der Sanden S, van Eek J, Martin DP, van der Avoort H, Vennema H, Koopmans M. Detection of recombination breakpoints in the genomes of human enterovirus 71 strains isolated in the Netherlands in epidemic and non-epidemic years, 1963-2010. Infection, Genetics and Evolution. 2011; 11(5): 886-94.

Wang CY, Li Lu F, Wu MH, Lee CY, Huang LM. Fatal coxsackievirus A16 infection. Pediatric Infectious Disease Journal. 2004a; 23(3): 275-6.

Wang JR, Tsai HP, Chen PF, Lai YJ, Yan JJ, Kiang D, Lin KH, Liu CC, Su IJ. An outbreak of enterovirus 71 infection in Taiwan, 1998. II. Laboratory diagnosis and genetic analysis. Journal of Clinical Virology. 2000; 17(2): 91-9.

Wang L, Wang J, Wang L, Ma S, Liu Y. Anti-enterovirus 71 agents of natural products. Molecules. 2015a; 20(9): 16320-33.

Wang LC, Kao CM, Ling P, Su IJ, Chang TM, Chen SH. CD4 T-cell-independent antibody response reduces enterovirus 71 lethality in mice by decreasing tissue viral loads. Clinical and Developmental Immunology. 2012; 2012: 580696.

Wang M, Jiang S, Wang Y. Recombinant VP1 protein expressed in Pichia pastoris induces protective immune responses against EV71 in mice. Biochemical and Biophysical Research Communications. 2013; 430(1): 387-93.

Wang SM, Lei HY, Huang KJ, Wu JM, Wang JR, Yu CK, Su IJ, Liu CC. Pathogenesis of enterovirus 71 brainstem encephalitis in pediatric patients: roles of cytokines and cellular immune activation in patients with pulmonary edema. Journal of Infectious Diseases. 2003; 188(4): 564-70.

Wang SM, Lei HY, Huang MC, Su LY, Lin HC, Yu CK, Wang JL, Liu CC. Modulation of cytokine production by intravenous immunoglobulin in patients with enterovirus 71-associated brainstem encephalitis. Journal of Clinical Virology. 2006; 37(1): 47-52.

Wang SM, Lei HY, Su LY, Wu JM, Yu CK, Wang JR, Liu CC. Cerebrospinal fluid cytokines in enterovirus 71 brain stem encephalitis and echovirus meningitis infections of varying severity. Clinical Microbiology and Infection. 2007; 13(7): 677-82.

Wang SY, Lin TL, Chen HY, Lin TS. Early and rapid detection of enterovirus 71 infection by an IgM-capture ELISA. Journal of Virological Methods. 2004b; 119(1): 37-43.

Wang Y, Zou G, Xia A, Wang X, Cai J, Gao Q, Yuan S, He G, Zhang S, Zeng M, Altmeyer R. Enterovirus 71 infection in children with hand, foot, and mouth disease in Shanghai, China: epidemiology, clinical feature and diagnosis. Virology Journal. 2015b; 12: 83.

Wang YF, Yu CK. Animal models of enterovirus 71 infection: applications and limitations. Journal of Biomedical Science. 2014; 21: 31.

Weber CA, Mehta PJ, Ardito M, Moise L, Martin B, De Groot AS. T cell epitope: friend or foe? Immunogenicity of biologics in context. Advanced Drug Delivery Reviews. 2009; 61(11): 965-76.

Wei R, Yang C, Zeng M, Terry F, Zhu K, Yang C, Altmeyer R, Martin W, de Groot AS, Leng Q. A dominant EV71-specific CD4+ T cell epitope is highly conserved among human enteroviruses. PLoS One. 2012; 7(12): e51957.

Wei SH, Huang YP, Liu MC, Tsou TP, Lin HC, Lin TL, Tsai CY, Chao YN, Chang LY, Hsu CM. An outbreak of coxsackievirus A6 hand, foot, and mouth disease associated with onychomadesis in Taiwan, 2010. BMC Infectious Diseases. 2011; 11: 346.

World Health Organization. Hepatitis B. Available from: http://www.who.int/csr/ disease /hepatitis/whocdscsrlyo20022/en/index3.html. Accessed February 7, 2016.

Wright HT Jr, Landing BH, Lennette EH, Mc AR. Fatal infection in an infant associated with coxsackie virus group A, type 16. The New England Journal of Medicine. 1963; 268: 1041-4.

Wu J, Cui D, Yang X, Lou J, Lin J, Ye X, Qin Z, Huang L, Zhao D, Huo Z, Xie G, Zheng S, Yu F, Lu L, Chen Y. Increased frequency of circulating follicular helper T cells in children with hand, foot, and mouth disease caused by enterovirus 71 infection. Journal of Immunology Research. 2014; 2014: 651872.

Wu TC, Wang YF, Lee YP, Wang JR, Liu CC, Wang SM, Lei HY, Su IJ, Yu CK. Immunity to avirulent enterovirus 71 and coxsackie A16 virus protects against enterovirus 71 infection in mice. Journal of Virology. 2007; 81(19): 10310-5.

Wu TN, Tsai SF, Li SF, Lee TF, Huang TM, Wang ML, Hsu KH, Shen CY. Sentinel surveillance for enterovirus 71, Taiwan, 1998. Emerging Infectious Diseases. 1999; 5(3): 458-60.

Wu Y, Yeo A, Phoon MC, Tan EL, Poh CL, Quak SH, Chow VT. The largest outbreak of hand; foot and mouth disease in Singapore in 2008: the role of enterovirus 71 and coxsackievirus A strains. International Journal of Infectious Diseases. 2010; 14(12): e1076-81.

Xie J, Jiao Y, Qiu Z, Li Q, Li T. 2010. Significant elevation of B cells at the acute stage in enterovirus 71-infected children with central nervous system involvement. Scandinavian Journal of Infectious Diseases. 2010; 42(11-12): 931-5.

Xu F, Yan Q, Wang H, Niu J, Li L, Zhu F, He S, Zhang S, Weng Z, Cheng T, Cai Y, He D, Chen Y, Ge S, Yeo AE, Zhang J, Ng MH, Xia N. Performance of detecting IgM antibodies against enterovirus 71 for early diagnosis. PLoS One. 2010; 5(6): e11388.

Xu L, He D, Li Z, Zheng J, Yang L, Yu M, Yu H, Chen Y, Que Y, Shih JW, Liu G, Zhang J, Zhao Q, Cheng T, Xia N. Protection against lethal enterovirus 71 challenge in mice by a recombinant vaccine candidate containing a broadly cross-neutralizing epitope within the VP2 EF loop. Theranostics. 2014; 4(5): 498-513.

Xu W, Liu CF, Yan L, Li JJ, Wang LJ, Qi Y, Cheng RB, Xiong XY. Distribution of enteroviruses in hospitalized children with hand, foot and mouth disease and relationship between pathogens and nervous system complications. Virology Journal. 2012; 9: 8.

Yan JJ, Su IJ, Chen PF, Liu CC, Yu CK, Wang JR. Complete genome analysis of enterovirus 71 isolated from an outbreak in Taiwan and rapid identification of enterovirus 71 and coxsackievirus A16 by RT-PCR. Journal of Medical Virology. 2001; 65(2): 331-9.

Yang C, Deng C, Wan J, Zhu L, Leng Q. Neutralizing antibody response in the patients with hand, foot and mouth disease to enterovirus 71 and its clinical implications. Virology Journal. 2011; 8: 306.

Yang F, Ren L, Xiong Z, Li J, Xiao Y, Zhao R, He Y, Bu G, Zhou S, Wang J, Qi J. Enterovirus 71 outbreak in the People's Republic of China in 2008. Journal of Clinical Microbiology. 2009; 47(7): 2351-2.

Yang KD, Yang MY, Li CC, Lin SF, Chong MC, Wang CL, Chen RF, Lin TY. Altered cellular but not humoral reactions in children with complicated enterovirus 71 infections in Taiwan. Journal of Infectious Diseases. 2001; 183(6): 850-6.

Yip CC, Lau SK, Woo PC, Yuen KY. Human enterovirus 71 epidemics: what's next? Emerging Health Threats Journal. 2013; 6: 19780.

Yoke-Fun C, AbuBakar S. Phylogenetic evidence for inter-typic recombination in the emergence of human enterovirus 71 subgenotypes. BMC Microbiology. 2006; 6: 74.

Yu CK, Chen CC, Chen CL, Wang JR, Liu CC, Yan JJ, Su IJ. Neutralizing antibody provided protection against enterovirus type 71 lethal challenge in neonatal mice. Journal of Biomedical Science. 2000; 7(6): 523-8.

Yu H, Chen W, Chang H, Tang R, Zhao J, Gan L, Liu B, Chen J, Wang M. Genetic analysis of the VP1 region of enterovirus 71 reveals the emergence of genotype A in central China in 2008. Virus Genes. 2010; 41(1): 1-4.

Yu N, Guo M, He SJ, Pan YX, Chen XX, Ding XX, Hao W, Wang YD, Ge SX, Xia NS, Che XY. Evaluation of human enterovirus 71 and coxsackievirus A16 specific immunoglobulin M antibodies for diagnosis of hand-foot-and-mouth disease. Virology Journal. 2012; 9: 12.

Yusof MA, Ali HM, Shariff HM, Ramli NK, Zawawi ZM, Aisyatun SN, Dennis JA, Saat Z. Subgenogroup B5 maintains its supremacy over other human enterovirus 71 strains that circulated in Malaysia from 2010 to 2012. Journal of General and Molecular Virology. 2014; 6(1): 1-5.

Zaini Z, Mcminn P. Complete genome sequence of a human enterovirus 71 strain isolated in Brunei in 2006. Genome Announcements. 2013; 1(4): e00522-13.

Zhang D, Shankar P, Xu Z, Harnisch B, Chen G, Lange C, Lee SJ, Valdez H, Lederman MM, Lieberman J. Most antiviral CD8 T cells during chronic viral infection do not express high levels of perforin and are not directly cytotoxic. Blood. 2003; 101(1): 226-35.

Zhang J, Weng Z, Du H, Xu F, He S, He D, Cheng T, Zhang J, Ge S, Xia N. Development and evaluation of rapid point-of-care tests for detection of enterovirus 71 and coxsackievirus A16 specific immunoglobulin M antibodies. Journal of Virological Methods. 2016; 231:44-7.

Zhang Y, Wang D, Yan D, Zhu S, Liu J, Wang H, Zhao S, Yu D, Nan L, An J, Chen L, An H, Xu A, Xu W. Molecular evidence of persistent epidemic and evolution of subgenotype B1 coxsackievirus A16-associated hand, foot, and mouth disease in China. Journal of Clinical Microbiology. 2010a; 48(2): 619-22.

Zhang Y, Zhu Z, Yang W, Ren J, Tan X, Wang Y, Mao N, Xu S, Zhu S, Cui A, Zhang Y, Yan D, Li Q, Dong X, Zhang J, Zhao Y, Wan J, Feng Z, Sun J, Wang S, Li D, Xu W. An emerging recombinant human enterovirus 71 responsible for the 2008 outbreak of hand foot and mouth disease in Fuyang city of China. Virology Journal. 2010b; 7: 94.

Zhao J, Xu J, Chen WW, Li YL, Tang Y, Li J, Wang HB, Guo TS, Zhao M, Li BA, Mao YL. The early diagnosis value of EV71 IgM class antibodies in the hand, foot, and mouth disease. Zhonghua Shi Yan He Lin Chuang Bing Du Xue Za Zhi. 2011; 25(2):140-2. (Article in Chinese)

Zhao M, Bai Y, Liu W, Xiao X, Huang Y, Cen S, Chan PK, Sun X, Sheng W, Zeng Y. Immunization of N terminus of enterovirus 71 VP4 elicits cross-protective antibody responses. BMC Microbiology. 2013; 13: 287.

Zheng ZM, He PJ, Cauffield D, Neumann M, Specter S, Baker CC, Bankowski MJ. Enterovirus 71 isolated from China is serologically similar to the prototype E71 BrCr strain but differs in the 5'-noncoding region. Journal of Medical Virology. 1995; 47(2): 161-7.

Zhou F, Kong F, Wang B, Mcphie K, Gilbert GL, Dwyer DE. Molecular characterization of enterovirus 71 and coxsackievirus A16 using the 5' untranslated region and VP1 region. Journal of Medical Microbiology. 2011; 60(Pt 3): 349-58.

Zhou F, Wang Q, Sintchenko V, Gilbert GL, O'sullivan MV, Iredell JR, Dwyer DE. Use of the 5' untranslated region and VP1 region to examine the molecular diversity in enterovirus B species. Journal of Medical Microbiology. 2014; 63(Pt 10): 1339-55.

Zhu J, Luo Z, Wang J, Xu Z, Chen H, Fan D, Gao N, Ping G, Zhou Z, Zhang Y, An J. Phylogenetic analysis of enterovirus 71 circulating in Beijing, China from 2007 to 2009. PLoS One. 2013; 8(2): e56318.

Zong W, He Y, Yu S, Yang H, Xian H, Liao Y, Hu G. Molecular phylogeny of coxsackievirus A16 in Shenzhen, China, from 2005 to 2009. Journal of Clinical Microbiology. 2011; 49(4): 1659-61.

Zou XN, Zhang XZ, Wang B, Qiu YT. Etiologic and epidemiologic analysis of hand, foot, and mouth disease in Guangzhou city: a review of 4,753 cases. Brazilian Journal of Infectious Diseases. 2012; 16(5): 457-65.

Appendix I: Nucleotide accession numbers of sequences reported in the present study

Isolate name	Accession number			Genotype
	5' UTR	VP4	VP1	
EV-A71				
MY-3898-12	KT908004	KT908026	NA	B5
MY-2949-12	NA	KT908027	NA	B5
MY-8352-12	KT908005	KT908028	NA	B5
MY-5105-12	KT908006	KT908029	NA	B5
MY-5313-12	KT908007	KT908030	NA	B5
MY-5390-12	KT908008	KT908031	NA	B5
MY-4703-12	KT908009	KT908032	NA	B5
MY-4285-12	KT908010	KT908033	NA	B5
MY-9836-12	KT908011	KT908034	NA	B5
MY-6937-12	KT908012	KT908035	NA	B5
MY-0757-12	KT908013	KT908036	NA	B5
MY-6407-13	KT908014	KT908037	NA	B5
CV-A16				
MY-2235-12	KT908015	NA	KT908038	B2b
CV-A6				
MY-6046-12	KT908016	NA	KJ815033	D1
MY-8586-12	KT908017	NA	KJ815034	D1
MY-2429-12	KT908018	NA	KJ815035	D1
MY-0446-12	NA	NA	KJ815036	D1
MY-3626-12	KT908019	NA	KJ815037	D2
MY-8299-13	KT908020	NA	KJ815038	D2
MY-6716-13	NA	NA	KJ815039	D2
MY-4657-13	KT908021	NA	KJ815040	D2
MY-0017-13	KT908022	NA	KJ815041	D2
MY-9784-13	KT908023	NA	KJ815042	D2
MY-8698-13	KT908024	NA	KJ815043	D2
MY-0319-13	KT908025	NA	KJ815044	D1

NA, not available

Appendix II: Schematic illustration of pUC57 vector and the restriction endonuclease recognition sites

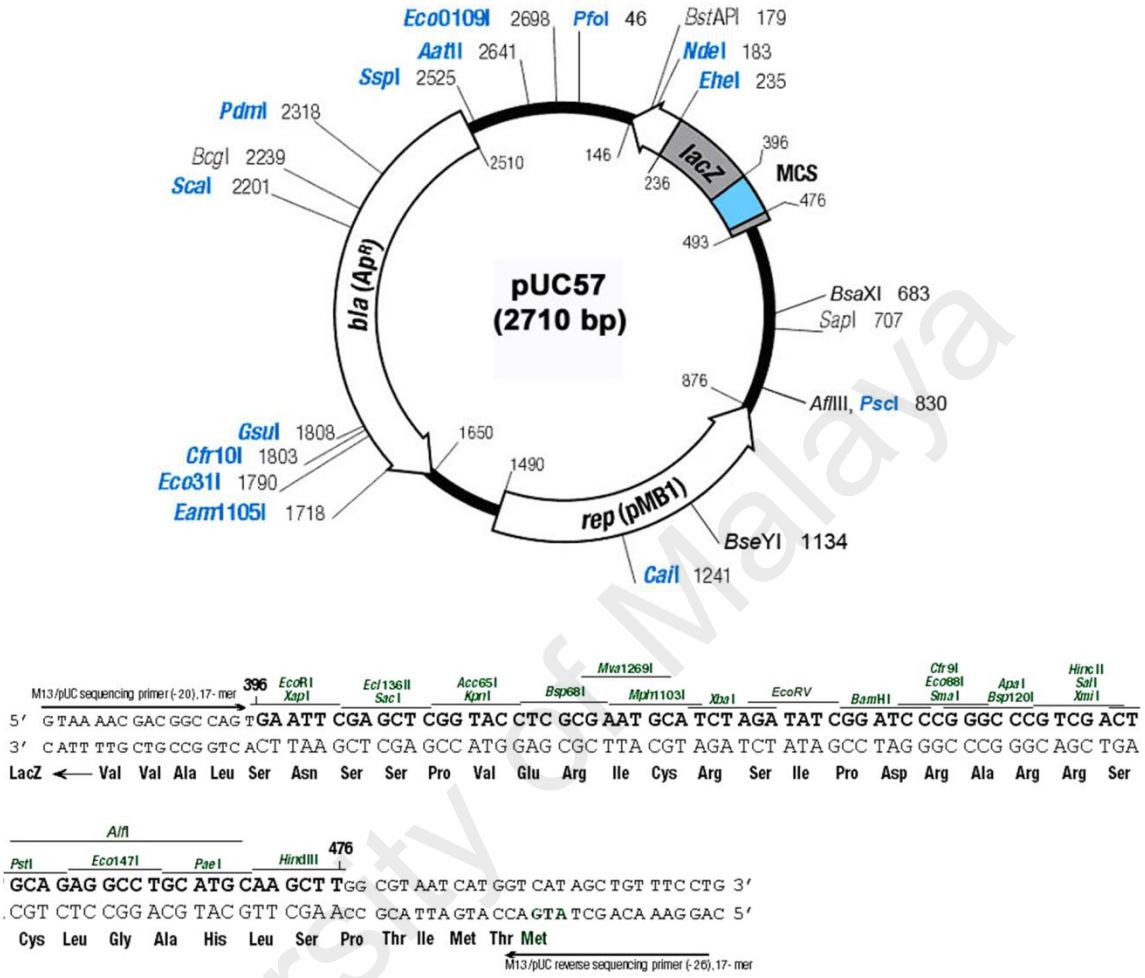

This figure is adapted from the pUC57 information sheet in GenScript webpage, http://www.genscript.com/vector/SD1176-pUC57_plasmid_DNA.html.

Appendix III: Schematic illustration of pET-52b(+) vector and the restriction endonuclease recognition sites

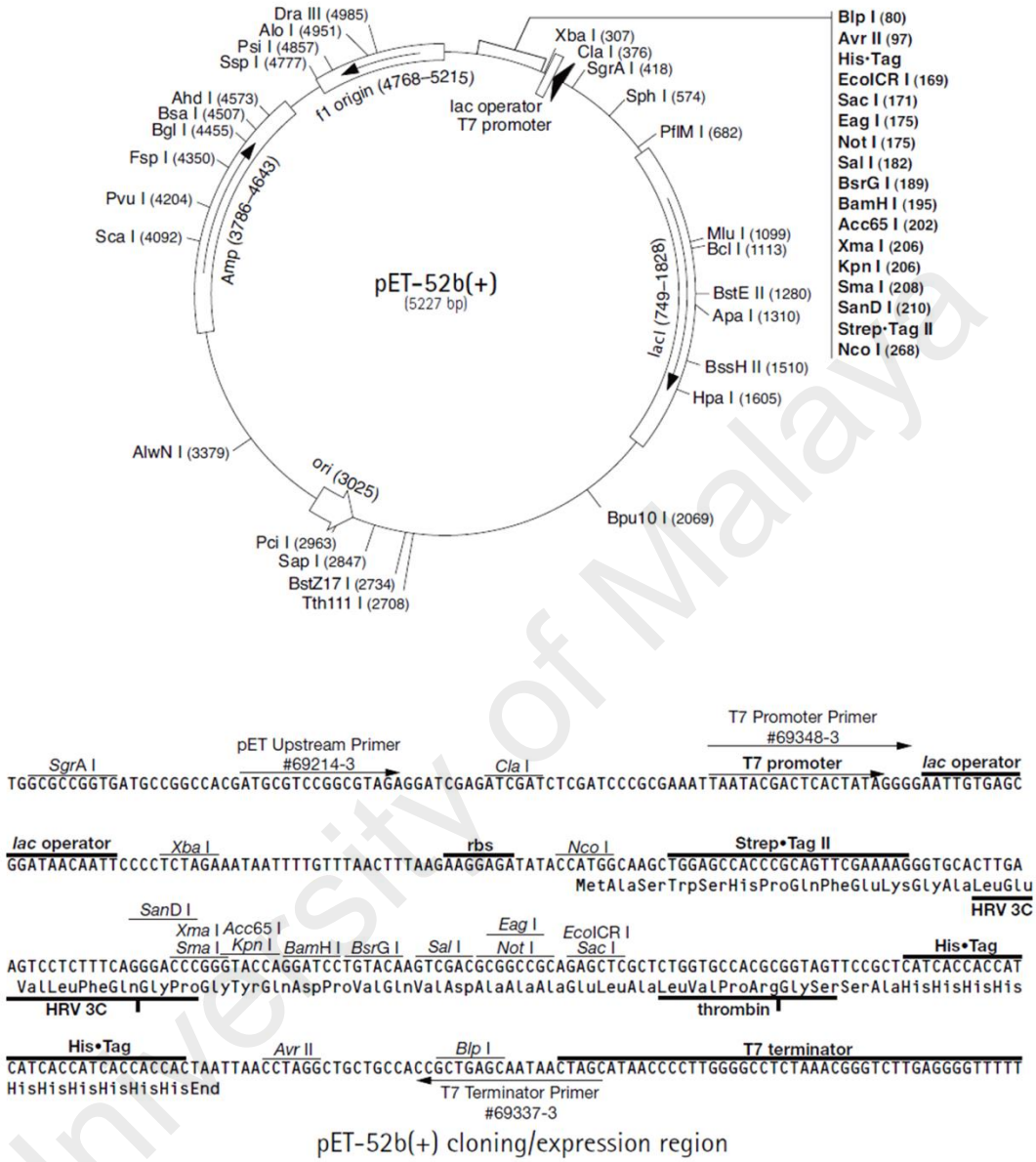

This figure is adapted from the pET-52b(+) information sheet (Novagen, Germany).

Appendix IV: Schematic illustration of pEGFP-N1 vector and the restriction endonuclease recognition sites

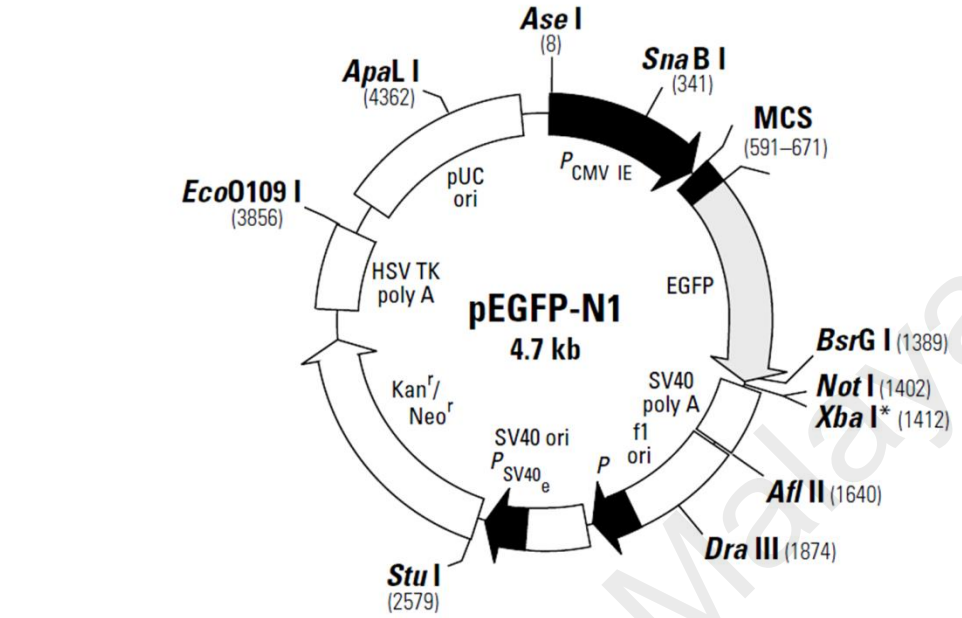

This figure is adapted from the pEGFP-N1 information sheet (Clontech Laboratories Inc., USA).

Appendix V: Antibody profiles for HFMD sera

Appendix VI: Amino acid sequence alignment of peptides with enteroviruses

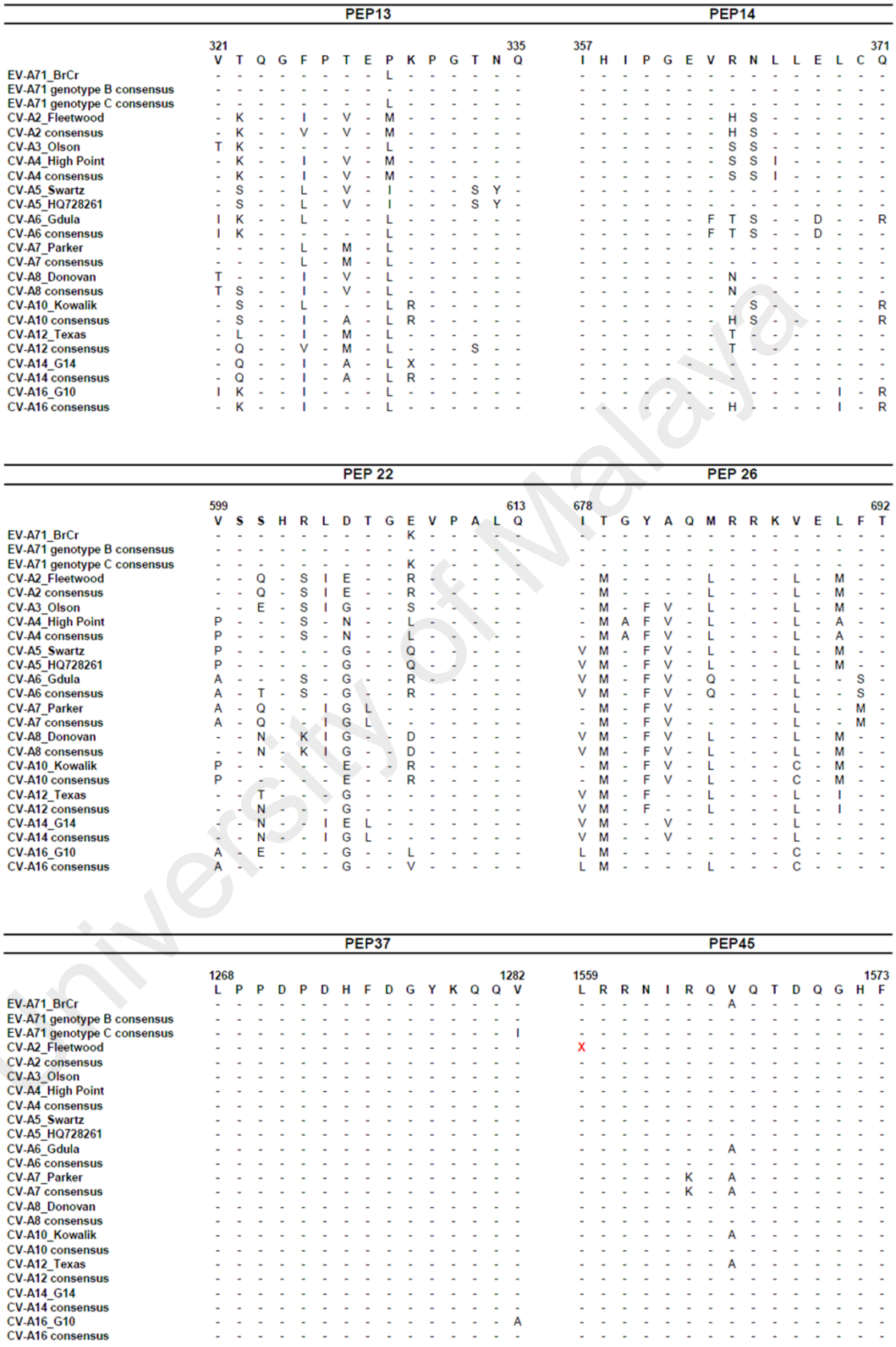

Appendix VI, continued.

	PEP53															PEP60													
	1800														1814	2073													2087
	E	P	D	E	Y	V	T	Q	A	A	L	H	Y	A	N	L	E	L	A	K	T	G	K	E	Y	G	L	T	M	T
EV-A71_BrCr	-	-	-	-	-	-	-	-	-	-	-	-	-	-	-	-	-	W	G	-	-	-	-	-	-	-	-	-	-	-
EV-A71 genotype B consensus	-	-	-	-	-	-	-	-	-	-	-	-	-	-	-	-	-	-	-	-	-	-	-	-	-	-	-	-	-	-
EV-A71 genotype C consensus	-	-	-	-	F	-	K	E	-	-	-	-	-	-	-	-	-	-	-	-	-	-	-	-	-	-	-	-	-	-
CV-A2_Fleetwood	-	-	-	-	-	-	-	-	-	-	-	-	-	-	-	S	-	-	-	R	-	-	-	-	-	-	-	-	-	-
CV-A2 consensus	-	-	-	-	-	-	R	E	-	-	-	-	-	-	-	-	-	-	-	R	-	-	-	-	-	-	-	-	-	-
CV-A3_Olson	D	-	-	-	-	-	-	-	-	-	-	-	-	-	-	-	-	-	-	R	-	-	-	-	-	-	-	-	-	-
CV-A4_High Point	-	-	-	-	-	I	R	E	-	-	-	-	-	-	-	-	-	-	-	R	-	-	-	-	-	-	-	-	-	-
CV-A4 consensus	-	-	-	-	-	I	R	E	-	-	-	-	-	-	-	-	-	-	-	R	-	-	-	-	-	-	-	-	-	-
CV-A5_Swartz	-	-	-	-	-	-	-	-	-	-	-	-	-	-	-	-	-	-	-	R	-	-	-	-	-	-	-	-	-	-
CV-A5_HQ728261	-	-	-	-	-	-	Q	-	-	-	-	-	-	-	-	-	-	-	-	-	-	-	-	-	-	-	-	-	-	-
CV-A6_Gdula	-	-	-	-	-	-	-	-	-	-	-	-	-	-	-	-	-	-	-	-	-	-	-	-	-	-	-	-	-	-
CV-A6 consensus	-	-	-	-	-	I	K	E	-	-	-	-	-	-	-	S	-	-	-	R	-	-	-	-	-	-	-	-	-	-
CV-A7_Parker	-	-	-	-	-	-	-	-	-	-	-	-	-	-	-	S	-	-	-	-	-	-	-	-	-	-	-	-	-	-
CV-A7 consensus	-	-	-	-	-	-	-	-	-	-	-	-	-	-	-	S	-	-	-	-	-	-	-	-	-	-	-	-	-	-
CV-A8_Donovan	-	-	-	-	F	-	R	E	-	-	-	-	-	-	-	-	-	-	-	-	-	-	-	-	-	-	-	-	-	-
CV-A8 consensus	-	-	-	-	-	I	R	E	-	-	-	-	-	-	-	-	-	-	-	-	-	-	M	-	-	-	-	-	-	-
CV-A10_Kowalik	-	-	-	-	-	-	-	-	-	-	-	-	-	-	-	-	-	-	-	R	-	-	-	-	-	-	-	-	-	-
CV-A10 consensus	-	-	-	-	-	-	K	-	-	-	-	-	-	-	-	-	-	-	-	-	-	-	-	-	-	-	-	-	-	-
CV-A12_Texas	-	-	-	-	-	-	-	-	-	-	-	-	-	-	-	-	-	V	-	-	-	-	-	-	-	-	-	-	-	-
CV-A12 consensus	-	-	-	-	-	I	K	E	-	-	-	-	-	-	-	-	-	-	-	R	-	-	-	-	-	-	-	-	-	-
CV-A14_G14	-	-	-	-	-	I	K	E	-	-	F	-	-	-	-	-	-	-	-	R	-	-	-	-	-	-	-	-	-	-
CV-A14 consensus	-	-	-	-	-	-	R	E	-	-	-	-	-	-	-	-	-	-	-	R	-	-	-	-	-	-	-	-	-	-
CV-A16_G10	-	-	-	-	-	-	K	E	-	-	-	-	-	-	-	-	-	-	-	R	-	-	-	-	-	-	-	-	-	-
CV-A16 consensus	-	-	-	-	-	-	-	-	-	-	-	-	-	-	-	S	-	-	-	-	-	-	-	-	-	-	-	-	-	-

In PEP45, the amino acid at position 1559 (indicated as X) is unable to translate due to the reported nucleotide sequences for that region is NUA. The consensus sequences represent the current circulating strains while BrCr, Fleetwood, Olson, High Point, Swartz, Gdula, Parker, Donovan, Kowalik, Texas, G14 and G10 are prototype virus strains.

Appendix VII: IFN-γ analysis (positive control)

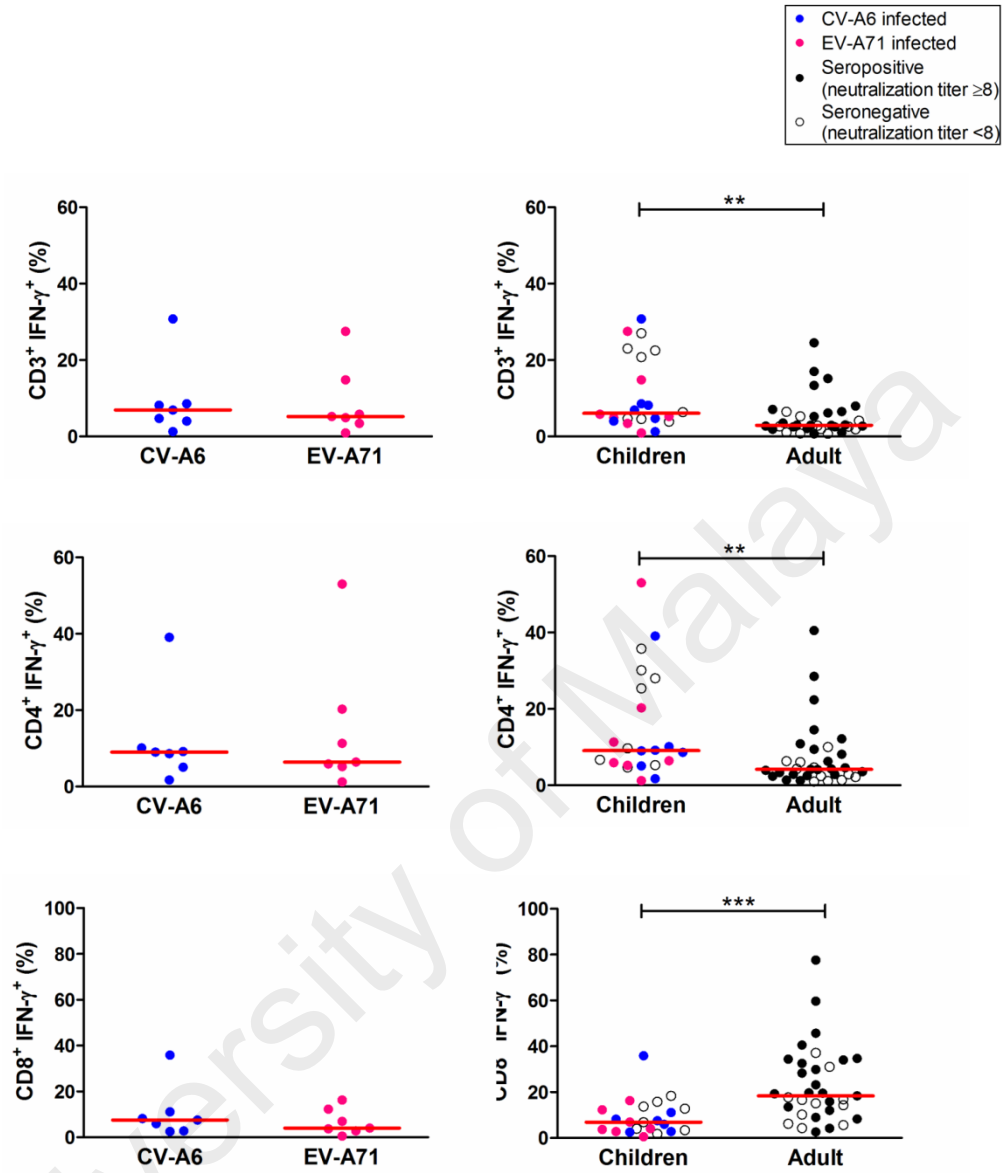

Appendix VIII: Granzyme B, perforin and CD57 in $CD8^+$ T cells (positive control)

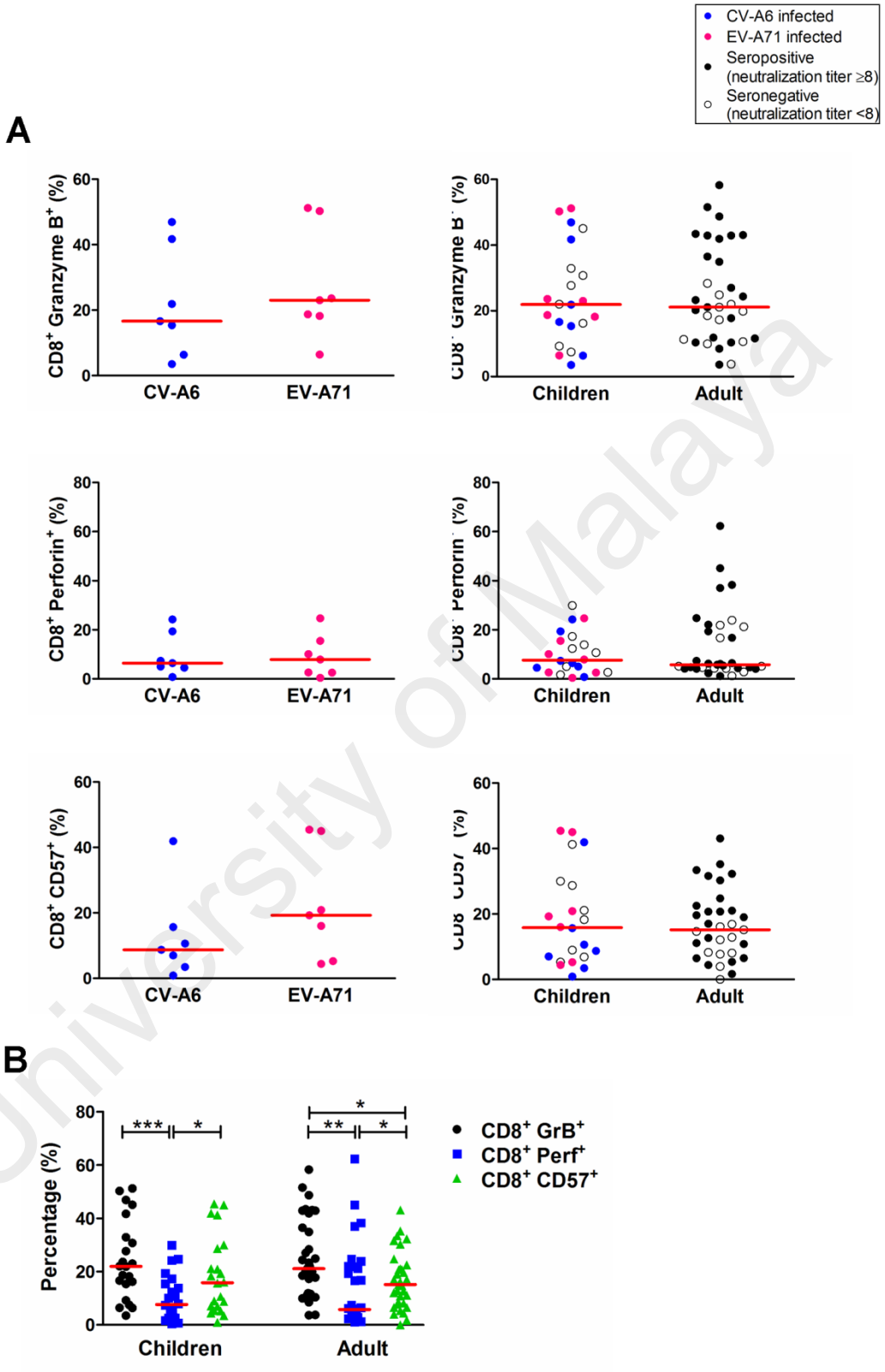

LIST OF PUBLICATIONS AND PAPERS PRESENTED

Publication

Aw-Yong KL, Sam IC, Koh MT, Chan YF. Immunodominant IgM and IgG epitopes recognized by antibodies induced in enterovirus A71-associated hand, foot and mouth disease patients. Submited (under reviewed).

Aw-Yong KL, Sam IC, Koh MT, Chan YF. Causative agents of hand, foot and mouth disease in University Malaya Medical Centre, Kuala Lumpur, Malaysia 2012-2013. Tropical Biomedicine. Accepted for publication.

Aw-Yong KL, Tan CW, Koh MT, Sam IC, Chan YF. Diagnosis of human enterovirus A71 infection in Malaysia using a commercial IgM-capture enzyme-linked imunosorbent assay and an IgM-colloidal gold immunochromatographic assay. Tropical Biomedicine. 2016; 33(2): 238-245.

Abstract in conferences

AwYong KL, Sam IC, Koh MT, Rosland HW, Chan YF. Hand, foot, and mouth disease caused by coxsackievirus A6, Malaysia, May 2012-April 2013. Poster presented at International Congress of the Malaysian Society for Microbiology 2013, Langkawi, Kedah, Malaysia.

Tropical Biomedicine 33(2): 238–245 (2016)

Diagnosis of human enterovirus A71 infection in Malaysia using a commercial IgM-capture enzyme-linked immunosorbent assay and an IgM-colloidal gold immunochromatographic assay

Aw-Yong, K.L.[1], Tan, C.W.[1], Koh, M.T.[2], Sam, I.C.[1] and Chan, Y.F.[1*]
[1]Department of Medical Microbiology, Faculty of Medicine, University Malaya, 50603 Kuala Lumpur, Malaysia
[2]Department of Paediatrics, Faculty of Medicine, University Malaya, 50603 Kuala Lumpur, Malaysia
[*]Corresponding author e-mail: chanyf@ummc.edu.my
Received 15 November 2015; received in revised form 6 December 2015; accepted 8 December 2015

Abstract. Hand, foot and mouth disease (HFMD) is a common childhood infection caused by many enteroviruses, including enterovirus A71 (EV-A71). As EV-A71 is associated with severe neurological disease, early diagnosis is critical for clinical and public health management. In developing countries such as Malaysia, laboratory capacity to carry out EV-A71 IgM detection is greater than that of the gold standard methods of virus culture or molecular detection. This study evaluated two diagnostic kits, EV-A71 IgM-capture enzyme-linked immunosorbent (ELISA) and EV-A71 IgM-colloidal gold immunochromatographic assay (GICA), which had previously only been assessed in China. The assays were tested with 89 serum samples from patients with suspected HFMD. The sensitivity, specificity, positive predictive value, and negative predictive value rates were 78.4%, 80.8%, 74.4%, and 84.0%, respectively, for the IgM-capture ELISA, and 75.7%, 76.9%, 70.0%, and 81.6% for the IgM GICA. These performance measures were similar between the two assays. Concordance between the two assays was 91.1%. The sensitivity rates were lower than those previously reported, likely because the multiple circulating EV-A71 genotypes in Malaysia differ from the C4 subgenotype found in China and used in the assays. Both assays had low false positive rates (12.5% and 16.7% for ELISA and GICA, respectively) when tested on sera from patients confirmed to have enteroviruses. Both diagnostic kits are suitable for early diagnosis of HFMD caused by EV-A71 in Malaysia, but confirmation with culture or PCR is still important.

INTRODUCTION

Hand, foot, and mouth disease (HFMD) is a common viral infection in children. HFMD usually results in mild and self-limiting illness, characterised by fever, vesicular lesions on the palms and soles and oral ulcers. The causative agents of HFMD are viruses from the genus of Enterovirus within the family of *Picornaviridae*, with enterovirus A71 (EV-A71) and coxsackievirus A16 (CV-A16) being the most commonly detected viruses. Over the last decade, EV-A71 was responsible for several large epidemics in the Asia-Pacific region, raising serious public health concerns (Solomon *et al.*, 2010; Chan *et al.*, 2011). EV-A71 infection can cause severe and potentially fatal neurological complications such as aseptic meningitis, brainstem encephalitis and acute flaccid paralysis, especially in children below 5 years old (Ooi *et al.*, 2010; Solomon *et al.*, 2010). Currently there are no effective antivirals and vaccines against EV-A71 (Tan *et al.*, 2014), hence early diagnosis of EV-A71 infection is critical for prompt public health measures to control the spread of virus and minimize the risk of fatality.

Traditionally, standard laboratory diagnosis of EV-A71 was achieved by immunofluorescence assay or virus culture of samples from the lesions, throat or rectum (Muir *et al.*, 1998). However, immunofluorescence is insensitive, and viral culture is time-consuming and labour intensive. Additionally, the yield of enteroviruses from clinical specimens may be low, as some enteroviruses, particularly the coxsackievirus A group, do not readily grow in cell culture (Lipson *et al.*, 1988). Neutralization test is used to detect specific antibodies that inhibit viral-induced cytopathic effect (CPE) (Muir *et al.*, 1998), but is not widely used as it is difficult to perform, requires the use of infectious virus in a biosafety level II laboratory, and availability of paired patient sera to confirm seroconversion. Molecular diagnosis methods such as reverse transcription polymerase chain reaction (RT-PCR) are far more sensitive and quicker, and are the new "gold standard" for enterovirus detection (Hamilton *et al.*, 1999; Robinson *et al.*, 2002). However it may not be widely available throughout developing countries where EV-A71 is more common, as it requires specialized equipment and well-trained personnel. Hence there is a need for a more accessible, reliable and rapid diagnostic assay for EV-A71 in laboratories without access to RT-PCR. A serological test such as enzyme-linked immunosorbent assay (ELISA) is an alternative as results can be obtained in 2-3 hours and most diagnostic laboratories will have access to the equipment, and IgM can be detected early in EV-A71 infection (Zhao *et al.*, 2011). The use of two commercially available EV-A71 IgM kits, EV-A71 IgM-capture ELISA and EV-A71 IgM-colloidal gold immunochromatographic assay (GICA), have been reported in China (Xu *et al.*, 2010; Yu *et al.*, 2012; Wang *et al.*, 2015) but it is critical to evaluate assays in different geographical settings, where there may be potential differences in circulating EV-A71 genotype and patient immune responses. In this study, we evaluated the performances of these two commercial assays in serum samples collected from HFMD patients in Malaysia.

MATERIALS AND METHODS

Serum specimens

Three panels of human sera (n=136) were used for the evaluation of EV-A71 IgM ELISA and IgM GICA, and were obtained from the diagnostic virology laboratory, University Malaya Medical Centre, in Kuala Lumpur, Malaysia. Panel A consisted of 36 residual serum samples obtained during a HFMD outbreak in 2000, and panel B consisted of 53 sera prospectively collected during an outbreak in 2012-2013. All patients from panels A and B showed clinical signs of HFMD (including ulcers in the mouth/tongue, rash/vesicles on the palms and soles, with/without fever), and were considered positive for EV-A71 or non-EV-A71 enteroviruses according to the virus cultured from throat swabs, vesicle swabs and/or rectal swabs. Swabs from patients in panel B were also tested by PCR for enteroviruses. Panel C, the non-HFMD (negative control) samples, consisted of 47 residual serum samples tested positive for IgM for other viral infections, such as dengue, chikungunya, measles, herpes simplex virus and varicella-zoster virus. This study was approved by the hospital's Medical Ethics Committee (reference number: 932.17). Our institution does not require informed consent for retrospective studies of anonymised samples.

Enterovirus detection and genotyping

Viral RNA was extracted using QIAamp Viral RNA Mini Kit (Qiagen, Germany) according to the manufacturer's instructions. To detect enterovirus, the 5'-untranslated region (5'UTR) was amplified with primers CoxbanS (5'-GTAMCYTTGTRCGCCWGTTT-3') and CoxbanR (5'-GAAACACGGACACCCAAA GTA-3', Arola *et al.*, 1995) using Access RT-PCR system (Promega, USA). The reaction was subjected to reverse transcription at 42°C for 60 min and reverse transcriptase inactivation at 94°C for 2 min, followed by 40 cycles at 94°C for 30 sec, 50°C for 1 min, and 68°C for 1 min, and final extension of 68°C for 7 min. The expected PCR products of 502 bp were visualized with 1.5% agarose gel stained with GelRed stain (Biotium Inc, Hayward, USA) under ultraviolet trans-

illumination. The purified amplicons were then sequenced with a 3730xl DNA Analyzer (Applied Biosystems). Sequencing results were subjected to BLAST search to identify the enterovirus serotypes.

Virus isolation

Clinical specimens (throat swabs, vesicle swabs and/or rectal swabs) were used for virus isolation. Specimens were inoculated into human rhabdomyosarcoma (RD) cell cultures in a 24-well plate. Viral cultures showing CPE were harvested and immunofluoresence assay was subsequently performed.

Immunofluoresence assay

Viral cultures showing CPE were harvested and centrifuged at 250 x g for 10 min. Cell pellets were resuspended with phosphate-buffered saline (PBS) and coated on poly-D-lysine treated microscope slides. After air drying, the cells were fixed with 3.7% paraformaldehyde and incubated for 10 min. The fixed cells were washed and permeabilized using 0.25% Triton X-100 (Sigma, USA) for 5 min. The cells were subsequently blocked with Image-iT FX Signal Enhancer (Invitrogen, USA) for 1 h. Enterovirus-infected cells were immuno-stained with Light Diagnostics Pan-Enterovirus Blend (Millipore, USA) as the primary antibody and FITC-labeled anti-mouse IgG conjugate (Millipore, USA) as the secondary antibody for 1 h at 37°C in a humidified chamber. Immunofluorescence was detected with a fluorescence microscope. All enterovirus-positive samples were further tested with Light Diagnostics EV-A71 monoclonal antibody 3324 (Millipore, USA) to confirm EV-A71.

EV-A71 IgM-capture ELISA

EV-A71 specific-IgM antibody in serum specimens were detected using EV-A71 IgM-capture ELISA (Beijing Wantai, China) according to the manufacturer's instructions. Briefly, aliquots of 100 µl/well of diluent and 10 µl/well of serum were sequentially added into microplates coated with anti-human IgM µ-chain, followed by 30 min incubation at 37°C. After washing five times with PBS, 50 µl of purified EV-A71 antigen and 50 µl of horseradish peroxidase (HRP)-conjugate anti-EV-A71 monoclonal antibody were added to the microplate, which was then incubated for 30 min at 37°C. The plate was washed five times with PBS, followed by addition of 50 µl of urea peroxide and 50 µl of TMB substrate, and further incubated for 15 min at 37°C in the dark. The reaction was terminated with 50 µl of 2.0 M sulfuric acid. Optical density (OD) of each well was read at 450 nm with a 630 nm reference filter with a microplate reader (BioTek Instruments, USA). The cut-off value was calculated as 0.1 + mean OD of the negative controls. If the mean OD of negative controls was lower than 0.05, this was treated as 0.05. A serum specimen was considered positive with a signal/cut-off (S/CO) value of ≥ 1.0.

EV-A71 IgM GICA

Serum EV-A71 specific-IgM was detected with EV-A71 IgM GICA kit (Beijing Wantai, China) according to the manufacturer's instructions. An aliquot of 15 µl of serum was added to the specimen diluent and mixed well. Aliquots of 80 µl of diluted samples were pipetted into the sample wells of the EV-A71 IgM GICA cassette and the results were read within 30 min. EV-A71-specific IgM antibodies were captured by immobilized EV-A71 antigen and formed an antibody-antigen complex on the test line. Serum specimens were considered positive if bands appeared at the test line and control line.

Statistical analysis

The sensitivity, specificity, positive predictive value (PPV), and negative predictive value (NPV) of EV-A71 IgM-capture ELISA and EV-A71 IgM GICA were calculated, and compared using Fisher's exact test. Statistical analyses were performed using GraphPad Prism version 5.0 (GraphPad Software, La Jolla, CA). Cohen's kappa (κ) was used to estimate inter-assay concordance, with a value of 1 indicating complete agreement. A *P*-value of <0.05 was considered significant.

RESULTS

Sera grouping

A total of 89 HFMD sera (36 sera from panel A and 53 sera from panel B) and 47 non-HFMD sera (panel C) were used for the evaluation (Table 1). Of these, 37 HFMD sera were from EV-A71-positive patients (confirmed by RT-PCR or culture), and 24 HFMD sera were positive for non-EV-A71 enteroviruses, which consist of CV-A4 (n=1), CV-A6 (n=10), CV-A16 (n=2), CV-B (n=1), echovirus 7 (n=6), rhinovirus (n=1) and untyped enteroviruses (n=3). The remaining HFMD sera were enterovirus RT-PCR-/culture-negative (n=28).

Performance characteristics

Overall sensitivity and specificity rates were moderately good for EV-A71 IgM-capture ELISA and IgM GICA, with 78.4% and 75.7% sensitivity and 89.9% and 85.9% specificity, respectively (Table 2). NPV rates were >90%, but PPV rates were moderate for ELISA (74.4%) and GICA (66.7%). Performances of the assays were also determined just for the HFMD cases, as this is the most likely group to be tested for EV-A71 IgM. Specificity (ELISA, 80.8% and GICA, 76.9%) and NPV (ELISA, 84.0% and GICA, 81.6%) decreased, while PPV were similar. There were no significant differences in sensitivity, specificity, PPV and NPV rates between the two assays.

Concordance between the results of the two assays for each category of sera is shown in Table 3. The overall concordance was 91.1%, with a κ value of 0.805. The concordance for testing the HFMD sera (panels A and B) was 92.1%, with a κ value of 0.841. The concordance for testing samples from EV-A71-positive cases was 97.3%, with a κ value of 0.924, whereas the concordance for testing EV-A71 negative cases was 91.9%, with a κ value of 0.622.

False positive rates of IgM-capture ELISA and IgM GICA

In sera from patients with HFMD but no confirmed EV-A71, anti-EV-A71 IgM was detected in 10/52 (19.2%) and 12/52 (23.1%) with IgM-capture ELISA and IgM GICA, respectively. Of those with confirmed non-EV-A71 enterovirus infection, anti-EV-A71 IgM was detected in 3/24 (12.5%) and 4/24 (16.7%) with IgM-capture ELISA and IgM GICA, respectively. These false positives were detected in patients confirmed to have echovirus 7 (n=2) and CV-A16 (n=1) using the IgM-capture ELISA assay, whereas the false positives in the IgM-GICA assay were seen in patients with echovirus 7 (n=1), CV-A16 (n=1) and CV-A6 (n=2). Two samples (one each with echovirus 7 and CV-A16) were positive with both assays. For the non-HFMD sera, only the IgM GICA recorded false positives, in 2/47 (4.3%) samples. Overall, the mean S/CO value (0.76±2.37) of the false-

Table 1. Classification of serum samples used for the evaluation of EV-A71 commercial diagnostic kits

Group	Panel A	Panel B	Panel C	Total
EV-A71[a]	24	13	N/A	37
Non-EV-A71 enterovirus[a,b]	12	12	N/A	24
Enterovirus RT-PCR-/culture-negative[a]	N/A	28	N/A	28
Non-HFMD	N/A	N/A	47	47
Total	36	53	47	136

[a]tested on throat swabs, vesicle swabs and/or rectal swabs from the same patient; all patients had suspected HFMD
[b]CV-A4 (n=1), CV-A6 (n=10), CV-A16 (n=2), CV-B (n=1), echovirus 7 (n=6), rhinovirus (n=1), untyped enteroviruses (n=3).
N/A, not applicable

Table 2. Comparative performances of the EV-A71 IgM-capture ELISA and EV-A71 IgM GICA in serum samples

		EV-A71 (n=37)		non-EV-A71					
		IgM positive	IgM negative	IgM positive	IgM negative	Sensitivity, % [95% CI]	Specificity, % [95% CI]	PPV, % [95% CI]	NPV, % [95% CI]
Overall analysis[a]	EV-A71 IgM-capture ELISA	29	8	10	89	78.4 (29/37) [62.6–88.9]	89.9 (89/99) [82.2–94.6]	74.4 (29/39) [58.8–85.6]	91.8 (89/97) [84.4–96.0]
	EV-A71 IgM-GICA	28	9	14	85	75.7 (28/37) [59.7–86.8]	85.9 (85/99) [77.5–91.5]	66.7 (28/42) [51.5–79.1]	90.4 (85/94) [82.6–95.1]
Analysis of HFMD cases[b]	EV-A71 IgM-capture ELISA	29	8	10	42	78.4 (29/37) [62.6–88.9]	80.8 (42/52) [67.9–89.4]	74.4 (29/39) [58.8–85.6]	84.0 (42/50) [71.2–91.9]
	EV-A71 IgM-GICA	28	9	12	40	75.7 (28/37) [59.7–86.8]	76.9 (40/52) [63.7–86.4]	70.0 (28/40) [54.5–82.0]	81.6 (40/49) [68.4–90.3]

[a]non-EV-A71 cases comprising non-EV-A71 enterovirus, enterovirus RT-PCR-/culture-negative, and non-HFMD cases (n=99) for overall analysis
[b]non-EV-A71 cases comprising non-EV-A71 enterovirus and enterovirus RT-PCR-/culture-negative cases (n=52), all of whom had suspected HFMD

Table 3. Concordance between EV-A71 IgM-capture ELISA and EV-A71 IgM GICA

EV-A71 IgM-capture ELISA		EV-A71 IgM GICA: EV-A71 +	EV-A71 -	Non-EV-A71 enterovirus +	Non-EV-A71 enterovirus -	Enterovirus RT-PCR-/culture-negative +	Enterovirus RT-PCR-/culture-negative -	Non-HFMD +	Non-HFMD -	Total
EV-A71	+	28	1							29
	-	0	8							8
Non-EV-A71 enterovirus	+			2	1					3
	-			2	19					21
Enterovirus RT-PCR-/culture-negative	+					6	1			7
	-					2	19			21
Non-HFMD	+							0	0	0
	-							2	45	47
	Total	28	9	4	20	8	20	2	45	136

positive samples was significantly lower than the mean S/CO value of 4.70±3.91 for the EV-A71-positive sera (data not shown).

DISCUSSION

In Malaysia, HFMD is endemic and outbreaks of EV-A71 infection occur every 2-3 years (NikNadia *et al.*, 2016). Early social distancing resulted in reduced HFMD cases in Sarawak, Malaysia in 2006 (Solomon *et al.*, 2010). Therefore, early diagnosis of EV-A71 would enable early interventions to curb the spread of infection and appropriately observe patients for complications. While PCR will detect the virus earliest, IgM has also been shown as a good early indicator for EV-A71 infection, as it may be detectable as early as 1 day of illness and peaks on day 5 (Zhao *et al.*, 2011), and is detectable for up to 94 days (Wang *et al.*, 2004). Serological detection of IgM would be suitable for most laboratories which do not have PCR or viral culture facilities. More importantly, the rapid and more convenient GICA assay showed comparable performance to the ELISA-based assay, suggesting that it can be used in clinics or rural settings with no laboratory facilities.

There are very few commercial EV-A71 IgM diagnostic kits available. In this study, we compared EV-A71 IgM-capture ELISA and IgM GICA assays in Malaysian patients, and found sensitivity rates (78.4% and 75.7%, respectively) that were lower than the 93.6% and 94.1% (IgM-capture ELISA), and 93.3% (IgM-GICA) reported earlier in China (Xu *et al.*, 2010; Yu *et al.*, 2012, Wang *et al.*, 2015). One possible reason might be the varying detection of antibodies resulting from different circulating EV-A71 genotypes found in Malaysia and China. In Malaysia, subgenotypes B4, B5 and C1 circulated in 2000, and only subgenotype B5 has been present after 2005, whereas the current predominant EV-A71 in China is subgenotype C4 (Chan *et al.*, 2011; Chan *et al.*, 2012). The purified EV-A71 antigen used in the diagnosis kits was subgenotype C4, hence this may explain the higher sensitivity reported in the China studies.

When testing serum from children with HFMD, the assays showed specificity rates of 80.8% and 76.9% for the IgM-capture ELISA and IgM GICA, respectively. These specificity rates were lower than the 88.6% reported by Xu *et al.* (2010), but higher than the 69.6% reported for the IgM-capture ELISA by Yu *et al.* (2012) and the 50% for the IgM GICA reported by Wang *et al.* (2015). The PPV rates of 74.4% (ELISA) and 70.0% (GICA) were moderate, although these rates would have been affected by the lower prevalence of EV-A71 in the HFMD outbreak in 2012-2013 (panel B), which had relatively more cases due to CV-A6. The false positives are likely due to detection of IgM which recognize common epitopes among enteroviruses (Xu *et al.*, 2010; Yu *et al.*, 2012). Increasing the cut-off values according to locally-

determined background seropositive rates may improve specificity and PPV.

PCR is known to be the most efficient diagnosis for EV-A71 (Ooi *et al.*, 2010); yet, in the present study, IgM was detected in 25.0% (ELISA) and 28.6% (GICA) of serum samples from patients with negative enterovirus RT-PCR. One possibility is the presence of low levels of virus RNA, which may be resolved by the use of real-time RT-PCR rather than the less sensitive conventional RT-PCR used in the present study. In addition, our RT-PCR is only limited to amplification of 5'UTR, so targeting other gene regions such as VP4/VP2 and VP1 should be considered.

One of the limitations of the present study is that the timings of disease onset are not known, and cannot be correlated with the IgM response. However, the value in this study is the use of samples from patients with confirmed enterovirus infection, in a different geographical location with different circulating enteroviruses to other previously reported evaluations, which were limited to China. The circulation of different serotypes of EV-A71 in Malaysia likely explains the lower test sensitivities seen here. Our study also showed that both EV-A71 IgM-capture ELISA and EV-A71 IgM GICA had comparable performance characteristics and concordance, despite the fact that point-of-care tests are generally felt to be inferior to ELISA-based assays. Therefore, the IgM GICA can be used in clinics or rural settings with no laboratory or ELISA facilities. Both diagnostic kits may be useful and convenient for the screening for EV-A71 infection during HFMD outbreaks in Malaysia, but confirmation (of patients with both positive and negative IgM results) with either culture or RT-PCR remains essential.

Acknowledgements. This study was supported by grants from the University of Malaya (High Impact Research Grant E000013-20001, University Malaya Research Grant RG522-13HTM and Postgraduate Research Grant PG036-2013B).

REFERENCES

Arola, A., Kalimo, H., Ruuskanen, O. & Hyypiä, T. (1995). Experimental myocarditis induced by two different coxsackievirus B3 variants: aspects of pathogenesis and comparison of diagnostic methods. *Journal of Medical Virology* **47**(3): 251-259.

Chan, Y.F., Sam, I.C., Wee, K.L. & AbuBakar, S. (2011). Enterovirus 71 in Malaysia: A decade later. *Neurology Asia* **16**(1): 1-15.

Chan, Y.F., Wee, K.L., Chiam, C.W., Khor, C.S., Chan, S.Y., Wan Nor Amalina, W.M.Z. & Sam, I.C. (2012). Comparative genetic analysis of VP4, VP1 and 3D gene regions of enterovirus 71 and coxsackievirus A16 circulating in Malaysia between 1997-2008. *Tropical Biomedicine* **29**(3): 451-466.

Hamilton, M.S., Jackson, M.A. & Abel, D. (1999). Clinical utility of polymerase chain reaction testing for enteroviral meningitis. *Pediatric Infectious Disease Journal* **18**(6): 533-537.

Lipson, S.M., Walderman, R., Costello, P. & Szabo, K. (1988). Sensitivity of rhabdomyosarcoma and guinea pig embryo cell cultures to field isolates of difficult-to-cultivate group A coxsackieviruses. *Journal of Clinical Microbiology* **26**(7): 1298-1303.

Muir, P., Kämmerer, U., Korn, K., Mulders, M.N., Pöyry, T., Weissbrich, B., Kandolf, R., Cleator, G.M. & van Loon, A.M. (1998). Molecular typing of enteroviruses: current status and future requirements. The European Union Concerted Action on virus meningitis and encephalitis. *Clinical Microbiology Reviews* **11**(1): 202-227.

NikNadia, N., Sam, I.C., Rampal, S., WanNorAmalina, W.M.Z., NurAtifah, M., Verasahib, K., Ong, C.C., MohdAdib, M. & Chan, Y.F. (2016). Cyclical patterns of hand, foot and mouth disease caused by enterovirus A71 in Malaysia. *PLoS Neglected Tropical Diseases* **10**(3): e0004562.

Ooi, M.H., Wong, S.C., Lewthwaite, P., Cardosa, M.J. & Solomon, T. (2010). Clinical features, diagnosis, and management of enterovirus 71. *Lancet Neurology* **9**(11): 1097-1105.

Robinson, C.C., Willis, M., Meagher, A., Gieseker, K.E., Rotbart, H. & Glodé, M.P. (2002). Impact of rapid polymerase chain reaction results on management of pediatric patients with enteroviral meningitis. *Pediatric Infectious Disease Journal* **21**(4): 283-286.

Solomon, T., Lewthwaite, P., Perera, D., Cardosa, M.J., McMinn, P. & Ooi, M.H. (2010). Virology, epidemiology, pathogenesis, and control of enterovirus 71. *Lancet Infectious Diseases* **10**(11): 778-790.

Tan, C.W., Lai, J.K.F., Sam, I.C. & Chan, Y.F. (2014). Recent development of antiviral agents against enterovirus 71 infection. *Journal of Biomedical Science* **21**: 14.

Wang, S.Y., Lin, T.L., Chen, H.Y. & Lin, T.S. (2004). Early and rapid detection of enterovirus 71 infection by an IgM-capture ELISA. *Journal of Virological Methods* **119**(1): 37-43.

Wang, Y., Zou, G., Xia, A., Wang, X., Cai, J., Gao, Q., Yuan, S., He, G., Zhang, S., Zeng, M. & Altmeyer, R. (2015). Enterovirus 71 infection in children with hand, foot, and mouth disease in Shanghai, China: epidemiology, clinical feature and diagnosis. *Virology Journal* **12**: 83.

Xu, F., Yan, Q., Wang, H., Niu, J., Li, L., Zhu, F., He, S., Zhang, S., Weng, Z., Cheng, T., Cai, Y., He, D., Chen, Y., Ge, S., Yeo, A.E., Zhang, J., Ng, M.H. & Xia, N. (2010). Performance of detecting IgM antibodies against enterovirus 71 for early diagnosis. *PLoS One* **5**(6): e11388.

Yu, N., Guo, M., He, S.J., Pan, Y.X., Chen, X.X., Ding, X.X., Hao, W., Wang, Y.D., Ge, S.X., Xia, N.S. & Che, X.Y. (2012). Evaluation of human enterovirus 71 and coxsackievirus A16 specific immunoglobulin M antibodies for diagnosis of hand-foot-and-mouth disease. *Virology Journal* **9**: 12.

Zhao, J., Xu, J., Chen, W.W., Li, Y.L., Tang, Y., Li, J., Wang, H.B., Guo, T.S., Zhao, M., Li, B.A. & Mao, Y.L. (2011). The early diagnosis value of EV71 IgM class antibodies in the hand, foot, and mouth disease. *Zhonghua Shi Yan He Lin Chuang Bing Du Xue Za Zhi* **25**(2): 140-142. (Article in Chinese)

MANUSCRIPT MS411-17

Causative agents of hand, foot and mouth disease in University Malaya Medical Centre, Kuala Lumpur, Malaysia in 2012-2013

Aw-Yong KL[1], Sam IC[1], Koh MT[2], Chan YF[1]

[1]Department of Medical Microbiology, Faculty of Medicine, University of Malaya

[2]Department of Paediatrics, Faculty of Medicine, University of Malaya

ABSTRACT

Hand, foot and mouth disease (HFMD) is a childhood illness, commonly caused by enterovirus A71 (EV-A71) and coxsackievirus A16 (CV-A16). In recent years, unusual HFMD outbreaks caused by coxsackievirus A6 (CV-A6) have been reported. From May 2012 to September 2013, enteroviruses were detected in 25 HFMD patients in University Malaya Medical Centre, Kuala Lumpur, Malaysia. The predominant serotypes were EV-A71 (48%) and CV-A6 (48%), followed by CV-A16 (4%). CV-A6 patients (mean age, 2.1) were significantly younger than EV-A71 patients (mean age, 3.3). There were no significant differences observed in clinical features between EV-A71 and CV-A6 patients. Since enteroviruses are difficult to differentiate clinically, the conserved 5' untranslated region (5' UTR) was used to identify enterovirus serotypes. Phylogenetic analysis of 5' UTR showed distinct clustering of viruses as EV-A71, CV-A16 and CV-A6. Further genotyping with capsid genes showed that all the EV-A71 sequences belonged to subgenotype B5, while the CV-A16 sequence belonged to subgenotype B2b. CV-A6 sequences were clustered into genotypes D1 and D2, with recent isolates from Seri Kembangan, Malaysia and China. In summary, 59.5% of HFMD cases in our centre in 2012-2013 were caused by EV-A71, CV-A16 and the newly emerging CV-A6. This study also demonstrated that 5' UTR is suitable for preliminary identification of enteroviruses during HFMD outbreaks, but specific capsid genes such as VP1 and VP4/VP2 are required for further genotyping. Apart from measures to control the spread of the virus during an outbreak of HFMD, identification of EV-A71 as the aetiological agent is important as EV-A71 is a major cause of severe neurological complications and potentially fatal.

HAND, FOOT, AND MOUTH DISEASE CAUSED BY COXSACKIEVIRUS A6, MALAYSIA, MAY 2012 – APRIL 2013

Kam Leng AwYong[1], I-Ching Sam[1], Mia Tuang Koh[2], Hannah Wardiah Rosland[2] and Yoke Fun Chan[1]*

[1]Department of Medical Microbiology, Faculty of Medicine, University of Malaya, 50603 Kuala Lumpur, Malaysia; [2]Department of Paediatric, Faculty of Medicine, University of Malaya, 50603 Kuala Lumpur, Malaysia

*Corresponding author email: chanyf@ummc.edu.my

Hand, foot and mouth disease (HFMD) is a common illness frequently occurring in infants and children. HFMD is characterized by fever, vesicular lesions on the palms and feet, ulcers in the oral mucosa, and sore throat. In Malaysia, the predominant etiological agents causing HFMD are enterovirus A71 (EV-A71) and coxsackievirus A16 (CV-A16). Lately, unusual HFMD outbreaks caused by coxsackievirus A6 (CV-A6) have been reported in Singapore, Taiwan, China, Japan, Finland, United States, Spain, and most recently in Thailand. Hence in the present study, we wanted to verify the occurrence of CV-A6-associated HFMD in Malaysia. From May 2012 to April 2013, a total of 35 throat swab specimens from HFMD patients were collected from the Paediatric Trauma and Emergency Department of the University Malaya Medical Centre, Kuala Lumpur. Viral RNA was extracted from the specimens. To identify enterovirus type in the specimens, we performed one step reverse transcription-PCR which amplified the 5' untranslated region of the viruses. Enteroviruses were detected in specimens from 20 HFMD patients (57.1%). Sequencing was performed for the 20 specimens. EV-A71 was detected in 12 patients (60%), CV-A16 was detected in 1 patient (5%), and CV-A6 was detected in 7 patients (35%). In conclusion, reports of HFMD outbreaks associated with CV-A6 are increasing. This study demonstrates that CV-A6 may be emerging as a new and major cause of epidemic HFMD, in addition to EV-71 and CV-A16.

CURRICULUM VITAE

PERSONAL PROFILE

Name : Aw Yong Kam Leng

Date of Birth : 18 July 1988

Nationality : Malaysian

Email : kamleng@hotmail.com

Contact Number : +6017-6229979

Address : 160-2-2 Blok S, Jalan Matang 2, Taman Sri Kuching, 51200 Kuala Lumpur, Malaysia.

EDUCATION AND QUALIFICATION

Dec 2012 till present	University of Malaya (UM)	
	Program	: Master of Medical Science
	Research Field	: Medical Microbiology (Virology)
	Status	: Thesis completed
	Graduation	: October 2016
July 2008 - May 2011	University of Malaya (UM)	
	Program	: Bachelor of Science (Bioinformatics)
	CGPA	: 3.62
May 2006 - Dec 2007	Jalan Ipoh Girls Secondary School, Kuala Lumpur	
	Program	: Malaysia Higher School Certificate
	CGPA	: 3.00

PUBLICATIONS

Aw-Yong KL, Sam IC, Koh MT, Chan YF. Immunodominant IgM and IgG epitopes recognized by antibodies induced in enterovirus A71-associated hand, foot and mouth disease patients. PLoS ONE. Submitted (under reviewed).

Aw-Yong KL, Sam IC, Koh MT, Chan YF. Causative agents of hand, foot and mouth disease in University Malaya Medical Centre, Kuala Lumpur, Malaysia in 2012-2013. Tropical Biomedicine. Accepted for publication.

Aw-Yong KL, Tan CW, Koh MT, Sam IC, Chan YF. Diagnosis of human enterovirus A71 infection in Malaysia using a commercial IgM-capture enzyme-linked imunosorbent and an IgM-colloidal gold immunochromatographic assay. Tropical Biomedicine. 2016; 33(2): 238-245.

CONFERENCES / WORKSHOPS

Aw-Yong KL, Sam IC, Koh MT, Chan YF. Immunodominant IgM and IgG epitopes recognized by antibodies induced in enterovirus A71-associated hand, foot and mouth disease patients. Poster presentation at EUROPIC 2016 congress, Les Diablerets, Switzerland, 4 - 8 September 2016.

Aw-Yong KL, Sam IC, Koh MT, Rosland HW, Chan YF. Hand, foot and mouth disease caused by coxsackievirus A6, Malaysia, May 2012 - Sept 2013. Poster presented at International Congress of the Malaysian Society for Microbiology 2013, Langkawi, Malaysia, 12 - 15 December 2013.

Aw-Yong KL. Participant at Chikungunya 2013, Langkawi, Malaysia, 28 - 30 October 2013.

Aw-Yong KL. Basic and clinical immunology course. University of Malaya, 23 - 27 July 2013.

Aw-Yong KL. BD FACSCANTO II operator training course. University of Malaya, 3 - 5 July 2012.

HONORS AND AWARDS

- University of Malaya Fellowship Scheme (Dec 2012 - May 2014)
- Graduate Research Assistantship Scheme (Sept 2014 - Feb 2015)
- Postgraduate Research Fund PG036-2013B (Dec 2013 - Nov 2015)

WORKING EXPERIENCE

- Research Assistant, University of Malaya (July 2011 - Dec 2012)
- Industrial Training Trainee, Community Health Development Division, Institute for Public Health (10 May 2010 - 4 July 2010)
- Teaching Assistant, Tadika Seri Murni (January 2006 - May 2006)